U
Universitetet
i Stavanger

FACULTY OF SCIENCE AND TECHNOLOGY

MASTER'S THESIS

Study programme/specialisation: Petroleum Geosciences Engineering	Spring semester, 2017 Open
Author: AMRIZAL	………………………………………… (signature of author)
Faculty Supervisor: SYLVIA NORDFJORD External Supervisor: -	
Title of master's thesis: **An Integrated Study of the Cretaceous Sequence Stratigraphic Development in the Northern Stord Basin, North Sea, Using 3D and 2D Seismic Data and Wells**	
Credits (ECTS): 30	
Keywords: *Sequence Stratigraphy* *Northern Stord Basin* *Cretaceous Period* *Seismic Interpretation* *Seismic Attribute Analysis* *Petroleum System and Exploration*	Number of pages: 139 one flash drive (USB) Stavanger, 21 June 2017

An Integrated Study of the Cretaceous Sequence Stratigraphic Development in the Northern Stord Basin, North Sea, Using 3D and 2D Seismic Data and Wells

by

Amrizal

Thesis

Presented to the Faculty of Science and Technology

The University of Stavanger

The University of Stavanger

June 2017

Acknowledgements

An Integrated Study of the Cretaceous Sequence Stratigraphic Development in the Northern Stord Basin, North Sea, Using 3D and 2D Seismic Data and Wells

Amrizal

The University of Stavanger, 2017

Supervisor: Sylvia Nordfjord

ABSTRACT

The Cretaceous interval of the northern Stord Basin is under-studied stratigraphic successions due to its minor significance for the oil and gas industry. Therefore, the available subsurface data is limited, especially well and high-resolution seismic data. However, state-of-the-art 3D broadband seismic data were recently acquired in the western part of the northern Stord Basin, giving an opportunity to develop a temporal and spatial distribution of reservoir and seal pairs, source rocks, and traps.

Nine key seismic surfaces were mapped (Base Cretaceous Unconformity, Top Unit A1, Top Unit A2, Downlap Surface 1, Unconformity 1, Top Unit D, Downlap Surface 2, Unconformity 2, and Top Shetland Surface) within the post-rift Cretaceous strata of the northern Stord Basin, which divide this interval into seven main seismic units (Units A-G). Seismic stratigraphic interpretation confirms that the eustatic sea-level rose during the Cretaceous period. However, it was interrupted by two base-level falls during the Berriasian and in the Cenomanian times. Several highs controlled the deposition in the study area, such as the Oseberg and the Troll Fault Blocks, the Bjørgvin Arc, and the Øygarden Fault Complex. All structural highs, except the Øygarden Fault Complex, were flooded the latest in the Turonian time.

Two complete and an incomplete second-order cycle sequences bounded by unconformities were identified in the study area. These sequences comprise a falling-stage systems tract (FSST 1), three lowstand systems tracts (LST 1, 2, and 3), two transgressive systems tracts (TST1 and 2), and two highstand systems tracts (HST 1 and 2).

The Åsgard deep-marine basin-floor fans (Unit A1) and the Agat and Tryggvason formations prograding shallow marine sandstones (Unit C and F) are two clastic-rich geometries within the Cretaceous interval in the study area. In addition, the Tryggvason and Ekofisk formations slumping-related chalky limestones (Unit G) are possibly also a good reservoir rock. The Sola (Unit C) and the Blodøks (Unit E) shales are potential source rocks interval, where the Sola shales are predicted to be in the early mature oil window, while the Blodøks shales are still in the immature oil window. The potential seal rocks are the intervening Åsgard claystones (Unit A2), other intra-formational claystones, and ultimately by the overlying Cenozoic sediments. The primary traps within the Cretaceous are stratigraphic traps, such as pinch-out in Unit A1 and truncation in Unit C and F. The lack of well data in the study area leads to the uncertainty of source rock maturity. Therefore, the hydrocarbon charging is expected to be from the Viking Graben in the east, which often is seen to be risky due to long-distance migration.

Table of Contents

x

List of Figures

List of Figures

1. INTRODUCTION

The northern North Sea is a mature hydrocarbon basin and belongs to one of the most prolific hydrocarbon provinces in the world. However, the northern Stord Basin, within the northern North Sea and situated on the eastern flank of the Viking Graben (Figure 1), is still an underexplored basin. The northern Stord Basin is covered by mainly 2D seismic reflection data sets with limited well control; hence, the low confidence of lateral and vertical sedimentary successions (Biddle and Rudolph, 1988). Recently new 3D seismic data were acquired in the northern North Sea and northern Stord Basin, which form part of this study.
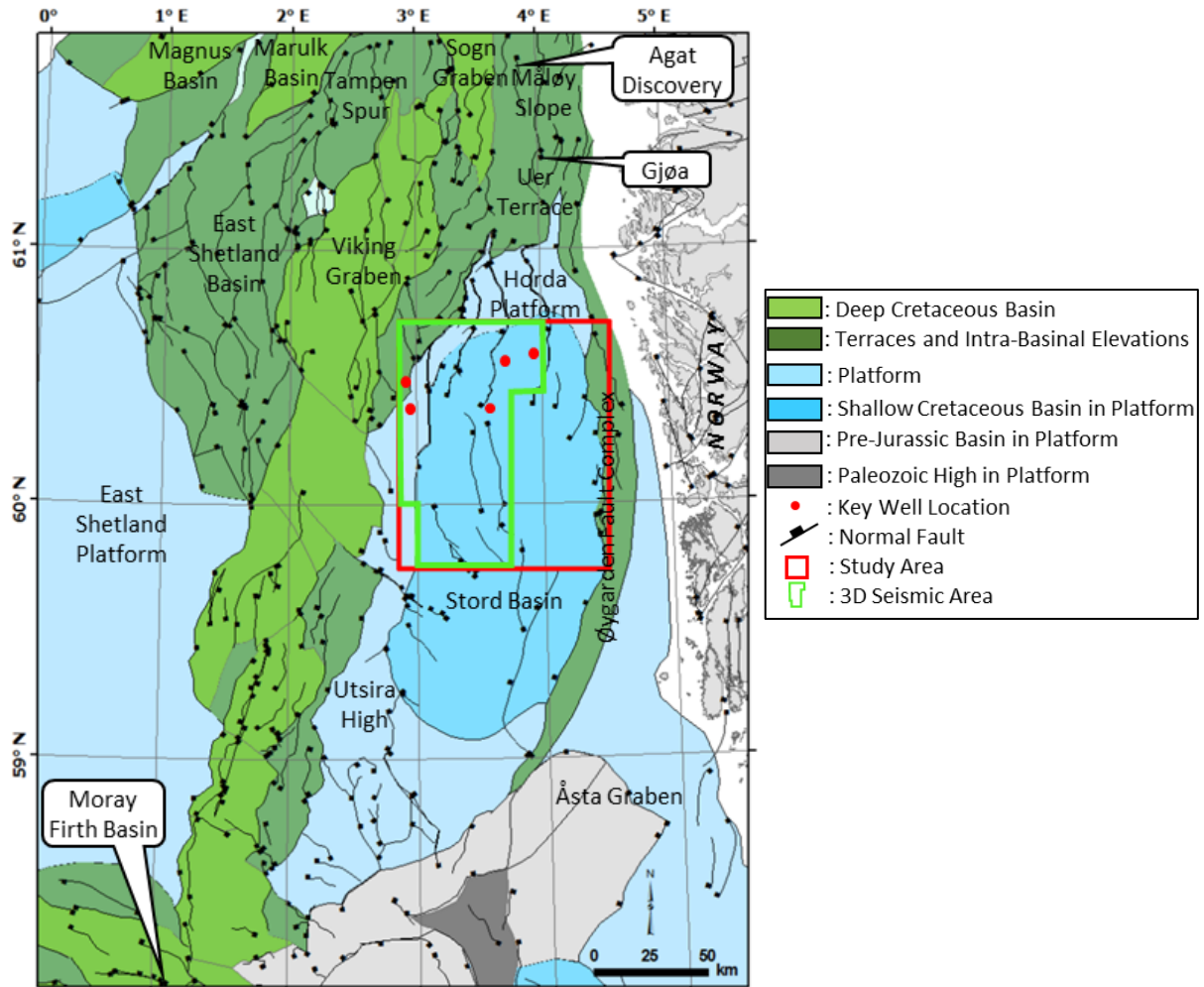
Figure 1: The location of the study area in the northern Stord Basin within the northern North Sea (red square) (modified from NPD, 2017). The Moray Firth Basin, the Agat discovery, and the Gjøa Field area are highlighted on the map.

1

Færseth (1996) and Fossen *et al.* (2016) described two phases forming the northern North Sea Rift: the Permo-Triassic rift and the subsequent Middle-Late Jurassic rift, initiated during deposition of the Brent Group. This was followed by passive post-rift infilling due to lithospheric cooling, with pulses of compression in the Late Cretaceous. Biddle and Rudolph (1988) suggested that Early Tertiary structural inversion might be associated with the initial opening of the North Atlantic Ocean and Alpine continent-continent collision.

The Stord Basin is bordered to the east by the Øygarden Fault Complex Terrace, to the southwest by the Utsira High, to the north by the Horda Platform, and to the south by a ridge separating it from the Åsta Graben (Figure 1). The north-south trend of the Stord Basin and the Åsta Graben forms the eastern part of the northern North Sea Basin (Sørensen and Tangen, 1995; Figure 1).

Generally, wells were drilled in the Stord Basin and its surrounding area to confirm the presence of Jurassic and older hydrocarbon-filled sandstone reservoirs. Fossen *et al.* (2016) reported Lower Triassic intervals overlying granitic-amphibolitic gneiss basement for the exploration discovery well 31/6-1, drilled at the high crest of a fault block on the Horda Platform in July 1983. Sørensen and Tangen (1995) described an exploration dry well targeting Jurassic units, 26/4-1, which was drilled in May-June 1987 in the western side of the Stord Basin. This well reached the upper part of the Triassic unit (Norwegian Petroleum Directorate, 2017). In June 2011, the 31/8-1 exploration well was drilled in the Stord Basin south of the Troll Field, to prove hydrocarbon presence in the Upper Jurassic Sognefjord and Lower to Middle Jurassic Johansen Formation (Dunlin Group). Biostratigraphy results showed that the well did not penetrate the upper Brent Group, and it resulted in water-bearing reservoirs with no reported oil shows (Norwegian Petroleum Directorate, 2017).

The Cretaceous play in the northern Stord Basin has received little attention, as the sediments were deposited during the post-rift stage and the underlying source rocks are inferred to be immature. The play also presents a challenge for exploration since these types of post-rift traps are commonly "subtle" four-way closures or difficult pinch-out traps (Gabrielsen *et al.*, 1995). Nevertheless, the Cretaceous play works in the Moray Firth Basin (Oakman, 2005), the northeastern North Sea Agat discovery, and the Gjøa Field area (Bugge et al., 2001), which have similar Cretaceous post-rift strata (Figure 1). According to Copestake *et al.* (2003), the

majority of hydrocarbon-bearing reservoirs in the Lower Cretaceous are in sandstones deposited in deep-water and mass-flow settings, except for the Tuxen Formation of the Danish sector. In contrast, most hydrocarbon-bearing reservoirs in the Upper Cretaceous are within chalk deposits in the Norwegian Sector (Surlyk, 2003). An important element for the Cretaceous play is the reservoir distribution.

According to Gabrielsen *et al.* (2001), the most important factors in reconstructing a post-rift depositional model to determine sandstone distribution are (paleo-) water depth and basin floor geometry. Thus, there is a need for improved understanding of the evolving depocenters and discontinuities of the Cretaceous play. The propose of this thesis is to analyze the potential of the Cretaceous play in the northern Stord Basin by using sequence stratigraphic methods, which may reveal prospective hydrocarbon intervals in a relatively underexplored area within a mature hydrocarbon basin.

1.1 OBJECTIVES

The primary objective of this thesis is to identify the tectonostratigraphic evolution of Cretaceous units in the northern Stord Basin, in order to gain understanding of the dynamics of Cretaceous units, erosion, and preservation of sedimentary strata. Furthermore, the objective is to build a sequence stratigraphic framework with identification of regionally important surfaces and units. The study uses state-of-the-art 3D broadband seismic data from the CGG Services (Norway) AS, which is complimented by 2D regional seismic lines from the TGS-NOPEC. The integration of 3D seismic stratigraphic interpretation, geomorphology tied to key well data, and interpretation of 2D seismic lines, define the gross stratigraphic architecture (specifically the stacking patterns of clinoform sets) and enables further subdivision of the sequences. It also helps in developing an understanding of the vertical and horizontal distribution of the reservoir and seal pairs as well as potential trapping candidates. Seismic attributes and isochore maps are important in predicting the depocenters through time. Finally, paleogeographic reconstructions aid in play mapping for the Cretaceous succession.

3

1.2 PREVIOUS STUDIES

Over the past decades, the northern North Sea has been comprehensively studied, especially the Viking Graben, one of the major Mesozoic rift basins. Yet, studies from the northern Stord Basin are limited. The study by Ågotnes (2016) focuses on the evolutionary model of the Stord Basin, concentrating on the Permian-Triassic rifting phase by using seismic interpretation of deep (9s TWT) 2D seismic lines. This work highlighted the first Permian-Triassic rifting phase that generated major displacements along the faults. It also established that the geometry and orientation of later Permian-Triassic faults in the Stord Basin were influenced by the Hardangerfjord Shear Zone and the Utsira Shear Zone, classifying this basin as a structural domain.

Sørensen and Tangen (1995) analyzed exploration plays in some marginal basins, including the Stord Basin. They identified the Late Jurassic Tau Formation and the Drake Formation (Toarcian shales) as potential Mesozoic source rocks in the Stord Basin. The main issue in this area is the maturation level of source rocks, due to restricted burial. However, the Tau Formation is deep enough for limited oil and gas generation in the central parts of Quadrant 26 (Sørensen and Tangen, 1995). The main reservoir intervals at Mesozoic level in this basin are expected from the Jurassic sequence. The minimum risk plays are rotated Jurassic fault blocks connected to potential locally mature kitchen areas, and maximum risk plays are Paleozoic level, since well data is limited in the Stord Basin.

Another study in the Stord Basin, conducted by Biddle and Rudolph (1988), focused on structural inversion during the Early Tertiary. Inversion is verified by the position of hanging-wall folds, which is parallel to the strike of reactivated faults. These structures occurred as the product of Alpine continent-continent collision and the opening of the North Atlantic Ocean. Jordt *et al.* (1995) investigated the tectonic development, sediment distribution and provenance area of Cenozoic interval in the central and northern North Sea. They explained that the changes in provenance areas and regional tectonic movements affected the development of Cenozoic depositional sequences in the North Sea. Moreover, the formation of depositional sequences and sequence boundaries occurred independently of eustatic sea-level changes.

There are no studies of the Cretaceous strata in the Stord Basin, but Cretaceous units deposited in other areas within the North Sea have been studied before. Oakman (2005) described the Lower Cretaceous play in the Moray Firth Basin (central North Sea) and Viking Graben (northern North Sea). The study explored the most significant Lower Cretaceous Aptian-Albian play in the Moray Firth Basin, and suggested depositional models depict sandstone distribution of proven Early Cretaceous units. He highlighted two depositional model concepts in Cretaceous units of the central North Sea, which are, Paleocene sands (Figure 2a) and a "Jurassic-upwards" pattern (Figure 2b). The Paleocene sands distribution shows that the sands are able to travel long distances via sub-basin fill and spill. The "Jurassic-upwards" pattern shows that sediment could not travel long distances from its provenance, so the sand units are from local intra-basins or highs (proximal to the basin). These concepts are reliable in predicting sand distribution at certain intervals, *e.g.*, the "Jurassic upwards" technique is used for the lowermost Cretaceous units, whereas, the Paleocene sands pattern is useful for the Upper Cretaceous sediments. The Agat sandstone (Lower Cretaceous) is also believed to be more like Paleocene sands (Figure 2a).

Bugge et al. (2001) described the Cretaceous strata in the northeastern North Sea recording significant tectonic activity. They highlighted that the Late Jurassic rifting probably continued into the Early Cretaceous, followed by minor tectonic episodes with basin floor subsidence and uplift of basin flanks and local highs. They identified several sandstone formations in the Cretaceous interval, *e.g.*, Åsgard, Agat, Tryggvason, and Kyrre formations. The Åsgard Formation sandstones (Ryazanian-Barremian) were sourced from uplifted and eroded areas within the basin and basin flanks; the Agat Formation (Albian) was deposited in a paleogeographic slope setting; while the Tryggvason (Early-Middle Turonian) and the Kyrre sands (late Turonian-Coniacian) were deposited after topography infill and are related to tectonic tilting events (Bugge *et al.*, 2001).
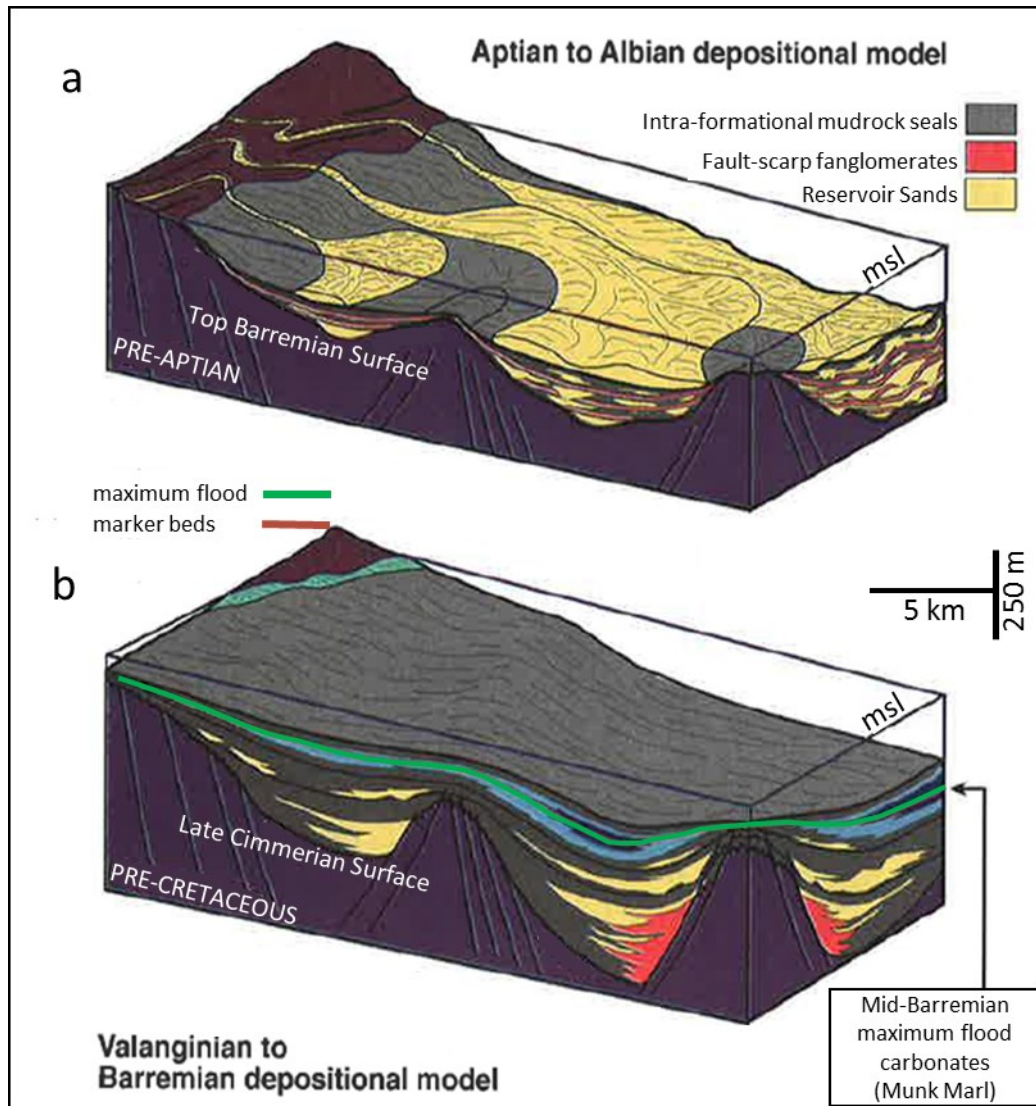
Figure 2: Sand distribution model in early Cretaceous units, which are, (a) Paleocene sands pattern, and (b) Jurassic-upwards (modified from Oakman, 2005). The Paleocene sands pattern corresponds to the Aptian-Albian depositional model, where the sands were able to travel long distances via sub-basin fill and spill. The Jurassic-upward pattern is related to the Valanginian-Barremian depositional model, where the sands could not travel long distances and the sediment source areas were from local highs.

Genaro *et al.* (2013) studied the syndepositional geomorphological characteristics of the Chalk Group (Late Cretaceous to Early Paleogene) in the Norwegian Central Graben by integration of regionally extensive 3D seismic data and numerous wells. The inversion tectonic and halokinetic forces have reshaped the morphology of the Norwegian Central Graben Basin

influencing the style of chalk sedimentation. Furthermore, bottom currents, sea level fluctuations and environment changes also affected the chalk depositional system. Das (2015) used 3D seismic stratigraphy and geomorphology to determine the depositional setting and specific seismic facies of the Central Graben Chalk Group. Eventually, she concluded that sea-level fluctuations, halokinetic and inversion tectonic activities, as well as bottom current circulations affected deposition of the Chalk Group in the Central Graben. Zanella and Coward (2003) reported that significant Late Cretaceous inversion structures only occurred in the southern part of the Central Graben (Danish sector), while the impact of inversion decreased northwards through the central North Sea.

Zachariah *et al.* (2009) concluded that local basin physiography strongly affected the Cretaceous post-rift stratigraphy during the Lower to Mid-Cretaceous in the northern Viking Graben. They interpreted the timing of syn-rift to post-rift transition as intra-Volgian age, by integrating 3D seismic and well data. Therefore, the BCU (Base Cretaceous Unconformity) reflection could not be used to represent the onset of post-rift, as it was a complex unconformity resulting from combined syn-rift and post-rift on the footwall crests, and a conformable contact in the grabens.

Gabrielsen et al. (2001) highlighted the post-rift basin configuration of the northern North Sea. They defined three phases of post-rift Cretaceous evolution of the northern North Sea: the incipient (Ryazanian-Latest Albian), the middle (Cenomanian-Late Turonian), and the mature (Early Coniacian-Early Paleocene). During the incipient post-rift, the inherited structures of the previous syn-rift stage had a large impact on sediment distribution. While in the middle stage, sediments continuously filled the internal basin relief. Eventually, the main structural features inherited from the syn-rift basin were completely covered by sediments in the mature post-rift phase due to subsidence cessation.

2. REGIONAL GEOLOGY

The northern North Sea is characterized by fault block rotation and is rigid compared with the central North Sea, which is influenced by Zechstein Salt deformation (Zanella and Coward., 2003). In the northern North Sea, a large pre-Permian (Devonian) basin formed due to gravitational collapse resulting from a thickened crust (McClay *et al.,* 1986). Zanella and Coward (2003) postulated that this was controlled by the pull-apart structure of Midland Valley-Solund fault zones in the south-east and the Great Glen-Møre-Trøndelag fault systems in the north-west.

This is supported by paleomagnetic data (Torsvik *et al.,* 1996), verifying the relatively lateral movement between Baltica and Laurentia during the Devonian. According to Beach *et al.* (1987), the main extension direction in the northern North Sea during the Triassic was north-west to south east; whereas Fossen *et al.* (2016) reported the extension direction of Permo-Triassic rift-related faulting in the North Sea as east-west.

The rift configuration in the North Sea is significantly affected by the pre-rift basement arrangement, which is oblique to the rift extension (Fossen *et al.*, 2016). Fossen *et al.* (2016) suggested the Øygarden Fault System, a west-dipping fault in the eastern part of Stord Basin, is proof of this. The fault dip changes direction towards the east and returns to west-dipping east of the Troll Field (Figure 3). The Hardangerfjord Shear Zone in the southern section also controls the continuity of the Øygarden Fault System. The combination of the Øygarden Fault System and the linked fault system along the east side of the Utsira High establishes the Stord Basin as a relatively isolated basin (Fossen *et al.,* 2016).

2.1 STRUCTURAL EVOLUTION

The northern North Sea experienced tectonic activity during pre-Triassic to Triassic rifting, Middle Jurassic to Early Cretaceous rifting, and Tertiary to Quaternary uplift. The oldest strata are uncertain due to limited well information (Biddle and Rudolph, 1988). Sørensen and Tangen (1995) inferred that several deep reflectors identified on the 2D seismic lines are probably Devonian in age, the same age as the adjacent onshore Hornelen Basin. Biddle and Rudolph

(1988) recognized active normal faulting of Triassic strata, represented by the expansion of the Triassic units on the hangingwall (Figure 4a and 4b). The 26/4-1 well calibrates the seismic interpretation and confidently distinguishes the Mesozoic interval (Sørensen and Tangen, 1995). However, the period of extensional tectonics within the Triassic is unclear due to a limited data set.
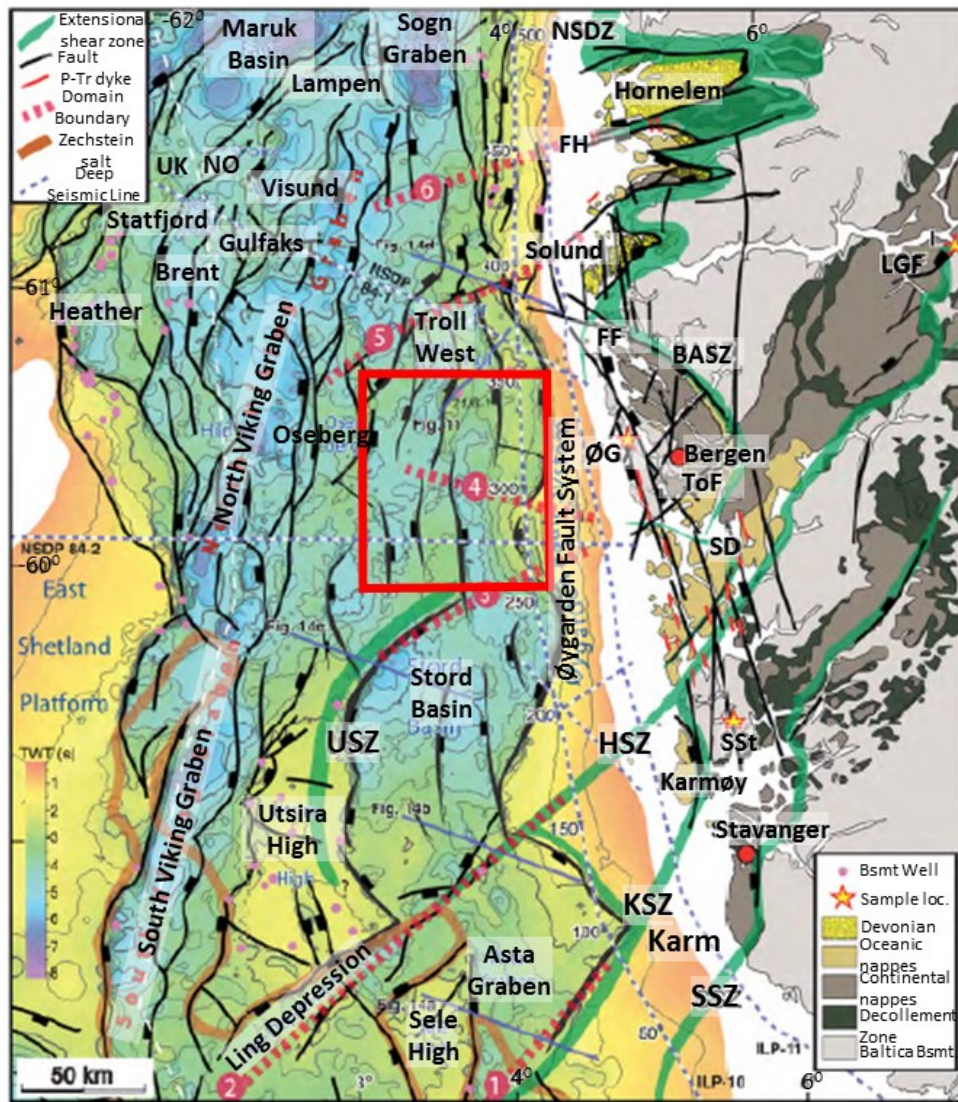
Figure 3: The top basement map (strata older than Permian is considered basement) of the northern North Sea Rift. The Øygarden Fault System is composed of two large west dipping segments and one small east dipping segment. The study area is highlighted as a red square on the map (modified from Fossen et al., 2016). FF, Fensfjord Fault; FH, Florø Horst; SSZ, KSZ, HSZ and BASZ, Stavanger, Karmøy, Hardangerfjord, and Bergen Arcs shear zones; NSDZ, Nordfjord–Sogn Detachment Zone; LGF, Lærdal–Gjende Fault; SD, Sunhordland Detachment; ToF, Totland Fault; USZ, Utsira Shear Zone; P–Tr, Permo-Triassic.
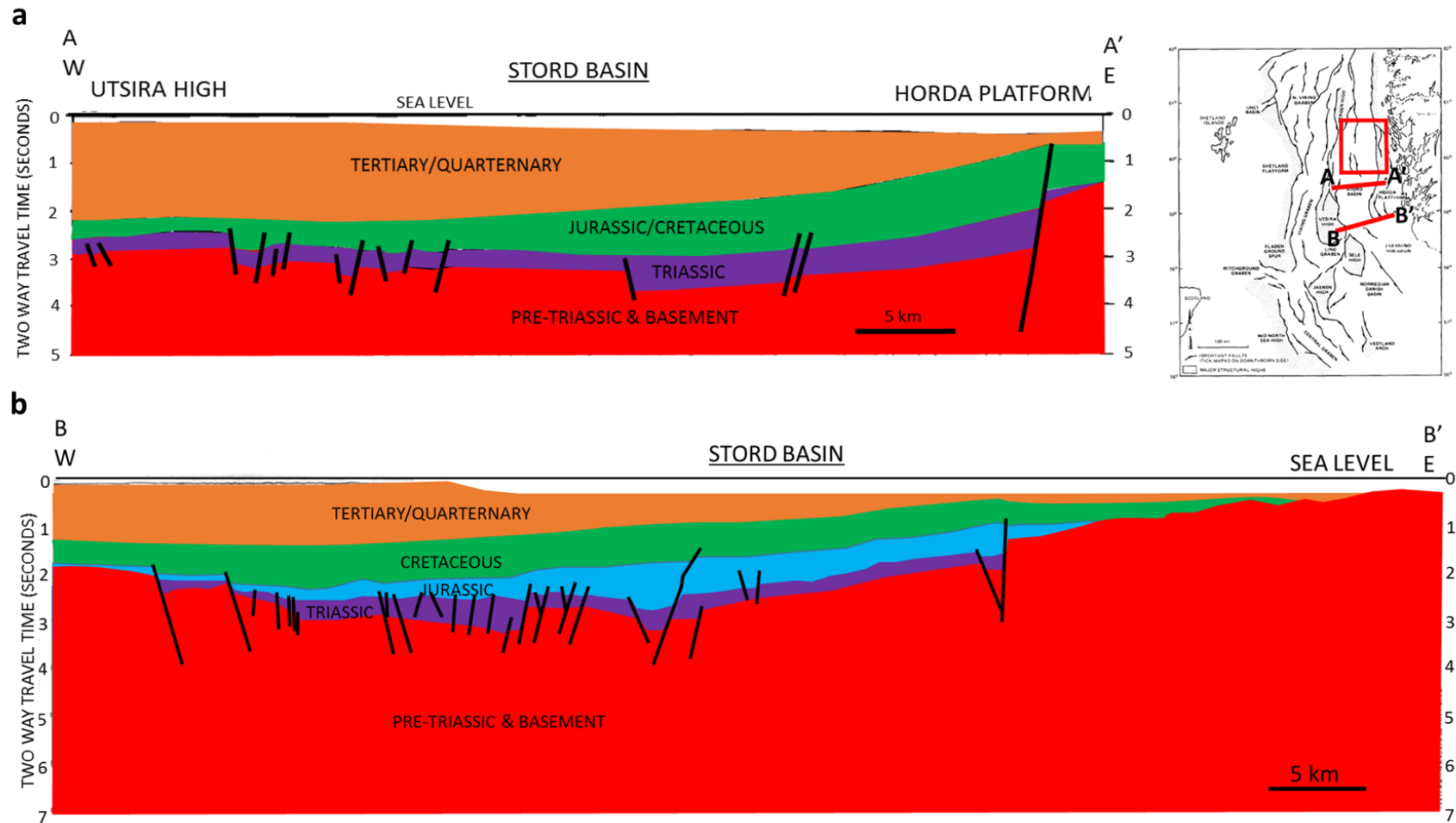
Figure 4: (a) Schematic cross section in the central part of the Stord Basin and (b) Schematic cross section in the southern part of the Stord Basin (modified from Biddle and Rudolph, 1988). Notice, the location of the study area is in the north of the Stord Basin, highlighted in red polygon on the inset map.

Additionally, Ågotnes (2016) concluded that throw accumulations during the Permian-Triassic rifting stage were higher than the throw from other extensional stages in the Stord Basin. These inherited structures controlled the structural and depositional setting of the basin. He also described the isolation of the Stord Basin to the south that occurred during the Permian-Triassic rifting phase.

Extensional tectonics also occurred during the Middle Jurassic, which resulted in reactivation of pre-existing normal faults and simultaneous generation of new faults (Figure 4; Biddle and Rudolph, 1988). The movement of growth faults and local depositional basins created thickness variations in Middle Jurassic sediments (Sørensen and Tangen, 1995). The displacement of these faults decreased upward to the lower part of Upper Jurassic units (Figure 4a and 4b). In the Upper Jurassic, the basin experienced tectonic quiescence similar to the Åsta Graben, (Sørensen and Tangen, 1995). In addition, Biddle and Rudolph (1988) ascribed the sag-like appearance as related to subsidence due to the decay of heat-flow during the Late Jurassic that continued during the Cretaceous until Early Tertiary. Coward *et al.* (2003), described the re-activation of normal faults that continued into the earliest Cretaceous and ceased in the Early Cretaceous, when minor fault reactivation occured due to sediment compaction. The reverse displacement of older normal faults, in the Early Tertiary and Quaternary uplift of the Norwegian mainland, was recognized as the last tectonic activity in the Stord Basin (Figure 4b; Biddle and Rudolph, 1988). They highlighted that the Quaternary uplift resulted in a westward tilt in the eastern part of the basin. This tectonic activity contributed to the formation of truncated features due to erosion of subaerial highs.

As mentioned earlier, Gabrielsen *et al.* (2001) divided the post-rift phase during the Cretaceous in the northern North Sea into three stages: the incipient, the middle, and the mature stage. They identified the Ryazanian-latest Albian incipient stage from previous syn-rift phase structures that controlled the basin arrangement and sediment supply. The middle stage occurred during Cenomanian-Late Turonian and was characterized by the geometries of the foregoing structural features. These structures were continuously drowned since the rate of subsidence is lower than the rate of sediment supply (Gabrielsen *et al.,* 2001). Finally, the Early Coniacian-Early Paleocene mature stage was inferred by a wide, saucer-shaped basin, where extra-basinal processes influenced basin infill and subsidence ceased.

2.2 CRETACEOUS LITHOSTRATIGRAPHY

According to Isaksen and Tonstad (1989), Cretaceous lithostratigraphy consists of two main groups: the Cromer Knoll and Shetland Group. They suggested the age of the Cromer Knoll Group is Late Ryazanian to Albian/Early Cenomanian and was deposited in an open marine environment (with low energy). This group comprises six formations in the Norwegian sector: the Åsgard, Tuxen, Mime, Sola, Rødby, and Agat formations. The Shetland Group is characterized by a siliciclastic facies in the northern North Sea and a chalk facies in the central North Sea. This group was deposited in an open marine environment during the Cenomanian to Danian, where the siliciclastic influx was limited until the Late Cretaceous. The Shetland Group consists of four chalk facies (the Hidra, Hod, Tor and Ekofisk formations) and six siliciclastic facies (the Svarte, Blodøks, Tryggvason, Kyrre, Jorsalfare, and Hardråde formations). According to the lithostratigraphy chart from NPD (2017), there are only four formations during the Early Cretaceous (Åsgard, Mime, Sola, and Rødby) and five formations during the Late Cretaceous (the Svarte, Blodøks, Tryggvason, Kyrre, and Hardråde) at Horda Platform (Figure 5). Since the focus of this study is in the northern North Sea area and the chalk facies are assumed absent in this area, only the siliciclastic facies will be considered in the Shetland Group subchapter.

2.2.1 The Cromer Knoll Group

The oldest Cretaceous formation is the Åsgard Formation (Figure 5), which is restricted to Early Cretaceous basins. The thickness of this formation varies: ~300 m in the northern Viking Graben, ~700 m in the Åsta Graben, and more than 1200 m in the Sogn Graben (Isaksen and Tonstad, 1989 and Bugge *et al.*, 2001). The characteristic lithology of this formation is light to dark grey calcareous claystones, light greenish-grey marlstones and stringers of limestone, where the quantity of glauconite, pyrite, and mica are common. The Åsgard Formation was deposited in a low-energy shelfal marine environment during the Late Ryazanian to Late Hauterivian (if the Tuxen Formation exists) and may extend to the Late Aptian to Early Albian (where either the Tuxen or the Sola Formation occurs) as considered by Isaksen and Tonstad (1989). Bugge *et al.* (2001) described the depositional environment of the Åsgard Formation

in the northeastern North Sea as a deep marine environment with a Late Ryazanian to Barremian depositional age.

The Tuxen Formation (Figure 5) is characterized by white to greyish-pink, calcareous claystones, and marlstones dominated by pelagic marls and chalk (Isaksen and Tonstad, 1989). This formation was deposited during the Late Hauterivian to Late Barremian, and its thickness varies from 1 m at highs to 100 m in the basins (Isaksen and Tonstad, 1989). Moreover, the Tuxen Formation interfingers parallel with claystones and marlstones of the Åsgard Formation in basinal areas of the Norwegian sector.

The Mime Formation (Figure 5) is indicated by white or light pink limestones and marls with smaller quantities of sand and silt, deposited in a transgressive shallow marine setting during the Late Valanginian to Albian (Isaksen and Tonstad, 1989). The thickness of this formation is shown to be 11 m, by the 34/10-18 well (well type), and 42 m, by the 17/4-1 well (well reference).

The Sola Formation (Figure 5) is composed of black or dark grey, finely laminated, pyritic and highly radioactive shales interbedded with stringers of limestone and marlstone. The thickness of this formation is between 20 and 200 m (Isaksen and Tonstad, 1989). Furthermore, Bugge *et al.* (2001) reported 90 m thick Aptian sediment in the westernmost Agat wells, in the northeastern North Sea. The Sola Formation onlaps and pinches out along the basin margin. The age of the Sola Formation is Mid-Aptian to Early Albian and was deposited in a marine environment with alternating oxic and anoxic bottom conditions (Isaksen and Tonstad, 1989). Moreover, Bugge *et al.* (2001) highlighted this formation was deposited during maximum flooding of the basin. They also mentioned that dark shales of this formation correspond to the organic-rich clays of the Fischschiefer in Germany. This suggests that the Sola Formation is a potential source rock.

The Rødby Formation (Figure 5) consists of red-brown marlstones with occasional glauconite and pyrite. This formation is typically 15-30 m thick, but it may reach more than 200 m in the Viking Graben (Isaksen and Tonstad, 1989). The depositional environment of the Rødby Formation is open marine and oxygenated with limited clastic sediment supply during the Albian (Isaksen and Tonstad, 1989). Additionally, Bugge *et al.* (2001) observed that the Rødby

Formation in the northeastern North Sea represents a more oxygenated setting, characterized by a gradual decrease in the radioactivity levels of background shales.

The Agat Formation (Figure 5) is identified by white to light grey, fine- to medium-grained sandstone, containing mica and glauconite with small amounts of pyrite. The thickness of this formation varies from 240 to 400 m (Isaksen and Tonstad, 1989). The Agat Formation was deposited during the Aptian to Albian (possibly Early Cenomanian) by debris flows and turbidity currents in a paleogeographic slope setting (Isaksen and Tonstad, 1989; Bugge *et al.*, 2001). Additionally, Oakman (2005) revealed the Aptian-Albian play, which is part of the most significant play in the central and northern North Sea that was deposited as a submarine fan in slope to basinal settings. He suggested that the sands could travel long distances via sub-basin fill and spill, especially if channelized, towards the low depositional area. Contrastingly, Bugge *et al.* (2001) explained that local slumping and sliding, indicated from seismic data in the northeastern North Sea, could have generated accommodation space for deposition of isolated sandstone bodies tens of meters thick.

2.2.2 The Shetland Group

The Svarte Formation (Figure 5) is characterized by medium to light grey, calcareous mudstones, interbedded with white to medium grey limestones, and contrasts with the clear to light grey sandstones that exists in the Agat area. The thickness of this formation is between 188 and 240 m in several wells of the Viking Graben, and the formation was deposited in an open marine environment during the Cenomanian (Isaksen and Tonstad, 1989).

The Blodøks Formation (Figure 5) is composed of red, green, grey, and black shales and mudstones with a low content of carbonate. The thickness is 7–28 m in several wells, but rarely exceeds 20 m (Isaksen and Tonstad, 1989). Bugge *et al.* (2001) described this formation as a strong and continuous reflection on seismic data, due to high impedance contrast, even though the thickness is below seismic resolution. The age of the Blodøks Formation is Latest Cenomanian to the Early Turonian, and it was deposited during a period of anoxic bottom conditions (Isaksen and Tonstad, 1989). This formation is associated with a condensed section

of organic-rich clay, which has source rock potential (Bugge *et al.,* 2001; Copestake *et al.,* 2003).

The Tryggvason Formation (Figure 5) is marked by light to dark grey, calcareous mudstones, interbedded with white to light grey, argillaceous limestones. The interbedded fine- to very fine-grained sandstones are common in the Agat area. The thickness of this formation is 145-326 m in the Viking Graben and 45 m on the western margin of the Horda Platform. It was deposited in an open marine environment during the Early to Mid-Turonian (Isaksen and Tonstad, 1989). Bugge *et al.* (2001) observed semi-concentric arcs in clay- and ooze-dominated sediments of the upper part of the Tryggvason Formation from attribute analysis. They interpreted these patterns as water escape structures or compaction patterns in, for instance, the Eocene Shales in the North Sea. They also stated that the onlap geometries on the upper part of the Blodøks Formation represent tectonic tilting related to basin-floor subsidence and basin flank uplift.

The Kyrre Formation (Figure 5) consists of medium grey to grey, silty to calcareous mudstones with rare limestone beds. Several fine- to very fine-grained sandstones are found in the Agat area. The well thickness of this formation varies between 270 and 1199 m, and was deposited in an open marine environment during the Late Turonian to Campanian (Isaksen and Tonstad, 1989). Furthermore, Bugge *et al.* (2001) described the depositional environment of this formation as deep marine in the Sogn Graben and the northern Viking Graben, and shallower in the eastern area of the Viking Graben. They suggested that the sandstones were deposited as submarine fan units within a transgressive and back-stepping trend. The prominent onlap features on top of the Tryggvason Formation in the northeastern North Sea, suggest another episode of tectonic tilting during the Late Turonian (Bugge *et al.,* 2001).

The Jorsalfare Formation (Figure 5) is composed of light to medium grey, calcareous mudstones, interbedded with thin, white to light grey, fine-grained limestones. This formation was deposited in an open marine environment during the Late Campanian to Maastrichtian, with recorded thickness in several wells between 145 and 365 m (Isaksen and Tonstad, 1989). Bugge *et al.* (2001) divided this formation into two parts: lower transgressive and upper regressive. Also, they implied that the basin flanks in the east of the northeastern North Sea were exposed at the end of the Cretaceous period, which is indicated by thinning and erosion.

The Hardråde Formation (Figure 5) is characterized by interbedded white or pale limestones and medium to light grey calcareous mudstones. The thickness of this formation in several wells varies from 10 to 291 m, while it is absent in the Troll area (Isaksen and Tonstad, 1989). The depositional environment of the Hardråde Formation is an open marine setting deposited during the Late Campanian to Maastrichtian (Isaksen and Tonstad, 1989).
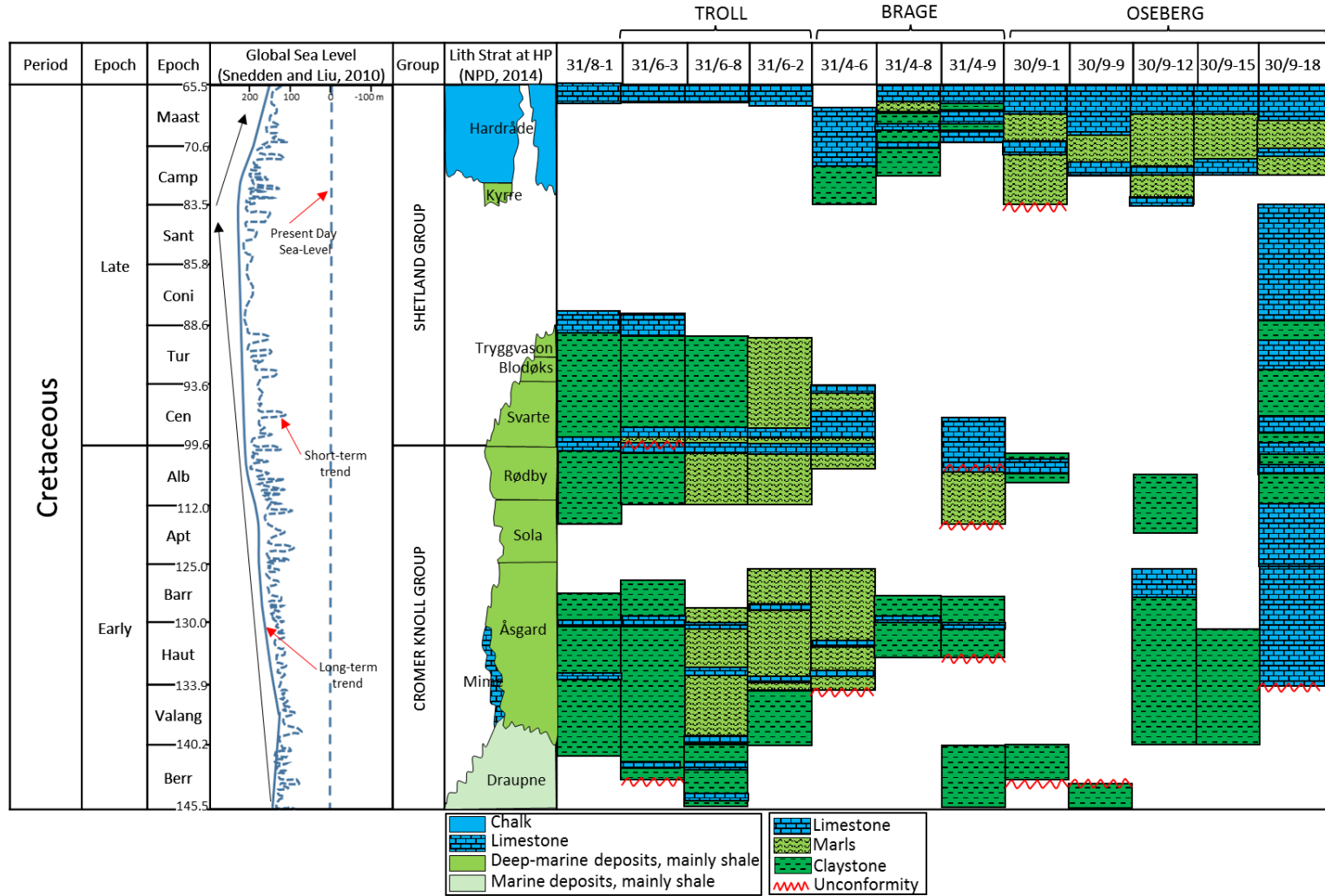
Figure 5: The Chronogram of several wells in the area around the northern Stord Basin (Troll, Brage and Oseberg Fields), lithostratigraphy chart from the Horda Platform (HP) and global sea level during the Cretaceous time. Generally, the global sea-level rise occurred during the Cretaceous, which is represented by the global sea-level curve. There are several time gaps observed from the chronogram, which are, the Berriasian-Valanginian, the Aptian, and the Coniacian-Campanian. The potential of the condensed section period is during the Aptian and the Coniacian-Campanian. The global sea-level is based on Snedden and Liu (2010). The lithostratigraphy chart follows NPD (2017). The location of the wells is shown in Figure 18.

17

3. SEQUENCE STRATIGRAPHY

Sequence stratigraphy is frequently applied as an analytical tool to examine the lateral and vertical evolution of stratigraphic successions, and is used as a predictive tool in the oil and gas industry. Van Wagoner *et al.* (1988) defined sequence stratigraphy as "*the study of rock relationships within a chronostratigraphic framework of repetitive, genetically related strata bounded by surfaces of erosion or nondeposition, or their correlative conformities.*" They proposed division of sedimentary layers into sequences, parasequences, and systems tracts. This provides a reliable method for describing sedimentary strata, building a framework for correlating and mapping facies, and interpreting the depositional environment.

Emery and Myers (2009) described sequence stratigraphy as "*the subdivision of sedimentary basin fills into genetic packages bounded by unconformities and their correlative conformities.*" They explained that the function of sequence stratigraphy is to provide the chronostratigraphic framework to determine the vertical and lateral distribution of sedimentary facies, thereby predicting the stratigraphy.
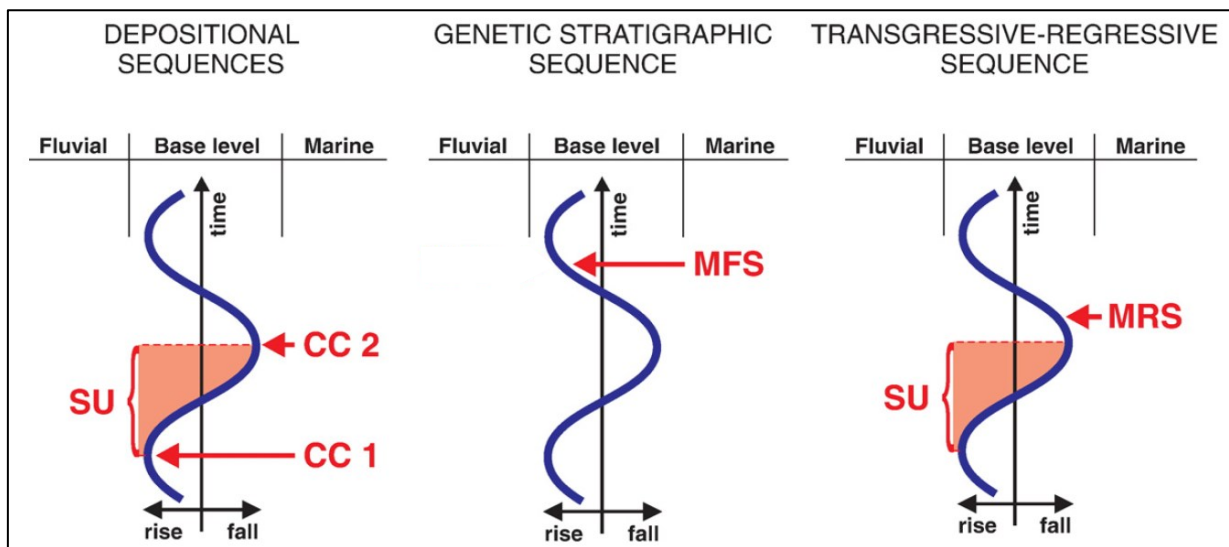
Figure 6: Three models of sequences (Catuneanu et al., 2009), which are, the depositional sequences (Posamentier et al., 1988), the genetic stratigraphic sequence (Galloway, 1989), and the transgressive-regressive sequence (Vail et al., 1977). Each sequence has different sequence boundaries. Abbreviations: SU — subaerial unconformity; CC 1 — correlative conformity sensu Posamentier and Allen (1999); CC 2 — correlative conformity sensu Hunt and Tucker (1992); MFS — maximum flooding surface; MRS — maximum regressive surface.

Catuneanu *et al.* (2011) described sequence stratigraphy as "*a methodology that provides a framework for the elements of any depositional setting, facilitating paleogeographic reconstructions and the prediction of facies and lithologies away from control points.*" The stacking pattern changes are controlled by the variation in sediment supply and the accommodation space at the time. They also concluded that the sequence stratigraphy framework facilitates interpretation of the depositional system evolution through time and space.

Events and stages (Sequence model)	Depositional Sequence I	Depositional Sequence II	Depositional Sequence III	Depositional Sequence IV	Genetic Sequence	T-R Sequence
HNR		HST	early HST	HST	HST	RST
end of T					— MFS —	
T	Sequence	TST	TST	TST	TST	TST
end of R						— MRS —
LNR		late LST (wedge)	LST	LST	late LST (wedge)	
end of RSL fall		- - - - -	— CC** —		- - - - -	
FR		early LST (fan)	late HST	FSST	early LST (fan)	RST
onset of RSL fall	— CC* —	— CC* —	- - - - -			
HNR		HST	early HST	HST	HST	

Legend:
— sequence boundary
— systems tract boundary
— within-sequence surface
- - - - - within-systems tract surface

BSFR — end of RSL fall — MFS — end of transgression — MRS — CC** — end of regression — onset of RSL fall

Figure 7: Summary of several approaches of sequence stratigraphy, modified from Catuneanu et al. (2011), showing the system tracks within one sequence and period of sequence boundaries. Abbreviations: HNR – highstand normal regression; T – transgression; LNR – lowstand normal regression; FR – forced regression; HST – highstand systems tract; TST – transgressive systems tract; LST – lowstand systems tract; FSST – falling-stage systems tract; RST – regressive systems tract; T-R – transgressive-regressive; BSFR – basal surface of forced regression; MRS – maximum regressive surface; MFS – maximum flooding surface; CC* – correlative conformity sensu Posamentier and Allen (1999); CC** – correlative conformity of Hunt and Tucker (1992); and RSL – relative sea-level.

Catuneanu *et al.* (2009) highlighted three types of sequences: depositional, genetic stratigraphic, and transgressive-regressive (T-R) sequences (Figure 6). The depositional sequence uses subaerial unconformities (negative accommodation) and their marine correlative conformities (positive accommodation) as sequence boundaries (Figure 7; Posamentier *et al.,* 1988); *i.e.,* negative accommodation is when the stratigraphic base level is located below the topographic profile, while positive accommodation is when the stratigraphic base level is above the profile. Galloway (1989) described the genetic sequence as a sequence bounded by maximum flooding surfaces (MFS), because MFS are easy to differentiate in all marine environments (Figure 7). The transgressive-regressive sequence is a composite sequence boundary that involves the marine portion of the maximum regressive surface and the subaerial unconformity (Figure 7).

3.1 SEISMIC STRATIGRAPHY

The basic principles of seismic stratigraphy were published synchronously with eustatic cycle charts (Vail *et al.,* 1977; Catuneanu, 2002). It was deduced that all stages of stratigraphic cyclicity were driven by global sea-level changes or eustasy. This concept was rapidly developed as the first generation of sequence stratigraphy, with the integration of well and outcrop data (Van Wagoner *et al.,* 1990; Catuneanu, 2002).

Catuneanu *et al.* (2011) highlighted that key stratigraphic surfaces can be used as systems tract boundaries since these surfaces mark changes in stratal stacking patterns. The basic types of stratal terminations (Figure 10), published with the evolution of seismic stratigraphy, facilitate in determining the configuration of seismic reflections (Mitchum at al., 1977; Mitchum and Vail, 1977; Catuneanu, 2002). The stratal termination terms have been applied in sequence stratigraphy to define the stacking pattern units and to produce characteristic features in identifying several surfaces and systems tracts (Van Wagoner *et al.,* 1988).

3.1.1 KEY STRATIGRAPHIC SURFACES

Key stratigraphic surfaces are the fundamental horizons bounding units with different stratal stacking patterns or genetic deposit types, *e.g.*, lowstand and highstand systems tracts, forced and normal regressive, and transgressive packages (Catuneanu *et al.,* 2009; Catuneanu *et al.,* 2011). These surfaces are significant in sequence stratigraphy analysis since they are related to different processes during the base level cycle. The following subchapters define the key stratigraphic surfaces.

SUBAERIAL UNCONFORMITY

The subaerial unconformity is a surface of erosion or nondeposition generated under subaerial circumstances by fluvial erosion or bypass, wind degradation, dissolution, pedogenesis, and karstification (Sloss *et al.,* 1949). Subaerial unconformities occur during base level fall, which will continuously extend basinward in a forced regression event. The forced regression causes fluvial processes to generate an erosional base level (Catuneanu, 2002). According to Hunt and Tucker (1992), the subaerial unconformity corresponds to a marine correlative conformity in the basin area, where the timing is related to the end of sea-level fall.

CORRELATIVE CONFORMITY

There are two interpretations of correlative conformity (Figure 7), which are based on Posamentier et al. (1988) and Hunt and Tucker (1992). Posamentier *et al.* (1988) defined the correlative conformity as a marine stratigraphic surface bounding the highstand normal regression and the lowstand forced regression, which means that this surface is located at the base of the basin floor fan. It represents the paleo-seafloor at the beginning of the forced regression event. The effect of Posamentier's concept is two sequence boundaries that will be intercepted within the area of forced regression (Hunt and Tucker, 1992). According to Hunt and Tucker (1992), this surface has the same meaning as 'basal surface of forced regression'.

Hunt and Tucker (1992) proposed the correlative conformity as a marine stratigraphic surface bounding the lowstand forced regression and the lowstand normal regression. This surface represents the paleo-seafloor at the end of the forced regression, correlating with the basinward

termination of the subaerial unconformity (Catuneanu, 2002). The correlative conformity can be identified at the top of the basin floor component in the deep marine depositional environment (Hunt and Tucker, 1992).

MAXIMUM FLOODING SURFACE (MFS)

The maximum flooding surface (Figure 7) is a stratigraphic surface that records the transition from transgression to highstand normal regression, and is also known as a downlap surface in shallow-water settings (Van Wagoner *et al.,* 1988; Galloway, 1989; Catuneanu *et al.,* 2011). This surface represents the paleo-seafloor at the end of the transgressive event and is overlaid by downlap features of the highstand clinoform deposits (Catunanu *et al.,* 2011). The maximum flooding surface forms during base level rise where the system shifts from a retrogradational to progradational trend.

MAXIMUM REGRESSIVE SURFACE (MRS)

The maximum regressive surface or transgressive surface (Figure 7) is a surface that separates the stacking pattern, from an underlying lowstand normal regression to an overlying transgression (Catuneanu *et al.,* 2011). This surface illustrates the paleo-seafloor at the end of the normal regression and occurs during base level rise where the system changes from coastal progradation to retrogradation (Catuneanu *et al.,* 2009).

TRANSGRESSIVE RAVINEMENT SURFACE (TRS)

The transgressive ravinement surface is a type of erosional surface that is affected by wave or tidal scouring in the coastal to shallow-marine area during the transgressive period (Swift, 1975; Allen and Posamentier, 1993; Catuneanu *et al.,* 2011). This surface merges with the maximum regressive surface and the maximum flooding surface, seaward and landward, respectively. Moreover, the surfaces are younger towards the basin and therefore diachronous in nature (Nummedal and Swift, 1987; Catuneanu *et al.,* 2011).

REGRESSIVE SURFACE OF MARINE EROSION (RSME)

The regressive surface of marine erosion is a subaqueous erosional surface that occurs during forced regressive periods by wave scouring of the shallow-water depositional system (Catuneanu *et al.,* 2011). The characteristic of this surface is younger in a basinward direction and, therefore, also diachronous in nature.

3.1.2 STRATAL STACKING PATTERNS

The stratal stacking patterns are defined by the geometries and facies relationships, which correspond to the sediment supply and accommodation (Catuneanu *et al.,* 2011). The stacking patterns can either be related to or independent of the shoreline. Shoreline-related stacking patterns occur during forced regression, normal regression, and transgression (Figure 8). The characteristics of forced regression (Figure 8a) is forestepping and downstepping of the shoreline, representing the impact of negative accommodation during phases of sea-level fall (Catuneanu, 2002). Normal regression (Figure 8b) is identified by forestepping and upstepping of the shoreline, depicting the influence of positive and overfilled accommodation during the early and late phases of sea-level rise (Catunenau, 2002). This pattern consists of lowstand normal regression (Figure 9A) and highstand normal regression (Figure 9B), which is primarily identified by the shape of the shoreline trajectory.

Transgression (Figure 8c) is shown by backstepping of the shoreline, the result of positive and underfilled accommodation (Catuneanu, 2002). Hansen and Hampson (2009) also used the shoreline and shelf-edge trajectories in determining the migration of the depositonal system through time.

Shoreline-independent stacking patterns form in the area—*i.e.,* sedimentation activities unaffected by shoreline changes—that can still be correlated regionally (Catuneanu *et al.,* 2011). For example, this stacking pattern can form by amalgamation of channel deposits in upstream-controlled fluvial settings, and channel confinement in deep-water settings (Catuneanu *et al.,* 2011).
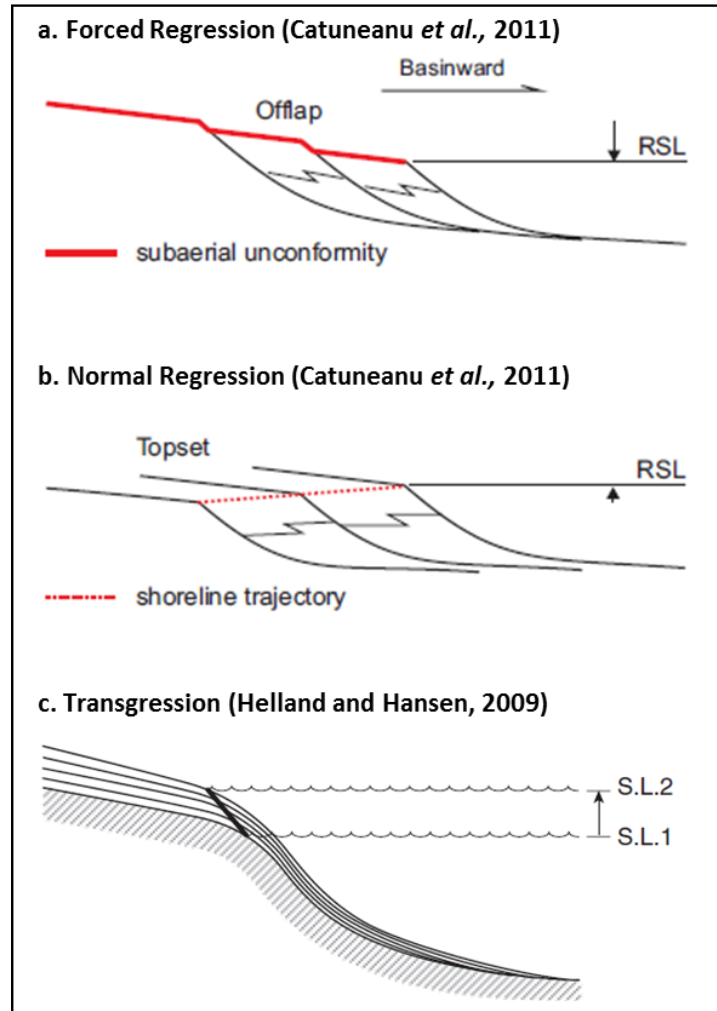
Figure 8: Shoreline-related stacking patterns from Catuneanu et al. (2011) and Helland and Hansen (2009), which consist of (a) forced regression, (b) normal regression, and (c) transgression. These stacking patterns are generated by shoreline shifts. Abbreviation: RSL – relative sea-level.

3.1.3 SYSTEMS TRACTS

A systems tract is defined by Brown and Fisher (1977) as *"a linkage of contemporaneous depositional systems, forming the subdivision of a sequence"*. A systems tract comprises a relatively conformable succession of strata bounded by unconformable or conformable sequence stratigraphic surfaces (Catuneanu *et al.,* 2011). The internal architecture of a systems tract varies from a succession of facies to a parasequence set. Changes of shoreline trajectory control the characteristics of the stacking patterns. There are five systems tracts that are commonly in use, interpreted by the interplay of sedimentation and base level changes.

FALLING-STAGE SYSTEMS TRACT (FSST)

The FSST (Figure 7) is the result of a forced regressive event and includes the sediments that accumulate after the initial relative base level fall, until before the next base level rise (Catuneanu *et al.,* 2011). This systems tract overlays the correlative conformity based on Posamentier and Allen (1999) and is capped by the Lowstand Systems Tract (LST) strata. In contrast, Hunt and Tucker (1992) put the correlative conformity on top of the falling-stage systems tract. This systems tract is age-equivalent to shallow marine sediments with rapidly prograding and offlapping stacking patterns (Hunt and Tucker, 1992). Catuneanu (2002) explained that the falling-stage facies depends on sea-level position relative to the shelf break.
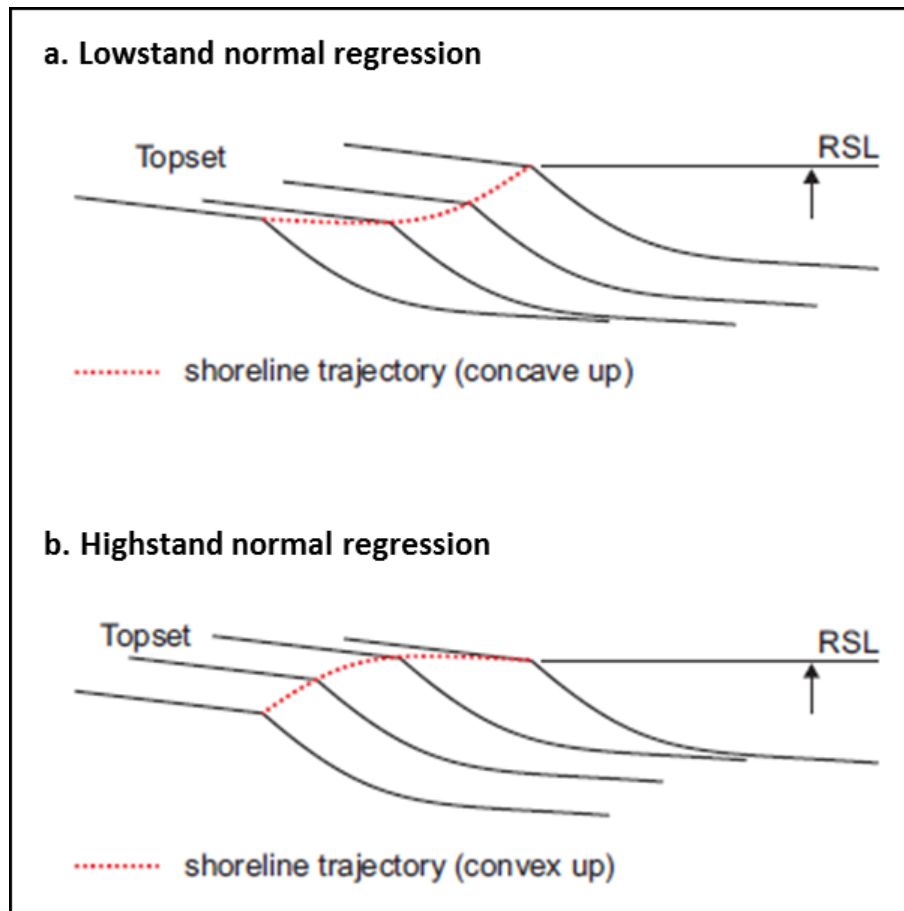
Figure 9: The two types of stratal stacking patterns of normal regressions, which can be differentiated by the patterns of shoreline trajectory (Catuneanu et al., 2011). (a) The concave up shoreline trajectory represents the lowstand normal regressions, while (b) the convex up shoreline trajectory indicates the highstand normal regressions. Abbreviation: RSL – relative sea-level.

LOWSTAND SYSTEMS TRACT (LST)

The LST (Figure 7) is formed during normal regression and is bounded at the base by the subaerial unconformity and the marine correlative conformity, and at the top by the maximum regressive surface (Catuneanu, 2002). This systems tract encompasses the accumulation of sediment during the beginning of relative base level rise. The LST is characterized by aggrading clinoforms that thicken downdip, with forestepping coastal plain, fluvial, and/or delta plain deposits as the topset sediments (Catuneanu *et al.,* 2011).

TRANSGRESSIVE SYSTEMS TRACT (TST)

The TST (Figure 7) consists of sediments generated during the beginning of the transgression to the maximum transgression of the coast, prior to the regression and deposition of the Highstand Systems Tract (described below; Catuneanu *et al.,* 2011). This systems tract is bounded at the base and top by the maximum regressive surface and the maximum flooding surface, respectively. The characteristics of the TST is retrogradational clinoforms correlated with condensed sections, backstepping, onlapping, and (potential) aggrading if the sediment supply is high enough (Galloway, 1989; Catuneanu *et al.,* 2011).

HIGHSTAND SYSTEMS TRACT (HST)

The HST (Figure 7) comprises deposits that are accumulated due to higher sediment supply than accommodation space during the final phase of relative base level rise (Catuneanu *et al.,* 2011). This systems tract lies above the maximum flooding surface and is covered by the subaerial unconformity and the correlative conformity, based on Posamentier and Allen (1999), or the basal surface of forced regression, based on Hunt and Tucker (1992). The characteristic of HST is prograding and aggrading clinoforms that thin downdip, where fluvial, coastal plain and/or delta plain deposits form the topset sediments (Catuneanu *et al.,* 2011).

REGRESSIVE SYSTEMS TRACT (RST)

An RST (Figure 7) is bounded by the maximum flooding surface at the base and by the maximum regressive surface above (Catuneanu, 2002). Typical sediments of this systems tract consist of HST, FSST, and LST (discussed above). The RST is a general term used for transgressive-regressive sequences and is applied when HST, FSST, and LST cannot be differentiated using subsurface data (Catuneanu *et al.,* 2011).

3.1.4 STRATAL TERMINATIONS

Emery and Myers (2009) described the reflection terminations as "*a two-dimensional seismic section by the geometric relationship between the reflection and the seismic surface against which it terminates".* The stratal termination is composed of downlap, onlap, toplap, truncation, and offlap (Figure 10). These terminations mostly represent shoreline shifts and sea-level changes (Catuneanu, 2002). Downlap (Figure 10) is termination of inclined strata against an initially horizontal or inclined surface (Mitchum *et al.,* 1977). It is diagnostic of normal or forced regressions (Catuneanu, 2002). Onlap (Figure 10) is termination of low-angle strata against a surface of greater initial inclination (Mitchum *et al.,* 1977). It may form in relation to transgression (Catuneanu, 2002). Toplap (Figure 10) is termination in the upper boundary of a depositional sequence, where the inclined strata forms (clinoforms) against an overlying lower angle surface (Mitchum *et al.,* 1977; Emery and Myers, 2009). The formation of toplap needs progradation of clinoforms with ideal bypass in the delta plain (Catuneanu, 2002). Erosional truncation (Figure 10) is the stratal termination against an erosional surface above it (Emery and Myers, 2009). Erosional truncation is characterized by the development of an angular unconformity or the development of erosional relief (Catuneanu, 2002). Offlap (Figure 10) is updip terminations of sedimentary units, where the progressive offshore shifts within a conformable sequence of rocks (Catuneanu, 2002). This termination is related to the forced regression during sea-level fall.
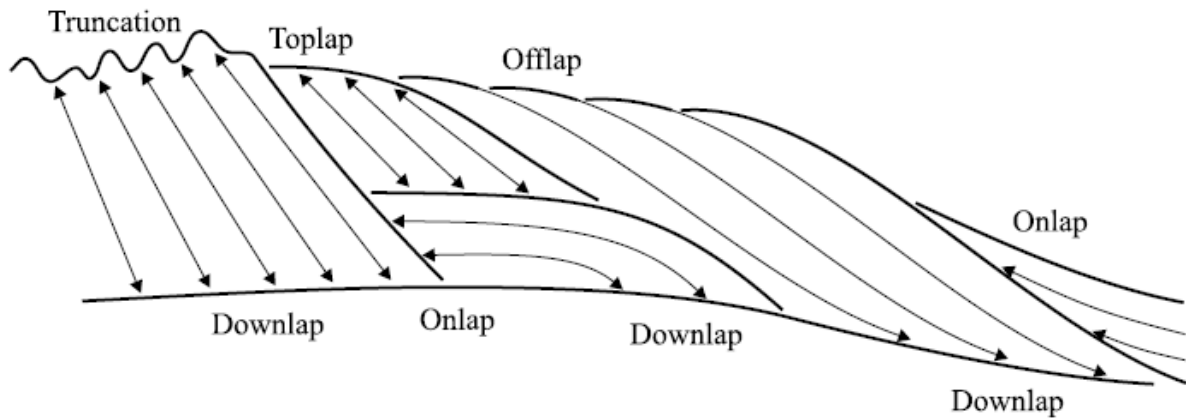
Figure 10: Modified stratal terminations from Emery and Myers (1996), in Catuneanu (2002). The arrows represent the position of surface dip compared to the dip of overlying strata.

3.1.5 PARASEQUENCES AND SEQUENCE HIERARCHY

Van Wagoner (1995) describes the parasequence as "*a relatively conformable succession of genetically related beds or bedsets bounded by flooding surfaces.*" The characteristic of parasequences is a regressive setting that generates a coarsening-upward sequence in shallow marine environments (Catuneanu, 2002).

Catuneanu (2002) explained that stratigraphic sequences are hierarchical and can be divided into different orders, depending on their relative importance. High-order sequences are more important, because these occur less frequently in the rock record, while low-order sequences are less important as these occur more frequently (Catuneanu, 2002). Miall (2010) highlighted that order level is useful when interpreting cycle frequency and in determining the cause of high or low frequency cycles. He also published a table to explain the stratigraphic cycles and their driving mechanisms and, finally, he compared them with definitions by several other authors (Table 1).

3.1.6 CLINOFORMS

Helland and Hansen (2009) ascribed the term clinoform to the complete sigmoidal 'topset-foreset-bottomset' depositional profile. A clinoform (Figure 11) has steeply dipping layers

28

(generally more than 1º) and expands basinward from the topset (Emery and Myers, 2009). The sediment caliber influences the slope angle, where a fine-grained deposit will build up a gentler slope than a coarse-grained deposit (Emery and Myers, 2009). Helland and Hansen (2009) divided clinoforms into two different systems, which are, shelf-slope-basin clinoforms and shoreline clinoforms. Shelf-slope-basin clinoforms occur on shelf margins and reach heights of several hundreds of meters or more. However, shoreline clinoforms include progradation of deltas, barrier-island shorelines and strandplains, but only reach up to a few tens of meters in height. Helland and Hansen (2009) also differentiated delta clinoforms into subaerial delta clinoforms and subaqueous delta clinoforms, based on the energy of the deltaic setting.

Table 1: The duration of sequence cycles and other terminology (Miall, 2010)

Sequence type	Duration (million years)	Other terminology
A. Global supercontinent cycle	200–400	First-order cycle (Vail et al., 1977)
B. Cycles generated by continental-scale mantle thermal processes (dynamic topography), and by plate kinematics, including:	10–100	Second-order cycle (Vail et al., 1977), supercycle (Vail et al., 1977), sequence (Sloss, 1963)
1. Eustatic cycles induced by volume changes in global mid-oceanic spreading centres		
2. Regional cycles of basement movement induced by extensional downwarp and crustal loading.		
C. Regional to local cycles of basement movement caused by regional plate kinematics, including changes in intraplate-stress regime	0.01–10	3rd- to 5th order cycles (Vail et al., 1977). 3rd-order cycles also termed: megacyclothem (Heckel, 1986), mesothem (Ramsbottom, 1979)
D. Global cycles generated by orbital forcing, including glacioeustasy, productivity cycles, etc.	0.01–2	4th- and 5th-order cycles (Vail et al., 1977), Milankovitch cycles, cyclothem (Wanless and Weller, 1932), major and minor cycles (Heckel, 1986)
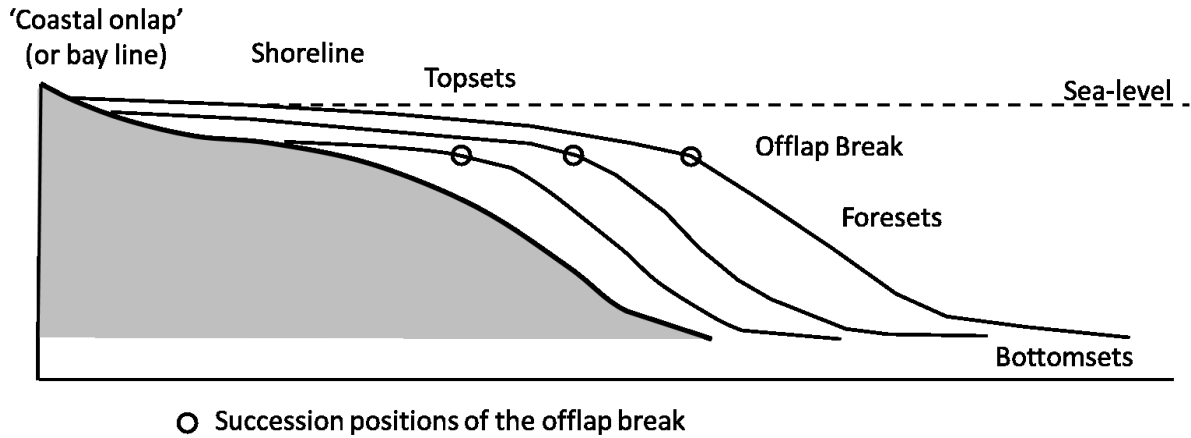
Figure 11: The prograding basin-margin unit profile consisting of topsets, foresets, and bottomsets (modified from Emery and Myers, 2009). The offlap break is the main break in the depositional profile, referring to the location between topsets and foresets.

3.2 CHRONOSTRATIGRAPHIC CHARTS

The objective of chronostratigraphic charts is to show the relationship between depositional systems in time and space and to surfaces of erosion, non-deposition, and condensation (Emery and Myers, 2009). The fundamentals of chronostratigraphic construction are the isochronous bedding planes, the seismic reflections representing bedding and time-line profiles. The period of the subaerial unconformity in the chronostratigraphic chart will be less towards the basin center than at the basin margin, while the duration of marine condensation in the chronostratigraphic chart is much longer towards the basin than towards the basin margin (Emery and Myers, 2009).

3.3 SEISMIC FACIES ANALYSIS

Mithcum *et al.* (1977) described seismic facies units as *"groups of seismic reflections whose parameters (configuration, amplitude, continuity, frequency, and interval velocity) differ from adjacent groups"*. Seismic facies can be used to identify facies and depositional environment (Emery and Myers, 2009). Roksandic (1978) highlighted the critical parameters in determining the reflection configuration, which comprise variations in continuity of reflections, amplitudes,

and frequencies. Figure 12 displays several types of reflection characteristics, which can be applied when interpreting sedimentary facies according to Roksandic (1978).

Ramsayer (1979) inferred that reflection geometry equals depositional geometry because reflections follow bedding planes. He also suggested that the internal reflection patterns of a sequence and their distribution could be used to interpret depositional environments, facies unit, and possible reservoir rocks. Hence, the seismic section has a function as a true chronostratigraphic correlation tool. However, seismic facies interpretation should be calibrated to well data because certain types of seismic reflections can be interpreted as several depositional environments.
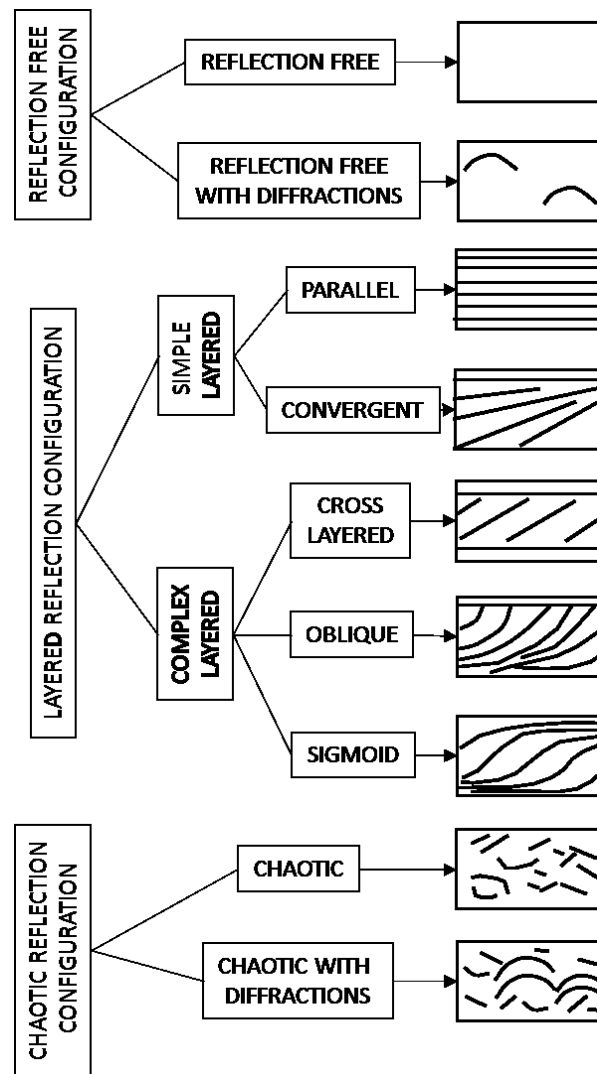
Figure 12: The basic types of reflection configuration in seismic facies analysis (Roksandic, 1978). Reflection free, layered and chaotic reflection forms can be utilized in analyzing sedimentary facies.

4. DATA AND METHODS

This study uses state-of-the-art 3D broadband seismic data from CGG Services (Norway) AS, which is complemented by 2D regional seismic lines from TGS-NOPEC. This thesis incorporates five key exploration wells, lithostratigraphic well tops, and age of formations, which was given by NPD (NPD, 2017). The seismic and well data, together with the principles of sequence stratigraphy, applied in this study will be presented here, with a focus on the seismic interpretation and software used.

4.1 DATA

4.1.1 3D SEISMIC DATA

This study is primarily based on CGG Northern Viking Graben NVG 3D seismic data. The survey is located in the Northern Viking Graben, North Sea, and encompasses a total area of 35 410 km^2. Figure 13 displays the entire CGGNVG 3D seismic survey in the Northern Viking Graben in the red polygon, while the blue polygon represents the area of this study, covering an area of approximately 5 310.66 km^2. Based on CGG (2017), this seismic survey applies CGG's full-bandwidth BroadSeis™-BroadSource™ solution, enhancing the image quality with no ghost effect.

The dataset was acquired in 2016, using a 12.5 m x 18.75 m grid size in a north-south direction. The geodetic datum and projection of this survey are European Datum 1950 and UTM 31N. The phase and polarity of this seismic survey are identified as increasing acoustic impedance at the seafloor. Figure 14 displays the strong peak between two small troughs recorded at the seafloor. According to Sheriff (2006), the CGG Northern Viking Graben NVG 3D survey has been processed as normal polarity and zero-phase signal. In addition, the variable wiggle display in Figure 14 shows the distance between the seismic inlines and crosslines, which are 12.5 m and 18.75 m between each line, respectively (125 m and 187.5 m every tenth trace).

The dominant frequency of the Cretaceous strata seismic interval is defined by using spectral analysis from the CGG Northern Viking Graben NVG 3D survey. Figure 15 displays the

spectral analysis from a seismic cube covering the Cretaceous strata, showing the peak and the frequency spectrum are 14-24 Hz and 10-30 Hz, correspondingly. The velocity is measured from synthetic seismogram from several key wells where the average velocity of Cretaceous strata is 2527 m/s. From the equations in Table 2, the vertical resolution of the Cretaceous interval is 26.3 m, the radius of Fresnel Zone before migration is 257.9 m, and the radius after the migration is 26.3 m.
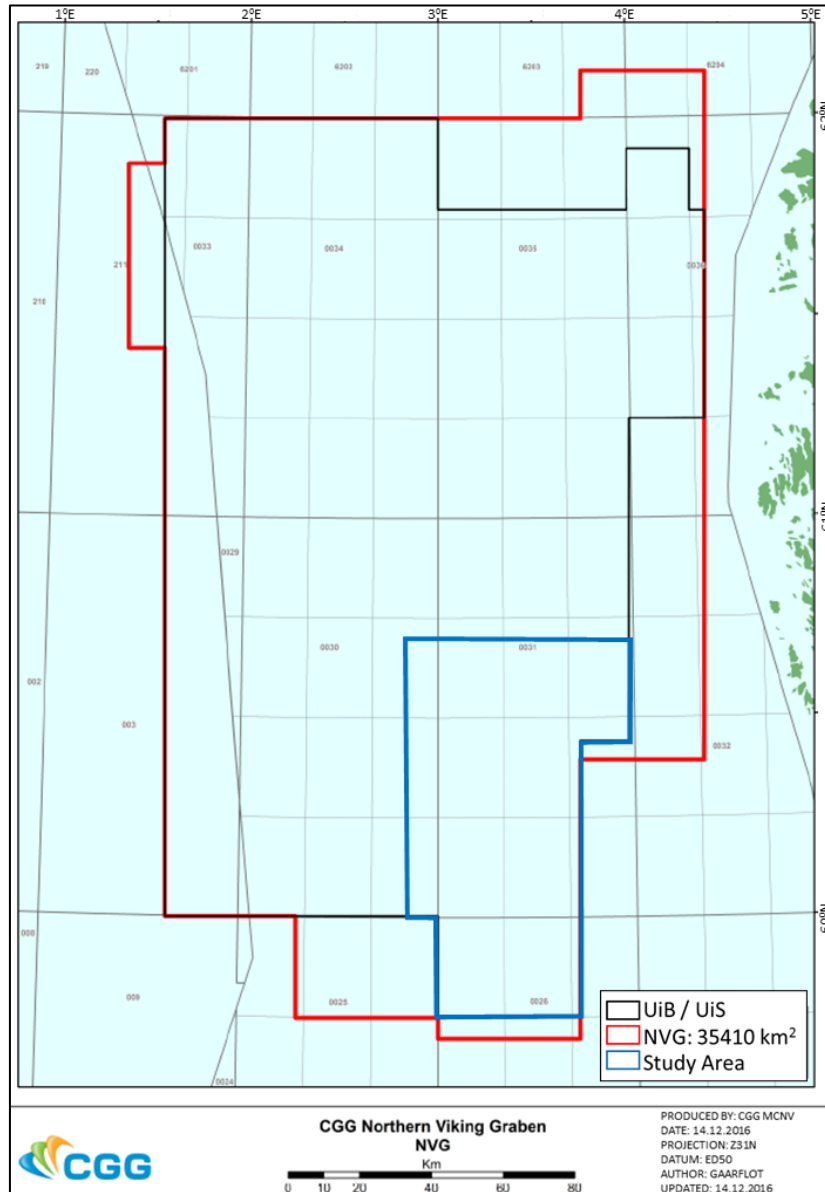
Figure 13: The location of the CGG NVG Seismic Survey with 3D Broadseis Broadsource data type (red polygon). The blue polygon marks the 3D seismic data coverage used in this study, a total of 5,310.66 km² in the northern Stord Basin, northern North Sea.

Table 2: The calculation of vertical and lateral resolutions of the CGGNVG 3D seismic survey in the study area. The velocity value is based on the synthetic seismogram result of several wells in the Cretaceous interval.

Parameters	Calculation
Wavelength (λ)	= 2527 m/s / 24 Hz = 105.3 m
Vertical Resolution	= 105.3 m / 4 = 26.3 m
Fresnel Zone Before Migration: Radius of Fresnel Zone	= 2527 m/s / 2 * (1 s / 24 Hz)$^{1/2}$ = 257.9 m
Fresnel Zone After Migration	= λ / 4 = 105.3 m / 4 = 26.3 m
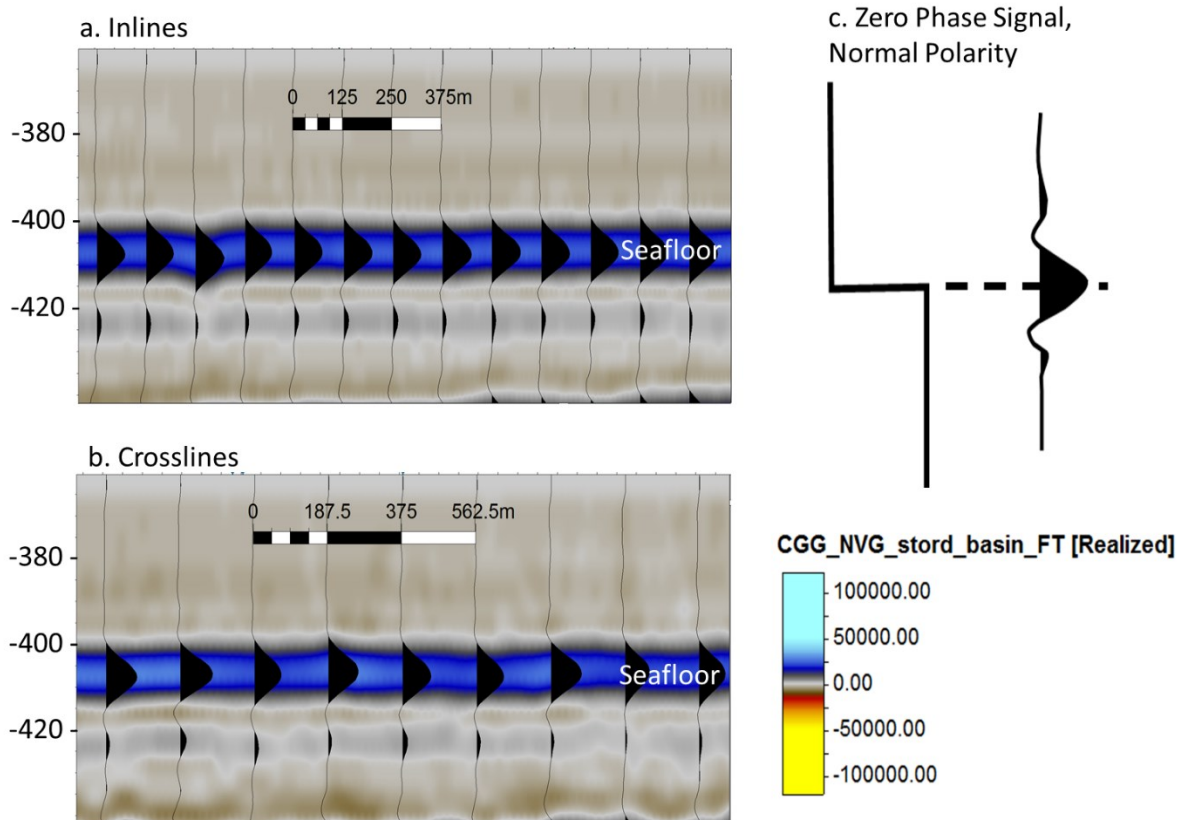
Figure 14: (a) The seismic inline cross section displays the seafloor wavelet reflection from the CGG northern Viking Graben NVG 3D seismic survey. (b) The seismic crossline cross section shows the variable wavelet reflection of the seafloor from the same seismic survey. c) A zero-phase signal, normal polarity model based on Sheriff (2006), which is similar to the wiggle of the seafloor in the CGG northern Viking Graben NVG 3D seismic survey, identified by the blue color.
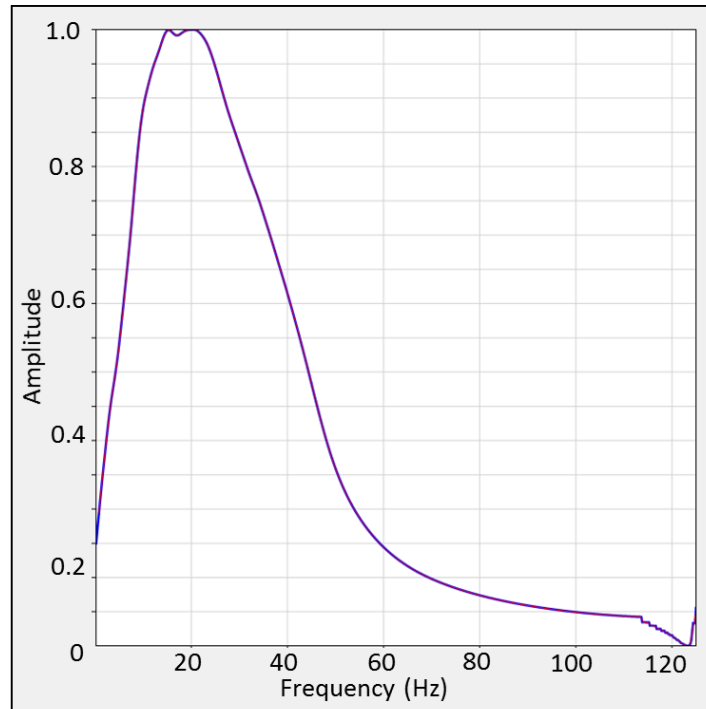
Figure 15: Spectral analysis of the Cretaceous interval from the CGG NVG Seismic Survey depicting the peak frequency between 14 and 24 Hz. The maximal peak frequency is used to identify the horizontal and vertical resolution of the seismic survey of the Cretaceous interval.

4.1.2 2D SEISMIC DATA

The 2D seismic data available for interpretation is part of the 2D North Sea Renaissance (NSR) data surveys, which are, NSR06, NSR07, NSR08, and NSR09 (Figure 16). TGS-NOPEC and Fugro Multi Client Services AS acquired these surveys during the period 2006-2009 on the Norwegian continental shelf. In addition to the NSR survey, the SG8043 survey on the Norwegian sector was used to complete the 2D seismic coverage of the study area.

The NSR06 seismic survey covers most of the study area, especially in the east where 3D seismic data is lacking. The NSR07 seismic survey consists of three lines across the central part of the study area. The NSR08 survey has a dense coverage, especially in the southern part of the study area. The NSR09 survey is composed of four seismic lines in the southern part and one seismic line in the northern part of the study area. The NSR seismic survey is high-resolution and has good data coverage. The SG8043 survey encompasses the northeastern part of the study area (Figure 16).
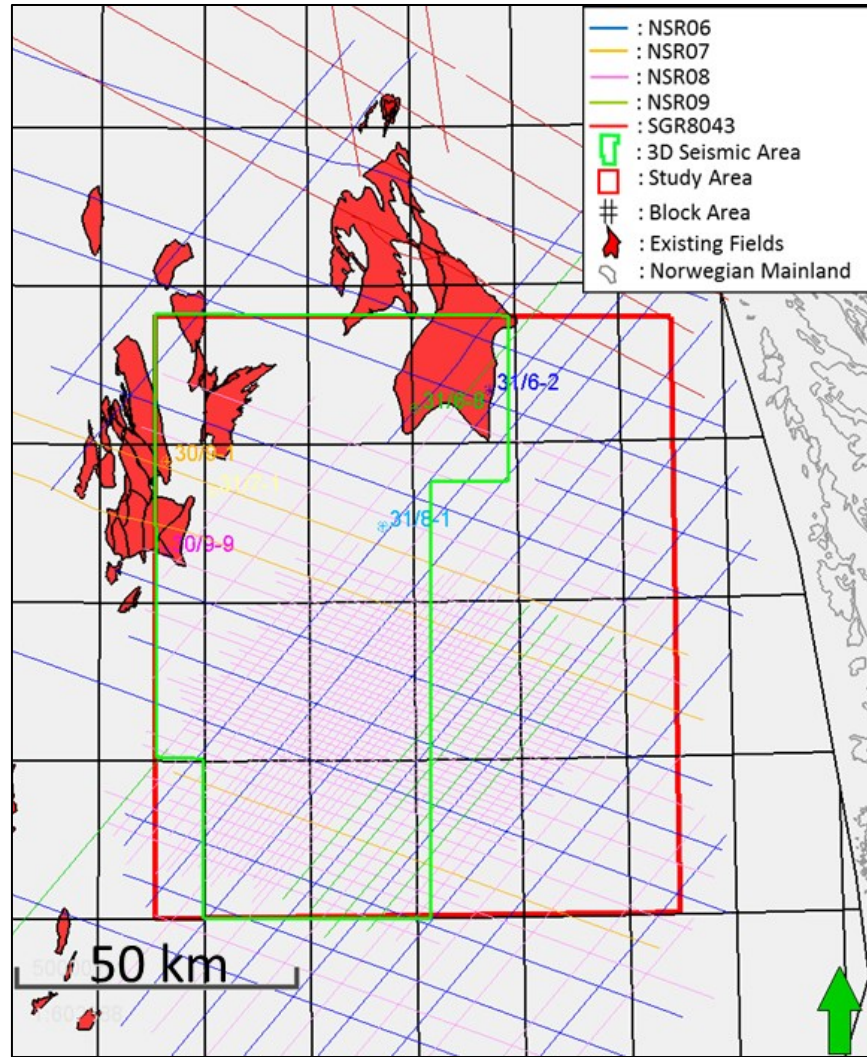
Figure 16: The 2D seismic surveys, North Sea Renaissance (NSR) and SG8043, covering the entire study area, notably in the eastern region where 3D data is absent.

By interpreting 2D seismic lines in the study area (especially outside the 3D seismic data area), regional tectonic features and stratigraphic events were identified, *e.g.,* the Øygarden Fault Complex and clinoforms. The 2D seismic lines were also used to identify key surfaces and strata terminations, which aid in generating a Wheeler's Diagram analysis.

The phase and polarity of these seismic surveys are identified by using the interface between seawater and seafloor (Figure 17). Figure 17 shows that these seismic surveys have been acquired with reverse polarity and zero-phase signal (based on Sheriff, 2006), which is opposite to the CGG-NVG 3D seismic survey.
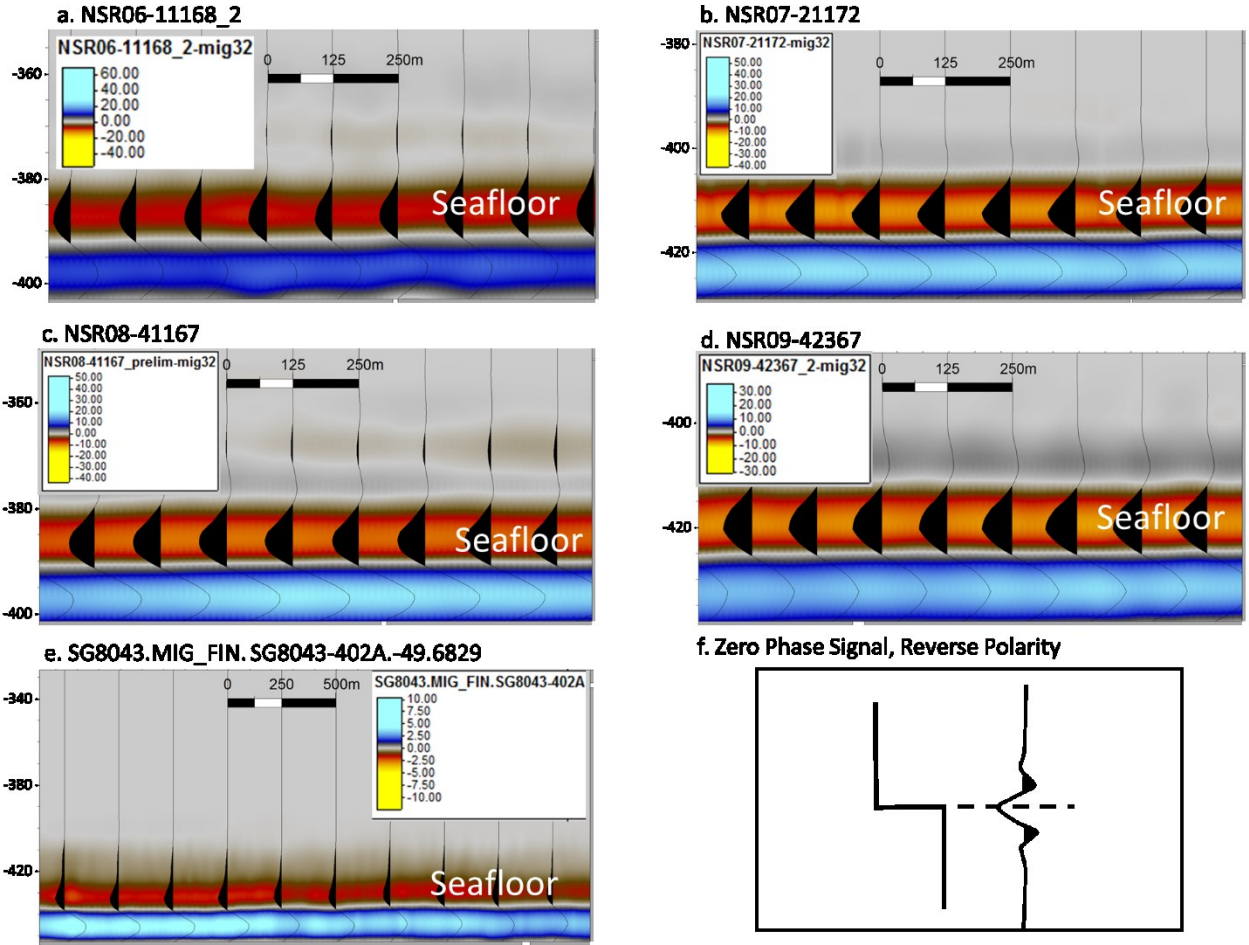
Figure 17: The NSR06, NSR07, NSR08, NSR09, and SG8043 2D seismic surveys, used in this study (a-e). The seafloor reflectors in these surveys show zero-phase signal and reverse polarity (f), based on Sheriff (2006). The cool colors represent positive amplitude, while the warm colors depict negative amplitude.

4.1.3 WELL DATA

This study utilizes five key exploration wells covering some hydrocarbon producing fields, such as the Troll and the Oseberg Field (Figure 18). These wells contain gamma ray, sonic, density, resistivity, and check-shot data that are used in stratigraphic well correlation and seismic-to-well tie.
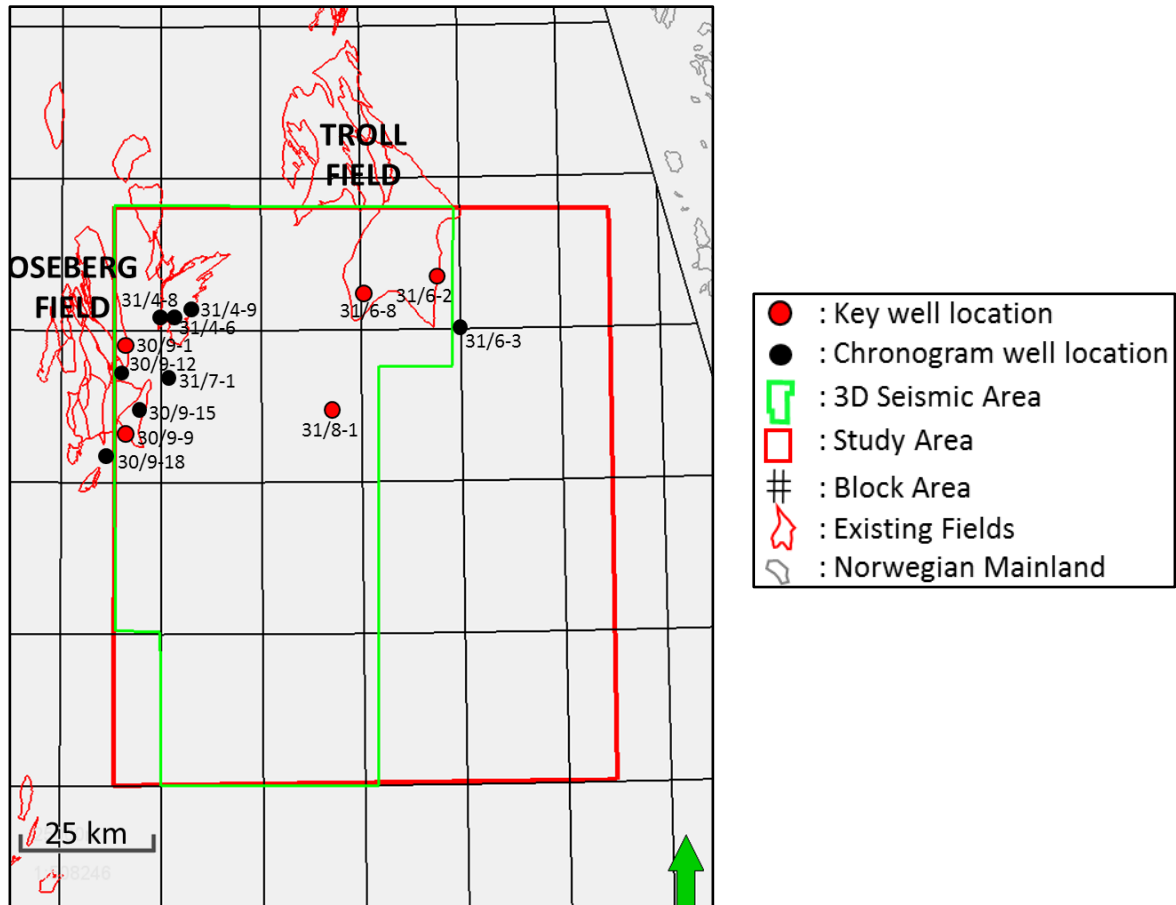
Figure 18: The location of five key and several additional wells used in the chronogram analysis, which are dominantly located in the northern part of the study area. Almost all key wells have the conventional well logs in Cretaceous strata and biostratigraphy data, which help in determining the major regional surfaces by using the sequence stratigraphic method.

Table 3 depicts the location, entered year, and Cretaceous sediment thickness of several key wells in this study. This consists of wells 30/9-1, 30/9-9, 31/6-2, 31/6-8 and 31/8-1. Overall, the thickest Cretaceous stratum from existing wells in the northern Stord Basin is 516 m. The seismic-to-well tie analysis was conducted on all key wells since most have sonic, density and check-shot data. However, the 31/8-1 exploration well, located in the northern Stord Basin, has no sonic data in the Cretaceous and younger sediment intervals and, therefore, requires calibration during seismic-to-well tie analysis. Biostratigraphy data is derived from 12 wells that are located in the northern Stord Basin surrounds (Figure 5, 18). This information is applied primarily to identify the stratigraphic cycles of the Cretaceous strata, thereby establishing the

sequence stratigraphy. The integration of biostratigraphy, lithostratigraphy, and seismic-to-well tie analysis defines the major regional surfaces in the study area.

Table 3: The key exploration wells used in this study in the Oseberg, Troll, and northern Stord Basin. Well tops are based on NPD (2017)

Well Bore Name	Location	Year	Thickness of Shetland Gp (m)	Thickness of Cromer Knoll Gp (m)	Thickness of Cretaceous Sediments (m)
30/9-1	Oseberg	1982	134	10	144
30/9-9	Oseberg	1989	114	0	114
31/6-2	Troll	1983	160	194	354
31/6-8	Troll	1985	115	41	156
31/8-1	Stord Basin	2011	116	400	516

4.2 METHODS

4.2.1 TOOLS

This study used Petrel E&P Software Platform 2015, as the leading software in interpreting the seismic reflection data. The CGGNVG 3D Seismic Data, NSR and SG8043 2D seismic surveys, and all key wells were loaded into the Petrel software to generate seismic-to-well tie, stratigraphic well correlation, and seismic interpretations. This software also aided in creating the time structure, time thickness, amplitude and variance attribute maps, which were applied in interpreting and analyzing the study area. Seismic facies analysis was also conducted to identify the depositional environment based on seismic characterization. In addition, the chronostratigraphic chart was used to determine the relative positions of the depositional packages in space and time (Emery and Myers, 2009).

4.2.2 SEISMIC-TO-WELL TIE

The purpose of this analysis is to provide a time-depth relationship between the seismic and well data and to recognize primary reflectors. Lithostratigraphic data from the Norwegian Petroleum Directorate was used as a guide on interpreting the chronostratigraphic succession of the Cretaceous interval. The stratigraphic well correlation was based on five key wells at the

Cretaceous strata level, using sequence stratigraphy methodology (Figure 19). The key wells were flattened at downlap surface 3 above the Cretaceous interval, and were divided into several key stratigraphic surfaces based on the well-log characteristics. There are three unconformities, two downlap surfaces and three transgressive surfaces, which can be identified from the log features (Figure 19).

All five key wells have sonic, density and check-shot data. Synthetic seismograms were produced by convolving the sonic and density logs, with an extracted wavelet to generate the synthetic predicted traces. A deterministic extraction was used for all wells in generating a wavelet from the relevant windows of the seismic. The power spectrum shows the peak frequencies are approximately 14-24 Hz (Figure 20), which is similar to the highest seismic frequencies from the spectral analysis (Figure 15). The synthetic seismogram in Figure 20 shows the consistent correlation between one of the key wells (31/6-8) and seismic data in the Cretaceous interval. Almost all wells have a fit correlation with seismic data, except in well 31/8-1 where small-time shifts are applied due to unavailability of a sonic log in the Cretaceous interval (Figure 19).

The seismic-to-well tie analysis eventually connects the well data in the depth domain and the seismic data in the time domain, and aids in identifying the key reflectors for interpretation. Figure 21 represents the relationship between seismic sections and key wells in the study area, which displays the relevant horizons based on the time-depth conversions and the synthetic seismograms.

4.2.3 INTERPRETATION STRATEGY

In order to generate the stratigraphic framework in the study area, three significant stratigraphic surfaces were recognized: the downlap surface, the erosional unconformity, and the transgressive surface. These three key horizons can be clearly identified from stratigraphic well correlation (Figure 19) and seismic data (Figure 21). In addition, the chronograms of the Cretaceous interval in the northern Stord Basin and its surrounding area have been created to analyze the period of erosion, non-deposition, and condensed section (Figure 5). Moreover, the chronograms were also utilized to identify the periodicity of the cycle frequency in this area.

The stratal terminations in the seismic data guided definition of the key stratigraphic surfaces. These stratigraphic surfaces determined several sequences in the Cretaceous strata, which aided in analyzing the tectono-stratigraphic sequences of this interval. Analysis was done by using time depth structure, total stratigraphic thickness in time, and seismic attribute maps of each interval bounded by the stratigraphic surfaces—fundamental tools in interpreting the sedimentary succession of Cretaceous strata.

Since the focus of this study is in the Cretaceous interval, the 3D seismic volume was cropped to this stratum, which made the interpretation and data capacity more effective and efficient. The interpretation of seismic horizons used guided autotracking with an interval of 16 traces (maximum), except parts of the BCU and transgressive surfaces, which were interpreted manually due to weaker amplitude and/or changes in polarity at the structurally high areas. A vertical exaggeration factor of 30 was applied to Cretaceous strata during seismic interpretation, as the succession is not very thick in the study area.

4.2.4 SEISMIC ATTRIBUTE

Taner (2001) defined Seismic attributes as *"all the information obtained from seismic data, either by direct measurements or by logical or experience-based reasoning"*. Emery and Myers (2009) explained the amplitude map can be used as a facies map if the amplitude of the reflection is correlated to the geological features. The average amplitude that is calculated as the root-mean-square of the amplitude (RMS amplitude) can be used to differentiate intervals of different seismic amplitudes. The characteristic of seismic amplitude depends on the density and or velocity contracts in the layer, which is mostly connected to the depositional facies. The variance cube measures the direct quantity of dissimilarity instead of the similarity of seismic data, resulting in a sharper, clearer image than previous coherency methods (Schlumberger, 2006). This means the variance cube measures the discontinuity in seismic data, which can be used to identify tilting and rotation, juxtaposition of high angle, and overlying post-rift strata.

In this study, RMS amplitude and variance attributes have been utilized to aid in analyzing the structural features (fault verification), seismic facies, and paleogeomorphology.
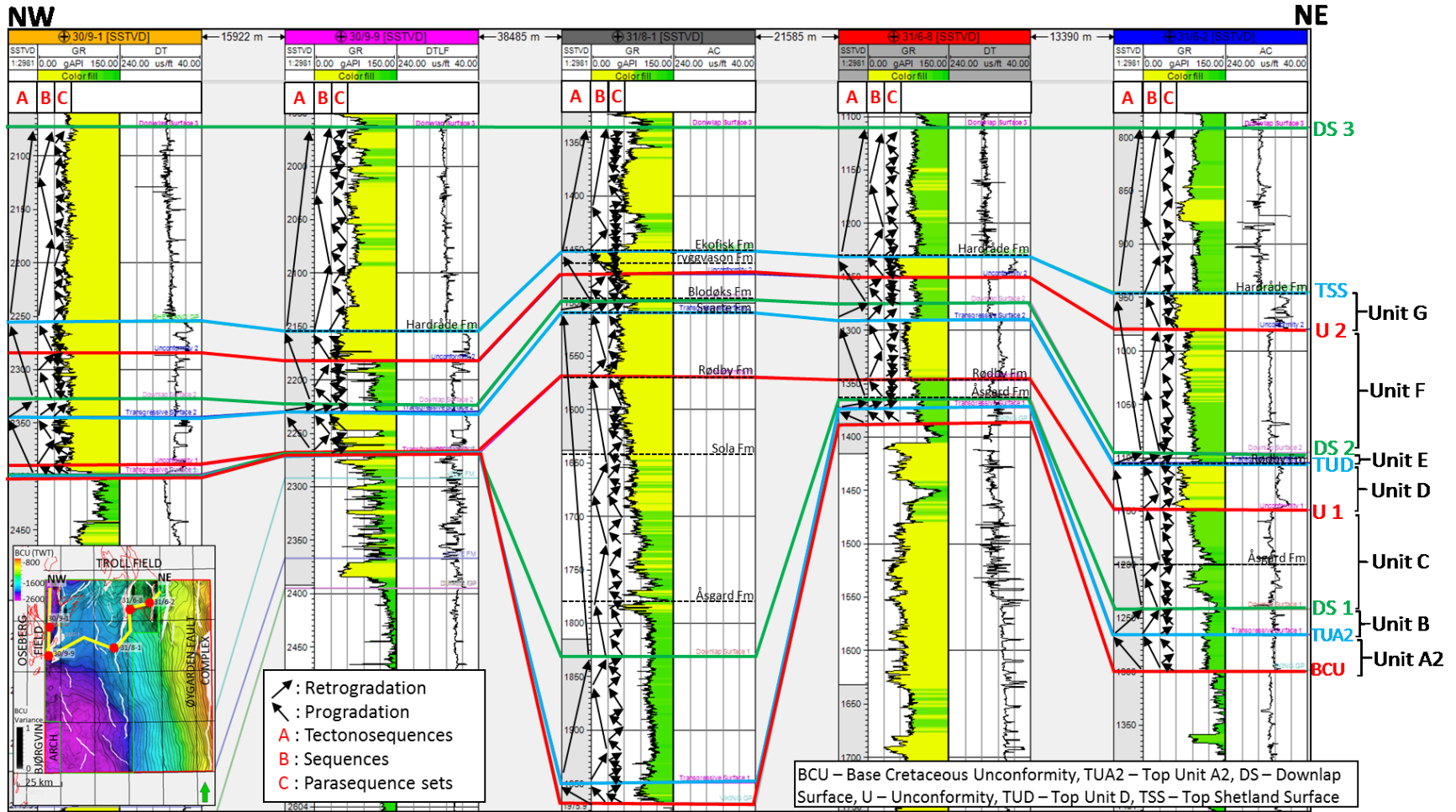
Figure 19: Stratigraphic well correlation by using the sequence stratigraphic method in five key wells in the study area. Lithostratigraphy is noted for each well based on NPD data (NPD, 2017). These wells were flattened at the Downlap Surface 3 above the Cretaceous strata. The red lines represent the unconformities, the green lines depict downlap surface, and the blue lines illustrate transgressive surface. The black arrows depict the progradational and retrogradational events in the different orders of the Cretaceous strata. Almost all wells have conventional well- logs in the Cretaceous interval, except for the 31/8-1 well where the sonic log starts at the Jurassic interval. The inset map shows the direction of well correlation on the BCU time structure map.
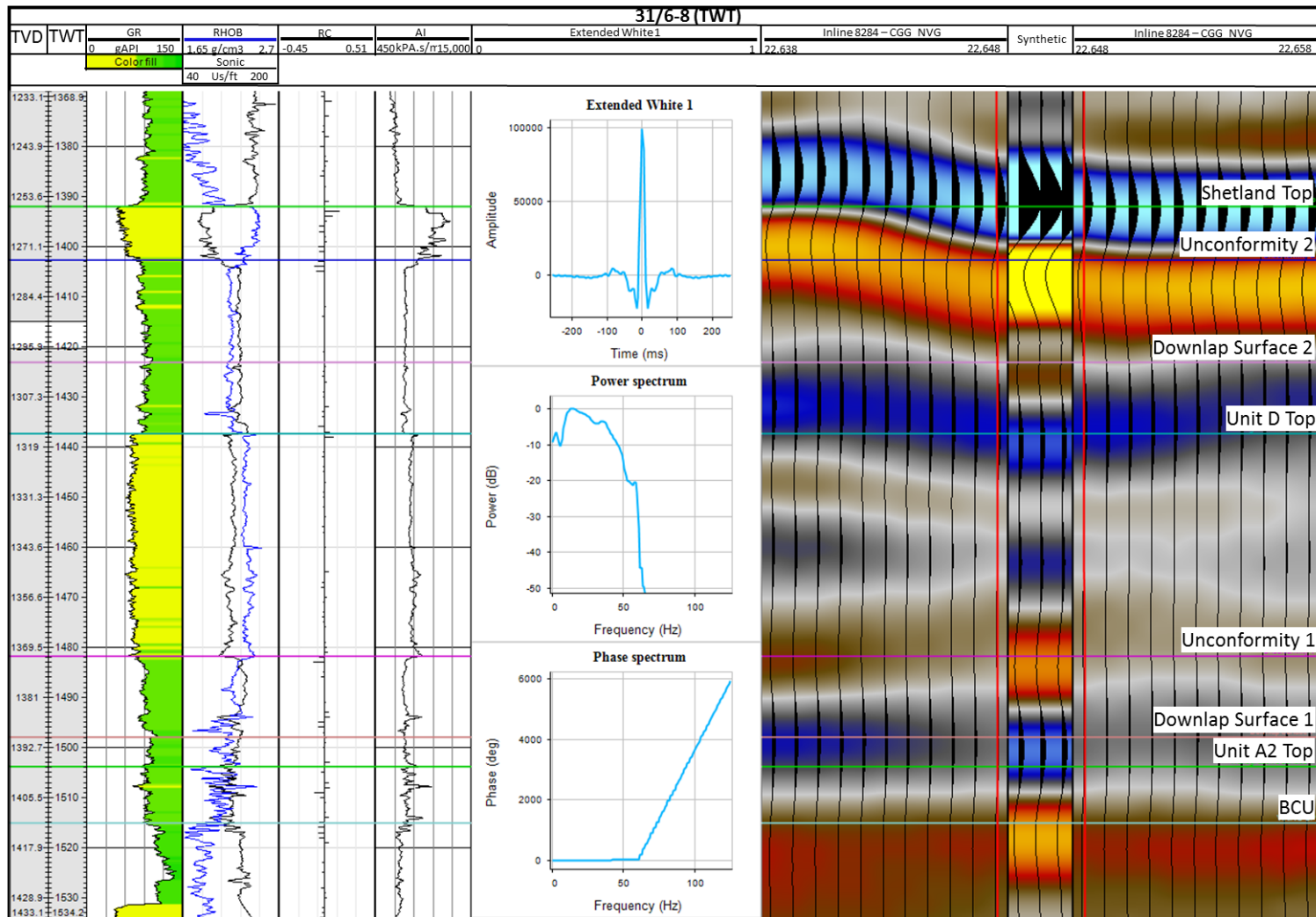
Figure 20: A seismic-to-well tie analysis of the 31/6-8 well on the Troll Field, defining interpreted surfaces of Cretaceous strata based on gamma ray, sonic, density, and acoustic impedance logs. The synthetic seismogram is also depicted here, as well as the seismic section, wavelet, power and phase spectrum. The peaks are characterized by the blue color, whereas the troughs are identified as the red color. The Top Shetland Surface, Downlap Surface 1, Downlap Surface 2, Top Unit A2, and Top Unit D are picked on the peak (blue) reflectors; while the BCU, Unconformity 1, and Unconformity 2 are picked on the trough (red) reflectors. Location of the well is exhibited in Figure 18.

43
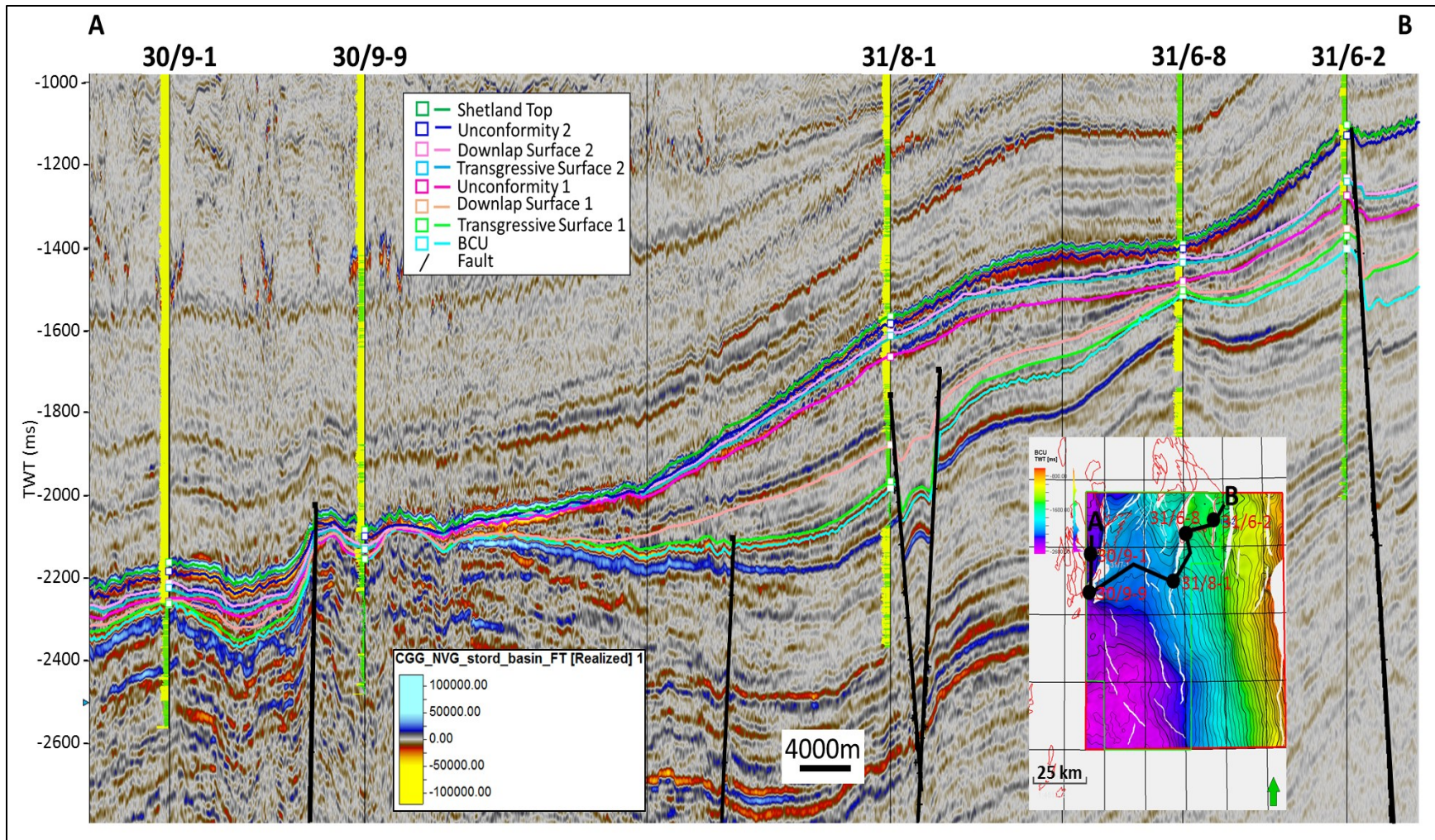
Figure 21: The 3D seismic line overlain by the five key wells (with GR trace) and the major horizons within the Cretaceous interval after applying the time-depth conversions. The time-depth conversion connects well and seismic data. The location of wells is shown on the inset map and in Figure 18.

5. OBSERVATIONS AND INTERPRETATIONS

5.1 SUBDIVISIONS AND SEISMIC STRATIGRAPHY OF THE CRETACEOUS INTERVAL

The seismo-stratigraphic units of the Cretaceous interval in the study area were recognized by significant changes in the amplitude and continuity of the bounding reflectors, stratal terminations, seismic facies, and geometry. The stratigraphic well correlation was also used for interpreting the key stratigraphic surfaces, as well as basis during seismic interpretation (Figures 19 and 21). Analysis of five key wells using log characteristics and seismic data lead to nine prominent stratigraphic surfaces. These surfaces are (Figure 19): the Base Cretaceous Unconformity (BCU), Top Unit A1 (TUA1), Top Unit A2 (TUA2), Downlap Surface 1 (DS 1), Unconformity 1 (U 1), Top Unit D (TUD), Downlap Surface 2 (DS 2), Unconformity 2 (U 2), and Top Shetland Surface (TSS).

These nine stratigraphic surfaces were used to subdivide the late Berriasian to Danian interval into seven main seismic units, termed Unit A, Unit B, Unit C, Unit D, Unit E, Unit F, and Unit G (Figure 22). Unit A was divided into two sub-units: Unit A1 and Unit A2. The seismic stratigraphic framework for the late Berriasian to Danian interval is observed in Figures 21 and 22, and is interpreted in Figure 36. It is also shown with reference to three main seismic sections—orientated N-S, NE-SW, and NW-SE—across the northern Stord Basin in Figures 23 and 24a-c.

The N-S trend of the Oseberg and Øygarden Fault Complex, as well as the NE-SW trending normal faults, are the dominant structures in the study area. These structures created some paleo-highs during the Cretaceous age, which may have acted as the sediment sources for this interval. These N-S and NE-SW normal faults are apparent on both the 2D and 3D seismic data (Figures 24a-c). Figure 25 illustrates the time-structure (TWT) maps of the Top Cretaceous (Top Shetland Surface), Base Cretaceous (BCU), and the other seismic surfaces within the Cretaceous interval showing variations of the topography in the northern Stord Basin throughout this time interval.
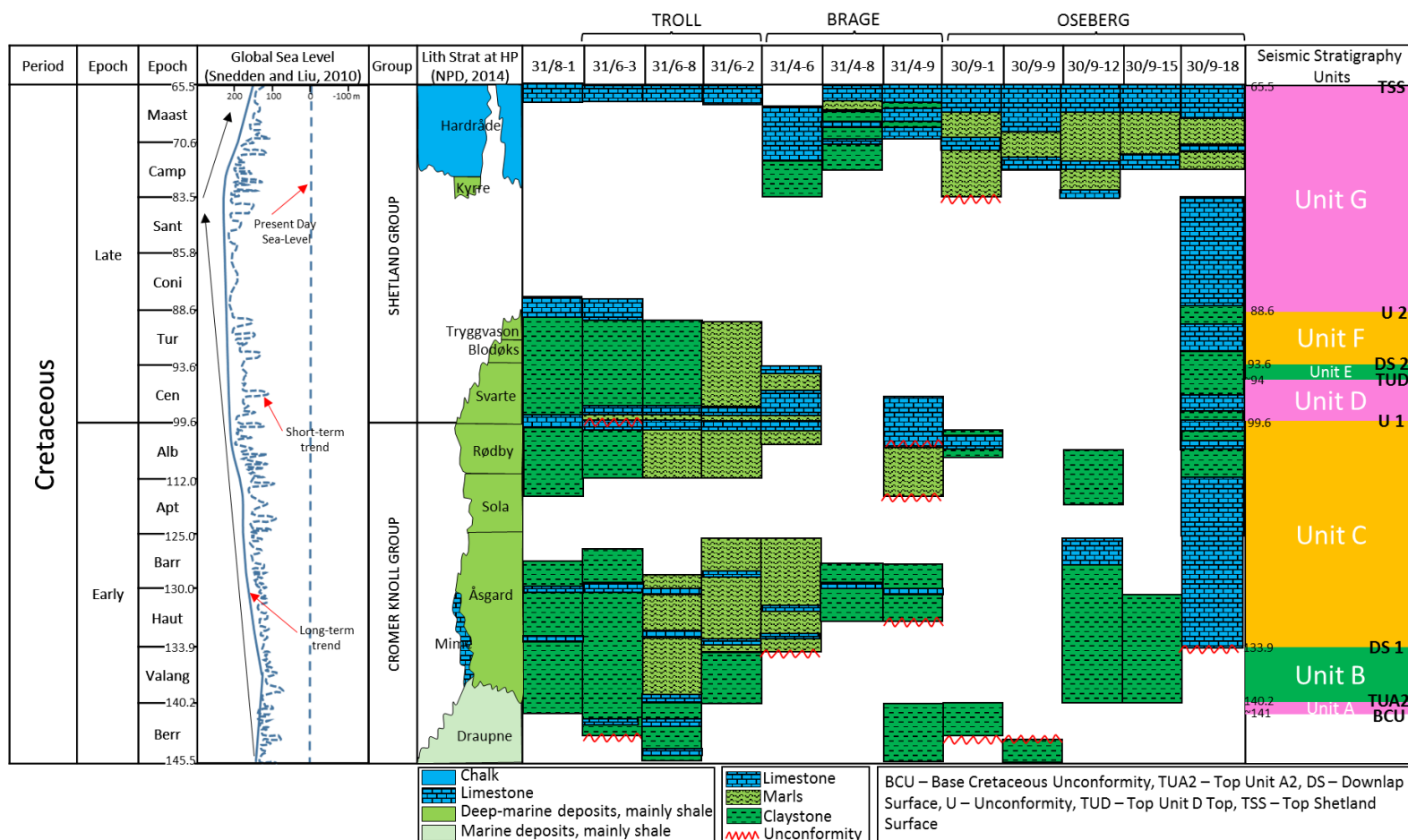
Figure 22: A Chronogram of 12 wells in the study area and its surrounds (Troll, Brage, and Oseberg Fault Block), lithostratigraphic chart from the Horda Platform (HP), and global sea-level during the Cretaceous. It highlights several time gaps during this period, such as, in the Berriasian-Valanginian, Aptian, and Coniacian-Campanian. The regional sea-level curve shows a rise in base-level during the Berriasian to Santonian, and a fall in the Campanian to Maastrichtian. However, the regional flooding during the Cretaceous period was interrupted by two main sea-level falls: in the Latest Berriasian and in the Cenomanian age. The inferred condensed section occurs during Aptian period in the basinal area, as well as during the Coniacian to Campanian age—supported by the global sea-level curve, which rose maximally during the Santonian time. In the right column, there are several seismic stratigraphy units bounded by the stratigraphic surfaces identified in this study. The global sea-level is based on Snedden and Liu (2010). The lithostratigraphic chart follows NPD (2017). The location of wells is shown in Figure 18.

46
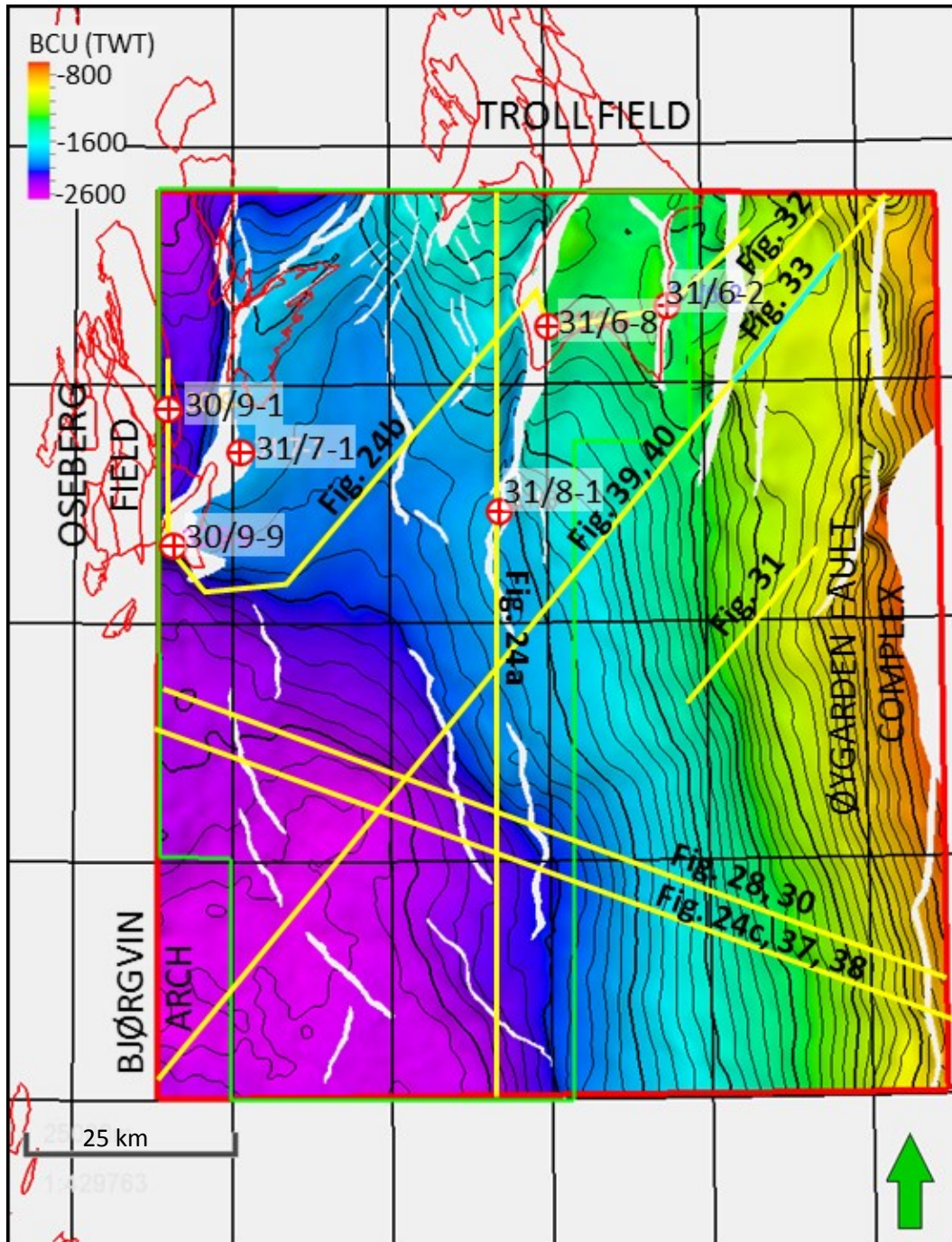
Figure 23: The BCU time-structure map overlain by several 2D and 3D seismic lines, which are illustrating the seismic stratigraphic framework in the northern Stord Basin. There are four major paleo-highs affecting the deposition and preservation in the study area: the Troll and the Oseberg Fault Blocks, the Bjørgvin Arc, and the Øygarden Fault Complex.

There are several structural highs in the study area: the Oseberg and the Troll Fault Blocks, the Bjørgvin Arch, and the Øygarden Fault Complex. The northern Stord Basin is a semi-enclosed basin, approximately 58 km long and 46 km wide, with an opening to the south (Figure 23).

The present-day depth of the Base Cretaceous Unconformity (BCU) reflection in the basin is around 2600 ms (~3285 m), shallowing up to 800 ms (~1010 m) on the flanks, and it dips towards the southwest (Figures 23 and 25). In general, the basin location is thought to be southwest of the study area.

Figure 26 shows the isochron maps for different interpreted units within the Cretaceous strata representing the change of topography through time. Depocenters change during deposition of Unit A to Unit G, with total maximum thickness reaching approximately 700 ms (~885 m) for the entire Cretaceous interval. The Cretaceous strata is absent in the Øygarden Fault Complex area (Figure 26).

5.1.1 UNIT A

Seismic Unit A consists of the Latest Berriasian age (~141-140.2 Ma), and is bounded at its base by the BCU and at its top by the Top Unit A2, respectively. Unit A1 and Unit A2 can be differentiated by the internal reflections and stratal terminations within these units (Figure 24c), which is described below. The boundary between Unit A1 and Unit A2 is not recognizable in well correlations since the wells are located on paleo-highs, hence the age of Top Unit A1 cannot be determined from wells (Figure 23).

5.1.1.1 UNIT A1

Unit A1 is the lower part of Unit A package, bounded by the BCU at the base and the Top Unit A1 above.

5.1.1.1.1 WELL LOGS

There is no well penetrating this unit.
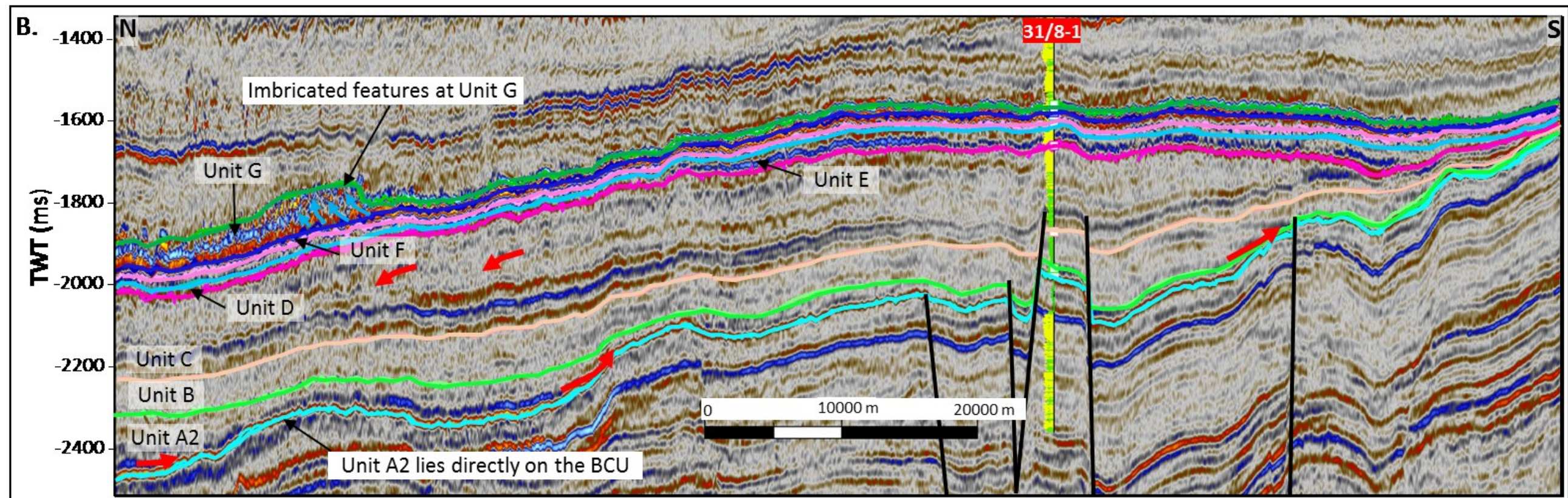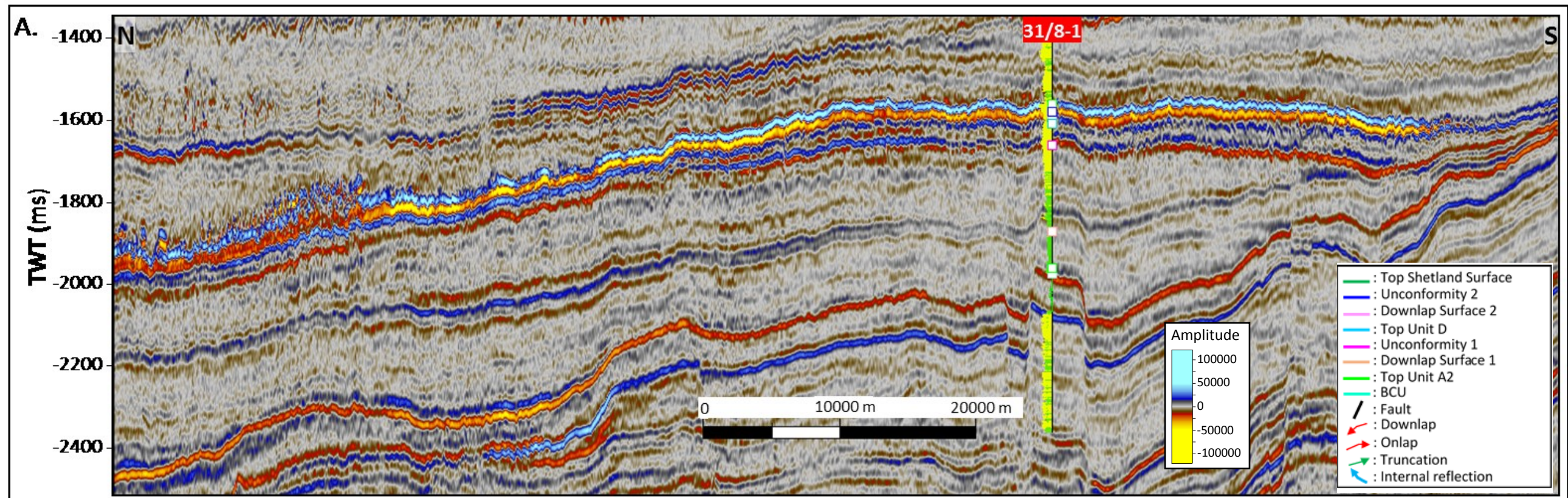
Figure 24a: (A) Uninterpreted and (B) interpreted 3D seismic lines crossing the 31/8-1 well (with GR), illustrating the different seismic units in the northern Stord Basin. Unit A2 onlaps toward the basin margin and overlies the BCU. The seismic unit thins towards the north, which is the location of the paleo-highs (Troll and Oseberg Fault Blocks). The stacking patterns of the gamma-ray log from the 31/8-1 well show progradational and retrogradational patterns (detail interpretation is shown in Figure 19). Imbricated features can be identified in Unit G, which is bounded by Unconformity 2 at its base and Top Shetland Surface at its top. The location of the section is shown in Figure 23.
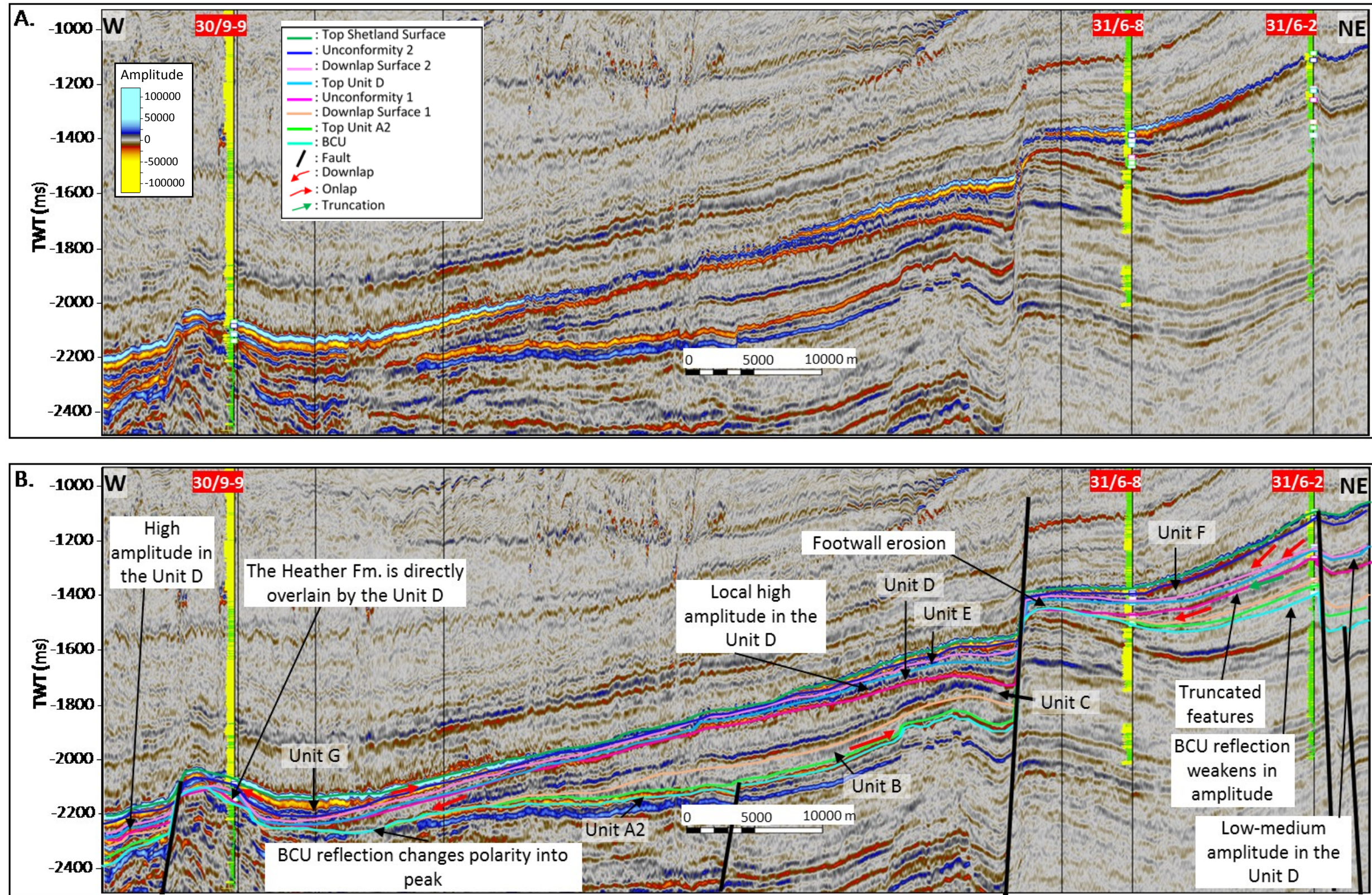
Figure 24b: A) Uninterpreted and (B) interpreted 3D seismic lines crossing the 30/9-9, 31/6-8 and 31/6-2 wells (with GR), illustrating the seismic units in the study area. The 30/9-9 well shows that Unit D (around 99.6 Ma) lies directly on the Heather Formation (approximately 168.3-163.5 Ma), located in the Oseberg Fault Block. The behavior of the BCU reflection can also be observed in this seismic line, such as, changes in polarity or weakening amplitude. Footwall erosion in the Troll Fault Block is observed, as several units were eroded in this area. The anomalous amplitude within Unit D, identified by high amplitudes, is interpreted as limestone stringers. The stratal termination—such as onlap, downlap, and truncation—are also defined on this seismic line. The location of the section is shown in Figure 23.
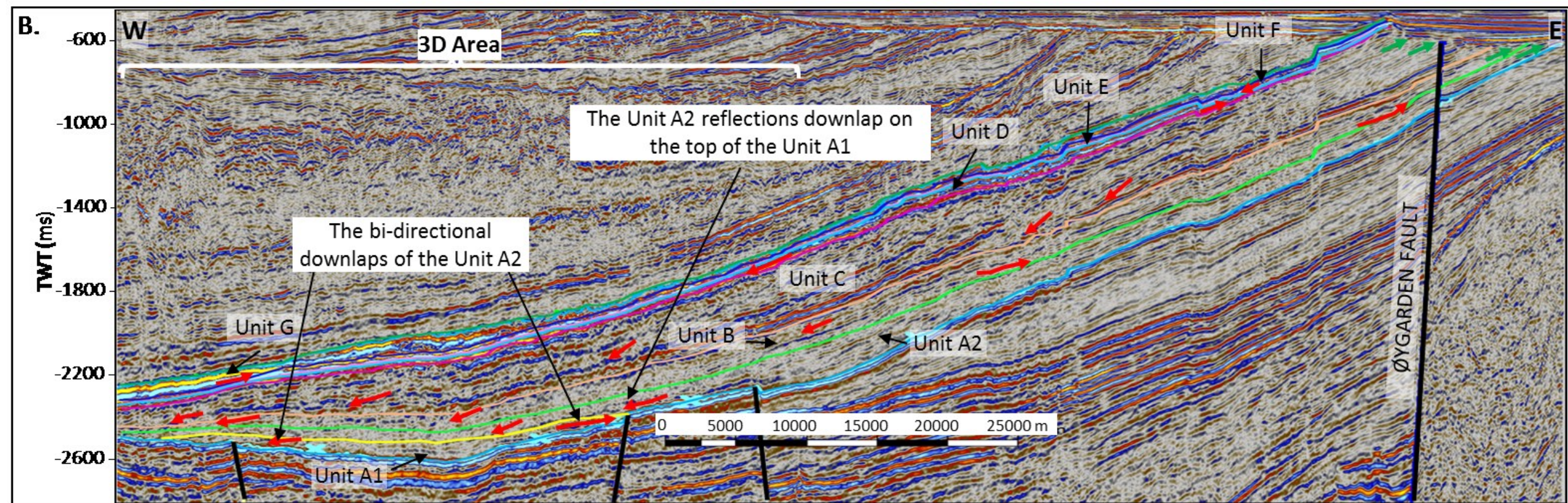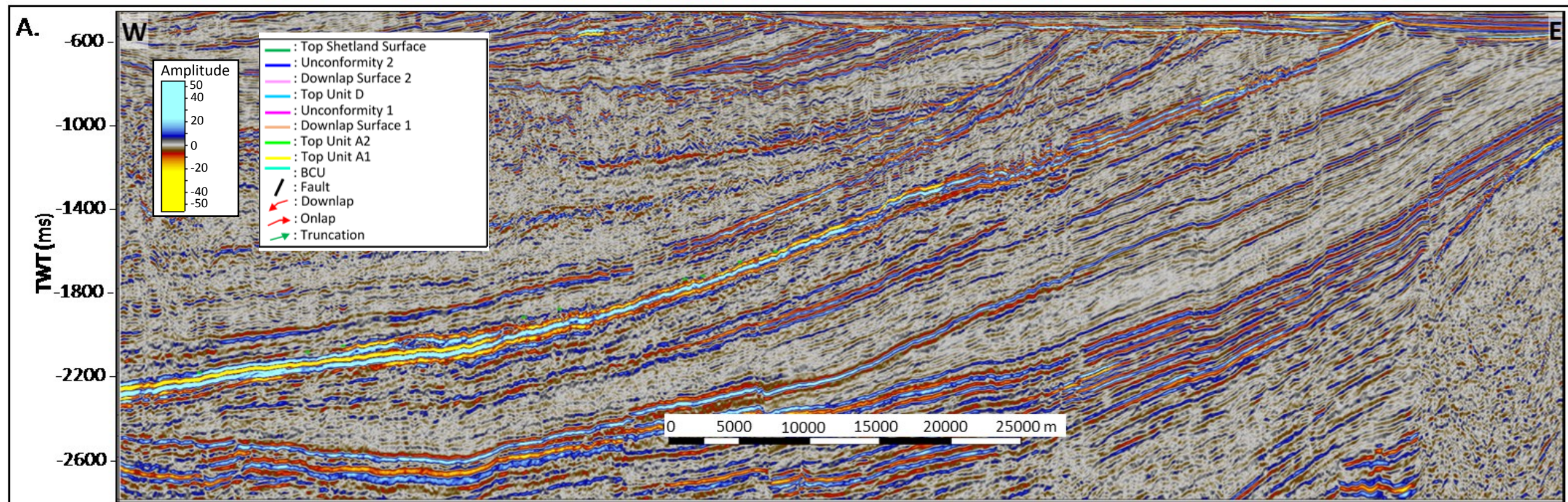
Figure 24c: A) Uninterpreted and (B) interpreted 2D seismic lines (NSR08-41165) displaying the distribution of the seismic units outside the 3D seismic area. The seismic character of Unit A1 is observed to be bi-directional downlaps and mounded shape, while Unit A2 reflections are observed to downlap onto Unit A1. The retrogradational stacking pattern can be identified from the stratal termination in Unit B, where the downlap features retreat toward east. The progradation of Unit C can still be observed in this seismic line as the thickest unit, while Units D, E, and F are much thinner in this seismic line. The internal reflections of Unit G infer an onlap character towards the basin margin. The location of the section is shown in Figure 23.
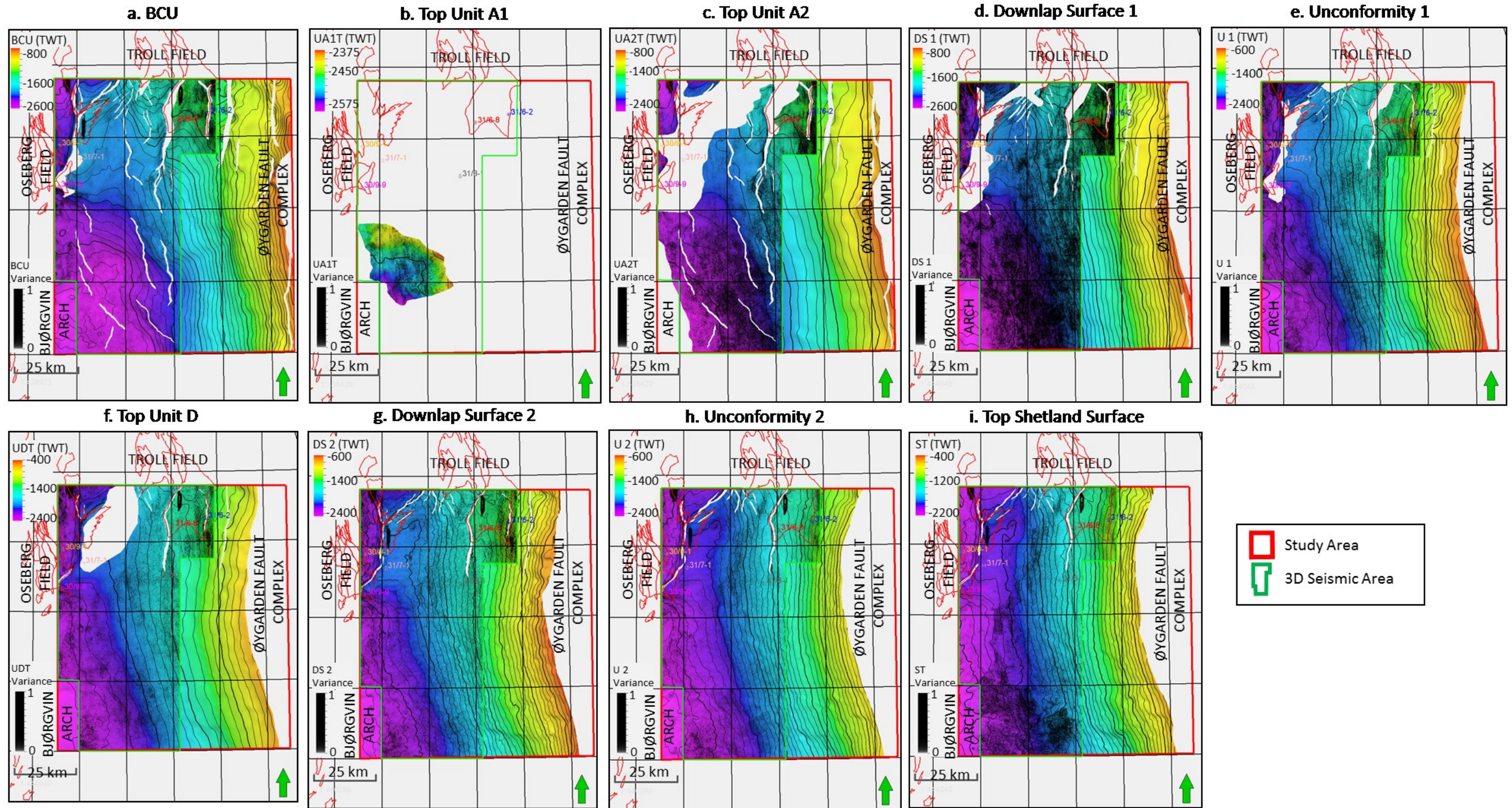
Figure 25: The time-structure maps (TWT) overlain by variance maps of each key stratigraphic surface within the Cretaceous strata in the northern Stord Basin. The basin position is assumed to be located in the southwestern part of the study area, while major paleo-highs consist of the Oseberg and the Troll Fault Blocks, the Bjørgvin Arch, and the Øygarden Fault Complex. Fault activities decreased gradually during the Cretaceous. Variance maps can be used in determining faults positions, offlap breaks, and slumping pattern. The warm colors represent the high areas while the cold colors display the low areas. The red polygon shows the study area and the green polygon identifies the 3D seismic area.
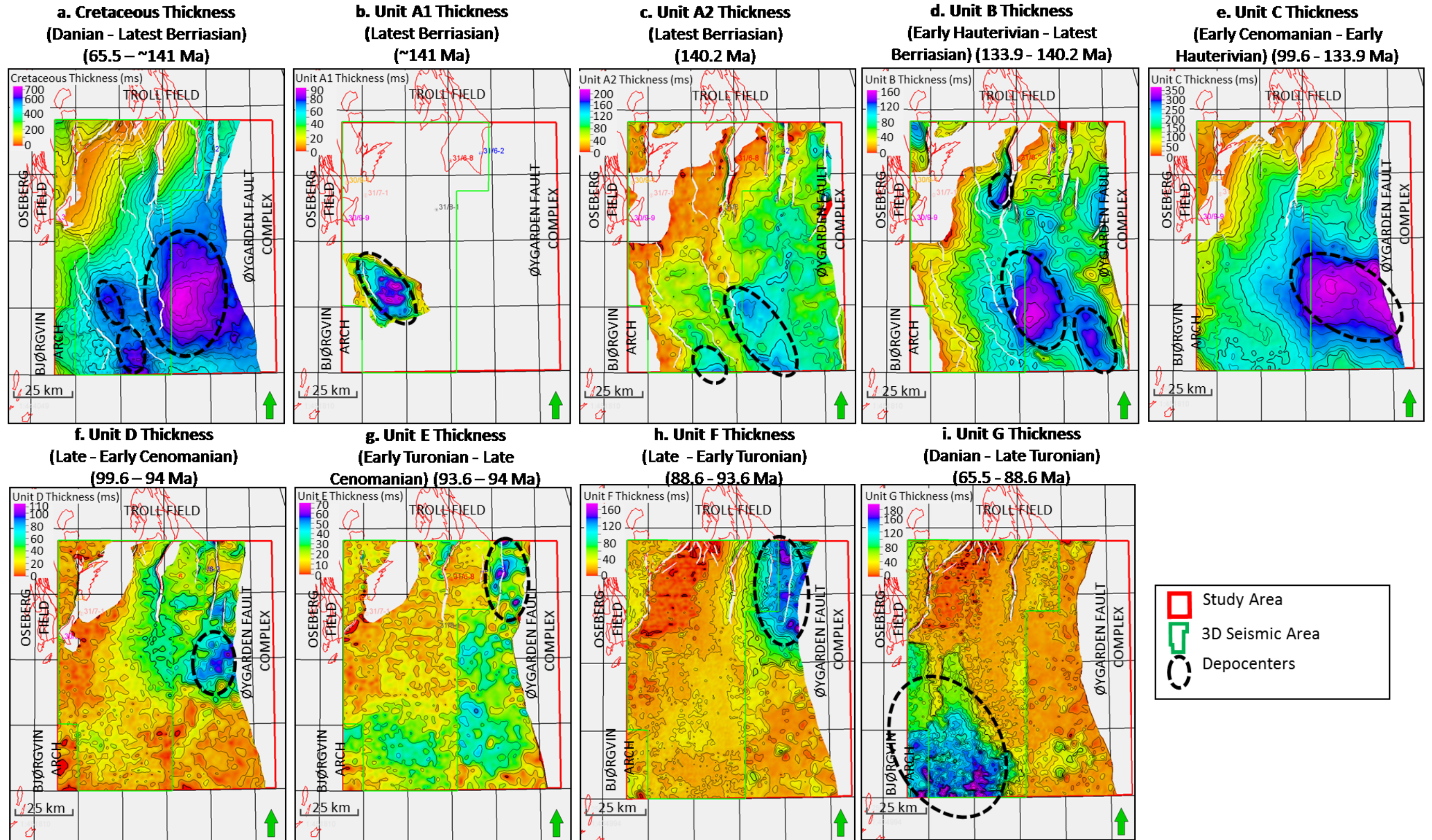
Figure 26: The isochron maps of the entire Cretaceous interval (a) and each unit (b-i) within the Cretaceous strata in TWT (ms). The thickest part of the interval is around 700 ms (~884 m), with the main depocenters in the south and southeast of the study area (a). The thickest unit is Unit C reaching 350 ms (~442 m); while the thinnest unit is Unit E reaching only 70 ms (~88.4 m). The blank zones in the study area represent non-deposition, or erosion. The black dashed circle represents the location of depocenters through time.

5.1.1.1.2 SEISMIC OBSERVATIONS

The character of the BCU reflection in Unit A is a strong trough amplitude, extensively continuous, and consistent (Figures 24a-c). Top Unit A1 is a medium to strong peak amplitude, and it is semi-continuous to continuous across the study area (Figure 24c).

Unit A1 is characterized by a mounded shape and progradation (Figures 24c and 27). The reflections within this unit show lateral semi-continuous to continuous, bi-directional downlapping onto the BCU, with medium to high amplitude anomalies (Figures 24c and 27). It is observed semi-continuous reflections, close to the flanks of the structural highs, to continuous reflections, toward the center of the basin (Figures 27c (ii) and 27c (iii)).

Figure 27 shows several seismic lines across Unit A1 combined with the variance and amplitude maps of Top Unit A1. The mound-shaped features in Unit A1 can be seen in Figures 27c (ii) and 27c (iii). However, the internal reflections of Unit A (A1 and A2) change from mounded shape (Figures 27c (ii) and 27c (iii)) to parallel in Figures 27c (i) and 27c (iv), indicating the limit of distribution of Unit A1. In addition, the variance map shows lobate geometries (Figure 27a), and the RMS amplitude map displays NNS-SSE offlap lineaments defined as high amplitude anomalies (Figure 27b). Figures 27c (ii) and (iii) show the progradational patterns of this unit toward the west. The offlap lineaments observed in the variance maps coincide with the position of the offlap breaks of internal reflection on the seismic lines (Figures 27c (ii) and 27c (iii)). The anomalously high amplitudes observed in the RMS amplitude maps of Unit A are due to the tuning effect, as BCU reflector significantly influences the amplitude map where Unit A is thin or absent.

5.1.1.1.3 MAPS AND OBSERVATIONS

The time-structure map (Figure 25b) of Unit A1 shows the configuration and the distribution of Top Unit A1, where present-day deepest part of Top Unit A1 is around 2575 ms (~3253 m) in the southwestern part of the study area. The paleo-highs affecting the deposition of Unit A were the Oseberg and the Troll Fault Blocks, the Bjørgvin Arc, and the Øygarden Fault Complex, where this unit was not deposited.
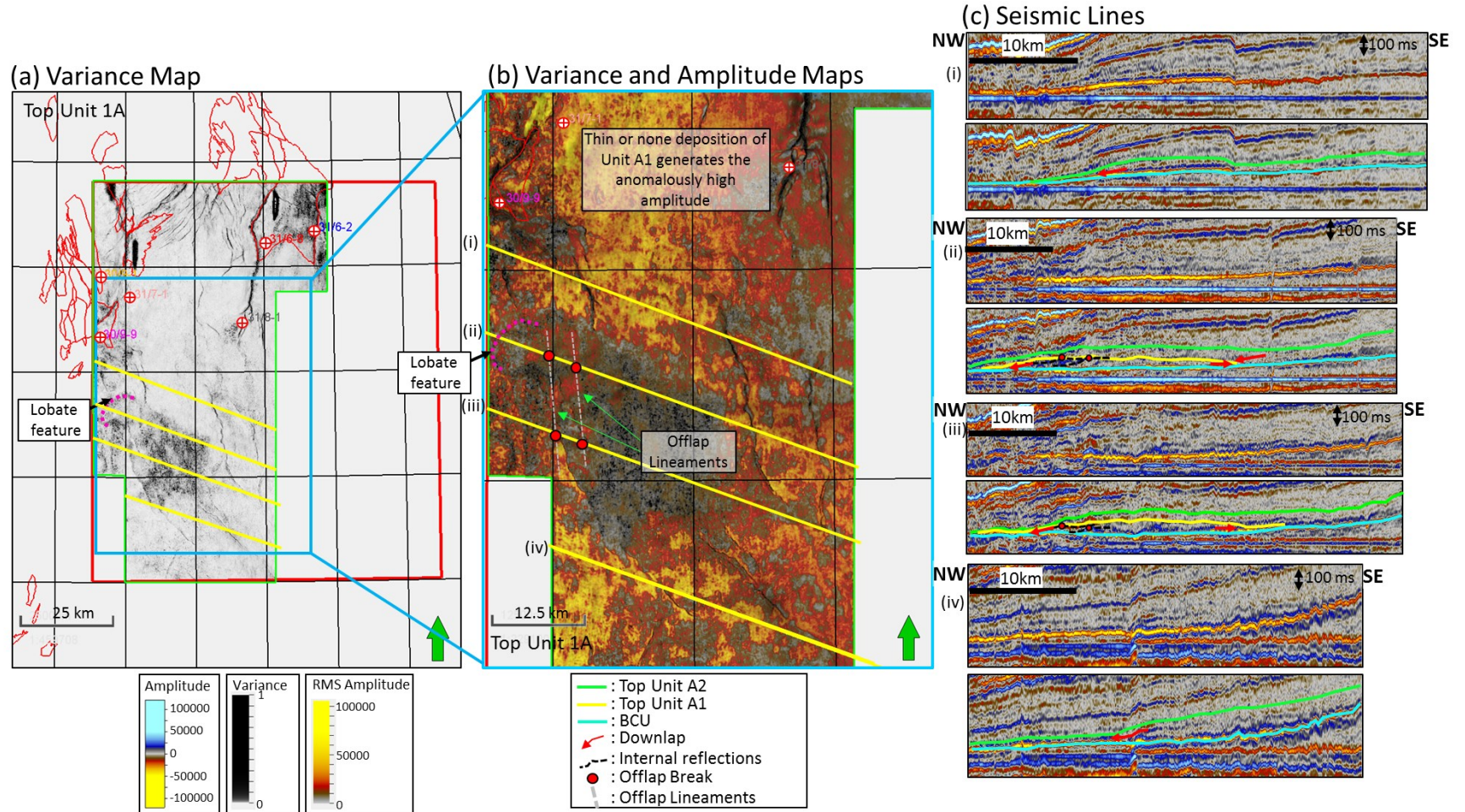
Figure 27: (a) Variance map, (b) variance and RMS amplitude maps, (c) two uninterpreted and two interpreted 3D northwest-southeast seismic lines showing the distribution of Unit A1 in the study area. The variance map shows the lobate geometry in the western part. The anomalously high amplitude surrounds this area is thought to be due to thin sediments or none deposition of Unit A1. The RMS amplitude map exhibits the offlap lineaments defined by high amplitude. Four seismic lines flattened on the Downlap Surface 0 (Heather Fm.) show the mounded shape in the seismic line (ii) and (iii), while the seismic lines (i) and (iv) display parallel reflections. The position of offlap breaks in the seismic lines fits with the north-south offlap lineaments in the RMS amplitude map. The mounded shape, lobate geometry, and offlap breaks position may represent a deep-marine basin-floor fan. The offlap lineaments record the offlap lineaments from the basin-floor fan. The area of this feature is approximately 25km in length, and 12 km in width with the thickest part of around 90 ms (~113 m).

55

The isochron map (Figure 26b) displays the northwestern-southeastern trend of Unit A1 depocenter, which is only located in the southwestern part of the study area. The maximum thickness of this unit reaching approximately 90 ms (~114 m). The dimension of this unit is around 25 km in length and 12 km in width (Figures 26b and 27).

5.1.1.1.4 INTERPRETATIONS

The strong trough amplitude of the BCU is interpreted as a response of high-impedance contrast between the Kimmeridge Clay Formation (organic-rich mudstones) and the Cretaceous limestones-claystones (Badley *et al., 1984*; Zachariah et al., 2009). For the Unit A1, the BCU reflection is the boundary between the underlying organic carbon-rich mudstones of the Draupne Formation, and overlying Lower Cretaceous sediment that has higher relative velocity.

The mounded geometry with the bi-directional downlaps, medium to high amplitude, and lobate geometry of Unit A1 (Figures 27a, 27c (ii), and 27c (iii)) indicates deposition of a deep marine basin-floor fan (Mitchum, 1985; Posamentier and Kolla, 2003). The lobate feature observed in the variance map, representing the different lithologies which is assumed between sandstone and background claystone. So, this geometry also supports basin-floor fan interpretation. In addition, the offlap lineaments with strong RMS amplitude (Figure 27b) can also be observed on the seismic data, indicating the offlap break of the prograding basin-floor fan.

The semi-continuous and continuous nature of the internal reflections in the Unit A1 suggest that the sediments were transported and re-deposited. In addition, the transition of reflections from semi-continuous in the basin margin to continuous in the basin center indicates that the sediments were re-deposited from the highs towards the lows of the basin.

There is a possibility sediment source was from the southeastern part of the study area (Øygarden Fault Complex), because both the trend of offset lineaments from the RMS amplitude map as well as the lobate features from the variance map confirm sediment source from the southeast and/or eastern part of the northern Stord Basin (Figure 27). In addition, paleogeography high was located in the eastern part of the study area and trend of depocenters is southeast-northwest (Figure 26b).

Even though there were some highs during this period (such as, the Oseberg and the Troll Fault Blocks, and the Bjørgvin Arc), Unit A1 is not found in close to that area and therefore does not fit with the trend of offset lineaments and of the lobate features defined in the variance map. This means that the structural high of the Øygarden Fault Complex, was active and was probably uplifted at this time causing sediment to re-deposit along its margins.

The limited distribution of this unit indicates a drop in the base-level at this time leading to an overall prograding seismic facies (Figures 27c (ii) and (iii)). The lowering base-level lead to the creation of less accommodation space, which focused the deposition to the topographically lowest area. In general, the BCU can be classified as the subaerial unconformity—since it represents the surface of erosion or none deposition under subaerial conditions (in the paleo-highs) or the correlative conformity—because there is no time gap between underlying and overlying sediments. In Unit A1, the BCU represents the correlative conformity since it is located in a more basinal setting. Top Unit A1 is similar to the intra lowstand systems tract surface, and it is the boundary between the forced regression and the normal lowstand regression. Unit A1 is equal with the falling-stage systems tract (FSST) (Catuneanu *et al.,* 2011)), as it is interpreted to be the result of a forced regressive event.

Overall, Unit A1 is interpreted to represent the Falling-Stage Systems Tract 1 (FSST 1) bounded by the Correlative Conformity 0 (CC 0) at its base (*i.e.,* the distribution of this unit is only in the basin center) and by the Intra Lowstand Systems Tract Surface 1 (ILSTS 1) at its top. This unit is thought to be representing basin-floor fan deposits of deep-marine depositional environment, with sediment sources coming either from the highs in the southeast and/or from the east of the study area (Øygarden Fault Complex).

Since there is no well penetrating this unit, the formation's name of Unit A1 refers to lithostratigraphic chart at Horda Platform from NPD, which is the Åsgard Formation (Figure 22). The seismic facies character may infer sandstone deposits as the lithotype for this unit, although a detailed study of the fan architecture needs to be conducted before this can be established. The dimension of this basin-floor fan is roughly up to 25 km in length, 12 km in width, and 90 ms (~113 m) in thickness (Figure 27).

5.1.1.2 UNIT A2

Unit A2 is the upper part of Unit A package, bounded at the base by the Top Unit A1 or the BCU and above by the Top Unit A2 (Figures 24a-c).

5.1.1.2.1 WELL LOGS

The characteristic of gamma ray response from Unit A2 varies slightly with the overlying formations (Figure 19). In almost all wells, gamma ray log shows coarsening upwards together with upward decreasing sonic values, transitioning from the underlying Draupne Formation to the overlying Cretaceous sediment. However, in the 30/9-9 well, gamma ray response displays significantly lower values (Figure 19). This is due to the limestone of Unit D directly overlying the BCU.

Towards the top of this unit, the boundary is identified by a change from low to slightly higher gamma ray values together with slightly increasing sonic value, which is not found in the wells 30/9-1 and 30/9-9 (Figure 19). The maximum thickness of this unit is 33 m in the 31/6-2 well.

The lithology description from three wells shows that this group consists of claystones. The claystones are characterized by varying in color from light olive grey, dark yellowish brown to moderate brown, light grey to medium light grey, in part olive grey, in part greenish grey, and they are soft, sticky, amorphous, very calcareous, and in part grading to argillaceous limestones.

5.1.1.2.1 SEISMIC OBSERVATIONS

As mentioned before, the character of the BCU reflection is a consistent, strong trough amplitude within the study area (Figures 24a-c). However, in some parts, the BCU reflection changes polarity to a peak or it is weakening in amplitude (Figure 24b). The BCU reflection records the conformable contacts between the underlying Late Jurassic and the Lower Cretaceous sediments, except on the structurally highs where the Lower Cretaceous sediments onlap and are therefore absent (Figure 24b). The 30/9-9 well indicates that the Heather Formation (Bathonian-Callovian? or 168.3-163.5 Ma) is directly overlain by Unit D in the Oseberg Fault Block (Upper Cretaceous (~99.6 Ma)) (Figures 19 and 24b). In addition, the

geometry of erosion and none deposition area follows the fault trends and they are therefore likely controlling the deposition, erosion and preservation of this unit. Other evidences are onlap of the overlying sediments onto structural highs and the truncation of the underlying sediments (Figure 24b).

The characteristic of Top Unit A2 reflector is a semi-continuous and low to medium peak amplitude (Figure 24c). This surface onlaps onto the highs (the Oseberg and the Troll Fault Blocks, and the Bjørgvin Arch) (Figure 24a) and it is truncated in the Øygarden Fault Complex area. The onlap and downlap features of the internal layers can be seen in Figure 24c. The seismic character of Unit A2 is progradational features, low to moderate amplitude with relatively continuous reflections. The progradational characteristic of Unit A2 can be only observed on 2D seismic line as foresets are not seen within 3D seismic area (Figure 28). The internal reflections of this unit downlap onto the assumed basin-floor with gently sigmoidal clinoform type (Figures 24c and 28). The offlap breaks are also identified in order to determine the character of the shelf-edge trajectory of this unit, which is ascending and concave-upward (Figure 28). The thickness of this unit becomes relatively thin towards north and northwest of the study area, where the BCU is shallower.

5.1.1.2.3 MAP AND OBSERVATIONS

The BCU time-structure map (Figure 25a) shows the topography of this surface in the study area. Still, the Oseberg and the Troll Fault Blocks, and the Øygarden Fault Zone were several active highs during this time. There were significant erosions in the Oseberg and Øygarden Fault Complex areas, while minor erosion took place in the Troll area (Figure 25a). The dipping direction of the BCU is towards southwest with the deepest part is around 2600 ms (~3285.1 m). Figure 25a displays the location of the faults that penetrated the BCU surface, which trend in N-S and NE-SW directions.

The time-structure map of Top Unit A2 (Figure 25c) illustrates the configuration and the distribution of this surface, which is dipping to the southwest of the study area. The deepest part of Top Unit A2 is approximately 2400 ms (~3032.4 m). The internal seismic reflections within Unit A2 onlap onto the paleo-high margins, such as the Oseberg and the Troll Fault Blocks, and

the Bjørgvin Arch. Compared to Top Unit A1, Top Unit A2 covers almost 2/3 of the study area. Several normal faults with NE-SW and N-S trends were still active during the deposition of this unit, affecting the distribution of Unit A2 (Figure 25c).
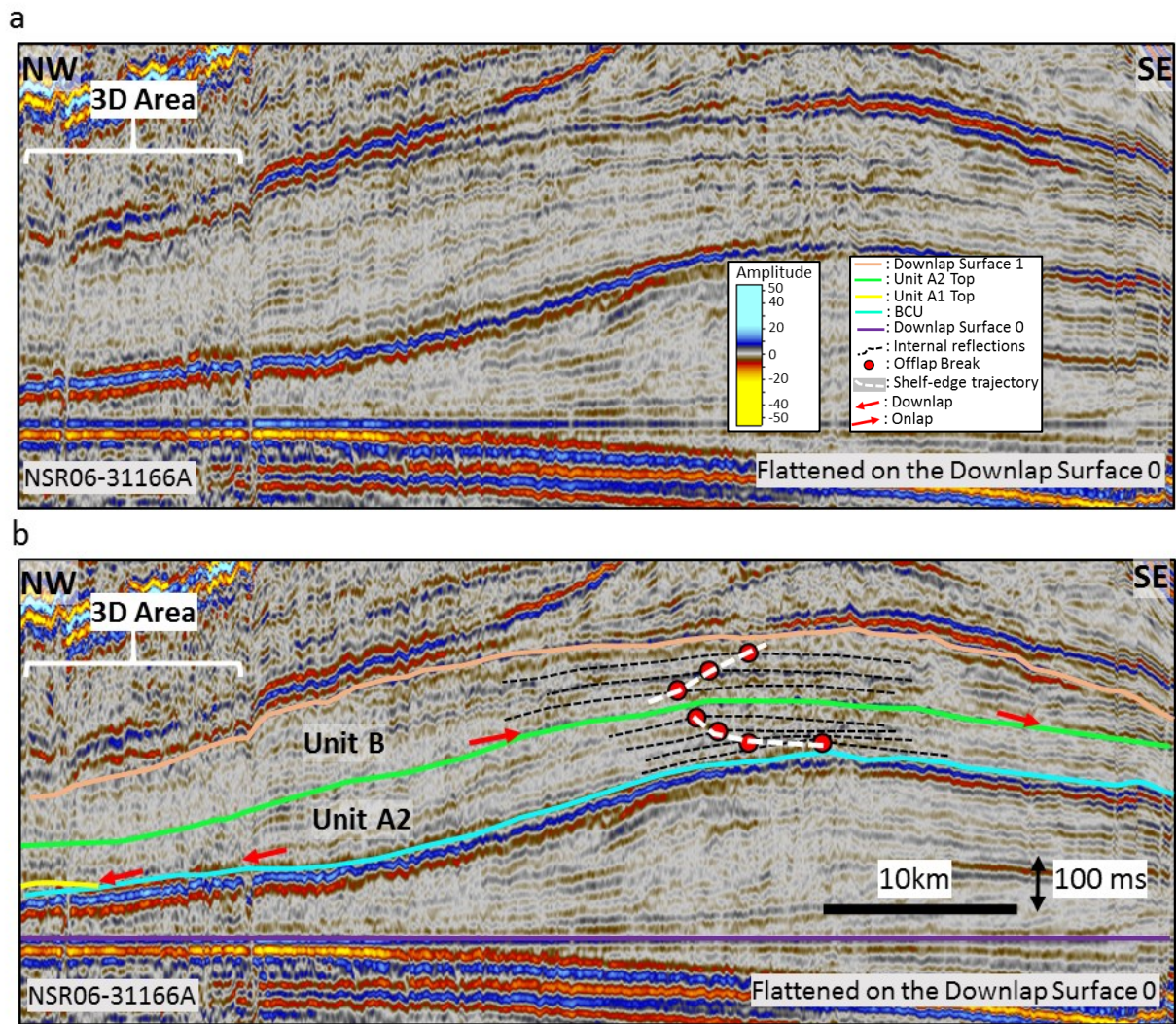
Figure 28: (a) Uninterpreted and (b) interpreted northwest-southeast 2D seismic lines representing the internal character of Unit A2 and Unit B. These seismic lines are flattened on the Downlap Surface 0 (Heather Formation). The progradation of the offlap breaks in Unit A2 exhibits ascending and concave-upward, which infers a lowstand normal regression (Catuneanu at al., 2011; Figure 9a). Whereas, the retrogradation of the offlap breaks in Unit B illustrates backstepping which suggest a transgressive accretionary (Hansen and Hampson, 2009; Figure 8c). The area of 3D seismic data is only in the western part of the seismic line. The location of the section is shown in Figure 23.

The isochron map of Unit A2 (Figure 26c) shows the depocenters location during deposition of this package. Two major depocenters were situated in the southwest and the south of the study area. The southwestern depocenter was bounded by two northwest-southeast faults while one northwest-southeast fault controlled the distribution of the southern depocenter (Figure 26c). The maximum thickness of this unit is about 160 ms (~202 m).

5.1.1.2.4 INTERPRETATIONS

The BCU reflection is the horizon that is easily identified in the crestal, slope, and basinal areas of the northern Stord Basin. For Unit A2, the BCU reflection is interpreted as the boundary between the underlying organic carbon-rich Draupne Formation mudstones and the overlying Lower Cretaceous marls and calcareous siltstones of the Unit A2 (Figures 19 and 22). In places where the BCU reflection weakens in amplitude or changes polarity to a peak, is interpreted to represent the erosional juxtaposition between non-Draupne shale against the Cretaceous interval (Figure 24b).

The 30/9-9 well shows that Unit D package (Upper Cretaceous (99.6 Ma)) directly overlies the Middle Jurassic Heather Formation (Bathonian-Callovian? or 168.3-163.5 Ma). This means that there was a significant time gap in the Oseberg Fault Block. The roughly time gap is at ~64 million years. The erosion in the Oseberg and the Troll Fault Blocks, Bjørgvin Arch, and Øygarden Fault Complex areas show that these highs were still active and acted as the sediment sources during deposition of Unit A2 package. These highs were the inherited structures from the previous tectonic episodes and seem to have controlled the deposition of Units A1 and A2.

The sediment source of southwestern depocenter was likely from the Bjørgvin Arc and Oseberg Fault Blocks, whereas the southern depocenter probably derived sediments from the Øygarden Fault Complex area. An intra-high between these depocenters (Figure 26c) means that the sediment source was probably not the same. According to Fossen *et al.* (2016), the north-south faults formed during the Permo-Triassic rifting phase in the northern North Sea and were reactivated during the Jurassic rifting phase, which also generated some of the northeast-southwest normal faults. These faults can still be observed at the BCU and Top Unit A2.

The progradation features, seen in NSR06-31166A 2D seismic line after flattened on Downlap Surface 0, represent the ascending and concave-upward shelf-edge trajectory (Figure 28). This trajectory has a similar pattern to lowstand normal regression (Catuneanu *et al.,* 2011; Figure 9a), which is interpreted as the rate of aggradation increases with time and the rate of progradation decreases with time. Therefore, Unit A2 is equated with the lowstand systems tract. Top Unit A2 can be classified as the maximum regressive surface or the transgressive surface separating the lowstand normal regression to transgression, based on Catuneanu *et al.* (2011). The dominant low amplitude, relatively lateral continuity of the reflections, and claystone descriptions from well data indicate that this unit is composed of mud-rich pelagic and hemipelagic deposits.

Overall, Unit A2 is interpreted to be the Lowstand Systems Tract 1 (LST 1), which is bounded at the base by the Intra Lowstand Systems Tract Surface 1 (ILSTS 1) or the Subaerial Unconformity 0 (SU 0) or Correlative Conformity 0 (CC 0) and above by the Transgressive Surface 1 (TS 1) (Figure 36). Unit A2 corresponds to the Åsgard Formation, which is by the well 31/8-1 recorded as the deposition of Åsgard mudstones (Figure 22). This unit is interpreted to have been deposited in a shelfal to slope marine environment during a gradual relative sea-level rise, which was controlled by the sediments were deposited further to the east. Due to the rising base-level, the accommodation space increased that lead to a change from progradational to aggradational patterns.

5.1.2 UNIT B

Unit B package comprises the Latest Berriasian to Early Hauterivian succession (140.2-133.9 Ma). This unit is bounded at the base by the Top Unit A2 and at the top by the Downlap Surface 1.

5.1.2.1 WELL LOGS

The typical gamma ray response of Unit B is fining upward together with upward increasing sonic log within this unit, based on three key wells (31/8-1, 31/6-8, and 31/6-2) (Figure 19).

The top of this unit is defined as the maximum gamma-ray value combined with high sonic data, except in the 30/9-1 and 30/9-9 wells (Figure 19). The maximum thickness of this unit based on key wells is around 118 m in the 31/8-1 well.

The lithology description from the 31/8-1 well shows that Unit B consists of claystones. The claystones are olive grey, moderate brown, occasional light grey to medium dark grey, light greenish grey in parts, soft, sticky, amorphous to occasional sub-blocky, very calcareous and grading to argillaceous limestone, no pyrite to locally trace pyrite nodules.

5.1.2.2 SEISMIC OBSERVATIONS

The character of the Downlap Surface 1 is a semi-continuous, low to medium peak amplitude (Figures 24a-c and 28). This surface onlaps onto some paleo-highs, such as the Oseberg Fault Block (Figure 24b), the Troll Fault Block (Figure 24a), the Bjørgvin Arch, and it is truncated in the Øygarden Fault Complex area (Figure 24c). The typical internal reflections of Unit A2 is semi-continuous, sub-parallel to convergent, low amplitude, and with low frequency. The internal reflections show onlap features towards the basin flanks which moves eastward (Figure 24c). The thickness of Unit B is thinner in the western part than in the eastern part (Figure 24c), where the internal reflections of this unit onlap directly onto the Top Unit A2 (Figure 24a-c).

Figure 28B shows the offlap break positions of the internal reflections of Unit B. The seismic line (Figure 28B) displays the offlap breaks moving gradually towards the basin margin, which represents a backstepping trend.

5.1.2.3 MAPS AND OBSERVATIONS

The Downlap Surface 1 time-structure map (Figure 25d) shows the dipping direction of this surface, which is towards southwest of the study area. The Oseberg and the Troll Fault Blocks, and the Øygarden Fault Complex were still highs during this time, while the Downlap Surface 1 covered the Bjørgvin Arch. The intensity of erosion seems to be less, compared to Top Unit A2 in the Oseberg and Troll Fault Blocks (Figure 25d). The deepest part of this surface is approximately 2600 ms (~3285 m). The NE-SW and N-S faults in the north were still active

and were still controlling the distribution of this unit. The minor NW-SE faults seems not to be active anymore during deposition of unit B.

The isochron map of Unit B (Figure 26d) illustrates the location of main depocenters during deposition of this package. The depocenter of Unit B was located in the south of the study area, while two minor depocenters were in the southeastern part of the study area and in the hanging wall of the Troll Fault Block. A northwest-southeast fault bound the sediments in the southern depocenter. There is an intra high located between the southern and the southeastern depocenters. In the Troll Fault Block, the fault affected the location of depocenters in hanging wall of this block. The maximum thickness of this unit is approximately 160 ms (~202 m).

5.1.2.4 INTERPRETATIONS

The onlap features and erosion in the Troll and Oseberg Fault Blocks, and Øygarden Fault Complex areas infer that these paleo-highs were active and uplifted during the Latest Berriasian to Early Hauterivian (140.2-133.9 Ma), while the Bjørgvin Arch had been covered by sediments of Unit B during this time. The sediment sources for the southern and southeastern depocenters were probably from the Øygarden Fault Complex whereas origin of the sediments of the Troll depocenters were from the Troll and Oseberg highs.

The retrogradational stacking pattern of this unit identified in the NSR06-31166A 2D seismic line when flattening on Downlap Surface 0, shows the backstepping (Figure 28B). These forms have similar trends with the transgression patterns of Hansen and Hampson (2009; Figure 8c), which is interpreted as accretionary transgression. It is a resulf of the relatively high gradient and morphology of the depositional foundation that existed at the start of the transgression. The backstepping features are also driven by relative sea-level rise causing the accommodation space to be higher than the sediment supply. In addition, the gamma ray pattern shows fining upwards, representing retrogradational stacking pattern (Figure 19). Therefore, Unit B can be classified as the transgressive systems tract (TST) according to Hansen and Hampson (2009) based on the stacking pattern and trajectory position (Figure 28B). This unit was deposited during the initiation of the transgressive event to the period of the maximum transgression. The Downlap Surface 1 is equal to the maximum flooding surface according to Catuneanu *et al.*

(2011) because it represents the end of the transgressive events. Also, downlap features of the highstand clinoform overlay this unit.

Overall, Unit B is interpreted as the Transgressive Systems Tract 1 (TST 1), bounded by the Transgressive Surface 1 (TS 1) at the base and by the Maximum Flooding Surface 1 (MFS 1) above (Figure 36). This unit represents the Åsgard Formation in the well 31/8-1 (Figure 22), indicating shelfal conditions with pelagic depositional environment, which was deposited until the maximum sea-level rise. It is also highlighted by the depocenters position retreating landward.

5.1.3 UNIT C

Unit C seismic package consists of the Early Hauterivian to Early Cenomanian deposits (140.2-133.9 Ma). The Downlap Surface 1 forms the base and the Unconformity 1 above bound the top of this unit.

5.1.3.1 WELL LOGS

In general, the character of gamma ray response of Unit C is coarsening upwards and is more irregular in nature for this unit. The sonic log shows a slight upward decrease in value within this interval (Figure 19). The top of this unit is defined by the low gamma ray value combined with low sonic values (except the 30/9-9 well) (Figure 19). In general, Unit C shows coarsening upwards of all four wells within the study area. The maximum thickness of this unit from key well data is around 73 m in the 31/8-1 well. The unconformity evidence is found in the 31/6-3 well in the Troll Fault Block (Figure 22).

The lithology description from four wells shows that this unit consists of claystones, marls, limestone stringers, and occasional dolomites. The characteristics of claystones are medium light grey to medium dark grey, sometimes medium light grey, blocky, crumbly, firm, very calcareous and grading to limestone, silty, microcrystalline to very fine crystalline calcite, non-glauconitic. The typical marls are medium grey to olive grey, medium light to light grey, soft to moderately hard, micro-pyrite, locally argillaceous grading to claystone. The limestone

stringers are characterized by white to medium grey, occasional olive grey, locally grading to marls, hardly microcrystalline. The typical dolomites are dark yellowish brown, blocky, and firm to hard.

5.1.3.2 SEISMIC OBSERVATIONS

The typical character of the Unconformity 1 reflection in Unit C is a strong trough amplitude, relatively continuous, and have consistent character within the study area (Figures 24a-c). The Unconformity 1 reflection onlaps towards the Oseberg Fault Block (Figures 24b) but it is truncated towards the Troll Fault Block and Øygarden Fault Complex (Figures 24b-c). There are erosional features in the Troll Fault Block where it was eroding the top of this unit (Figure 24b). The typical internal reflections of Unit C are continuous to semi-continuous reflection, gentle sigmoidal clinoforms, medium to low amplitude, and low frequency. The downlap features of this unit seems clearly in both 2D and 3D seismic data (Figures 24b, 24c, 29, and 30).

The erosional activity of Unit C occurred intensively in the Troll Area. This can be observed in the seismic cross sections in Figures 24b and 29. Figure 29 displays the variance map and the RMS amplitude maps of this unit, as well as two 3D seismic lines. From this figure, it can be clearly observed the NNW-SSE discontinuity lineaments in the variance attribute map, whereas the RMS amplitude map displays the only slight variation. Two seismic lines crossing these discontinuity lineaments show the progradational features of internal reflections within Unit C, which downlap onto the Downlap Surface 1. When flattening these seismic lines on the Downlap Surface 1, it can be observed the thickness difference between hanging wall and footwall of this unit in the Troll Area. Also, the truncation of the internal reflections can be seen in the eastern part of the seismic line in this group (Figure 29c (i)). The erosional thickness measured from topset within the Unit C to the Unconformity 1, which is 110 ms (~139 m; Figure 29c (i)). Figure 29c (ii) exhibits the progradational pattern of the seismic facies of this unit that is consistent with gamma-ray signature found in wells.
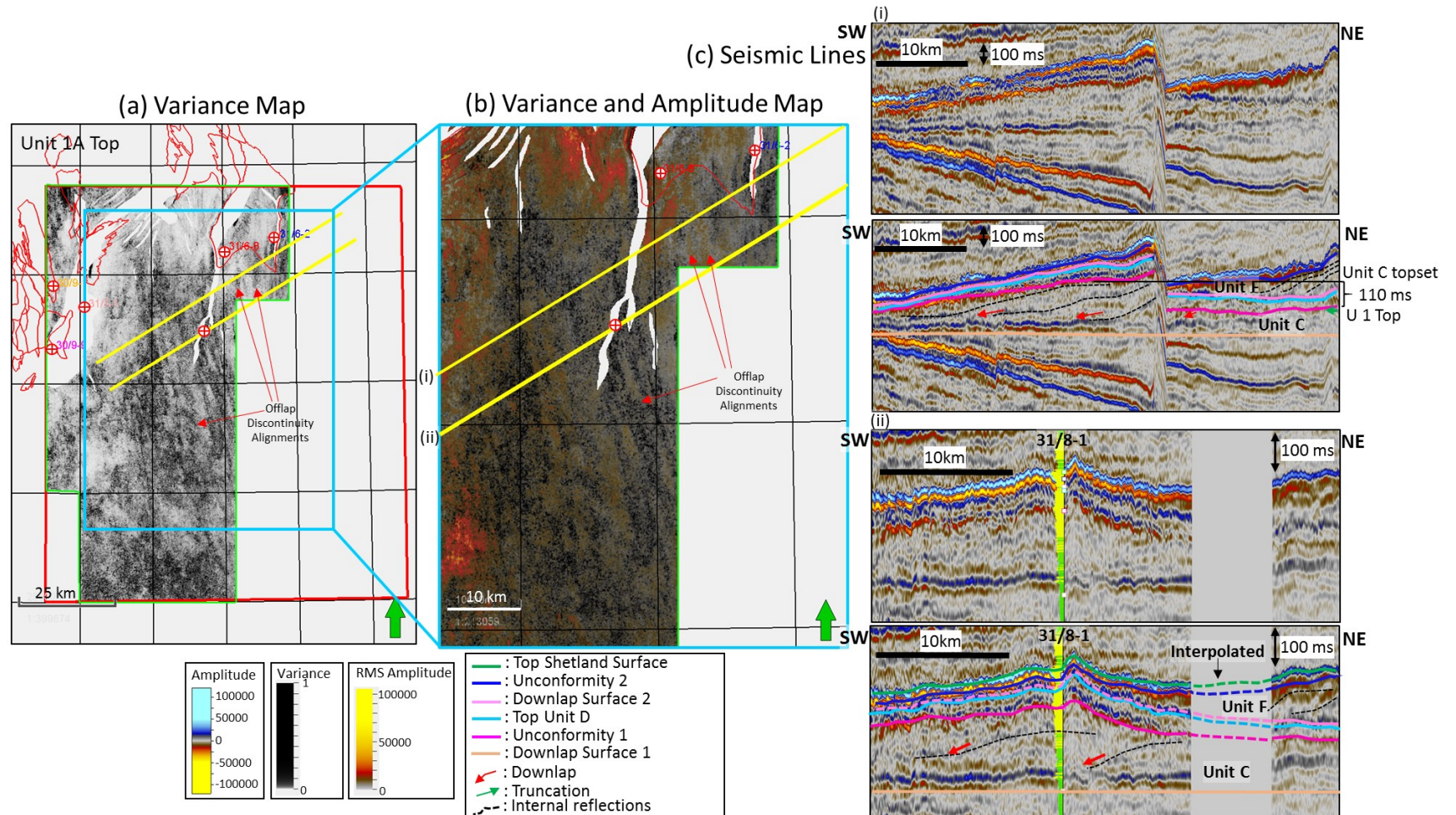
Figure 29: (a) Variance map, (b) variance and RMS amplitude maps, (c) two uninterpreted and two interpreted southwest-northeast 3D seismic lines illustrating the internal character of Unit C in the study area. The variance map exhibits the offlap discontinuity alignments with the northwest-southeast trend. The RMS amplitude map displays offlap discontinuity alignments defined by high amplitude values. The progradation of this unit can be observed in the seismic lines (i) and (ii), which are both flattened on the Downlap Surface 1. The seismic line (i) defines the thickness of erosion of this unit measured from Unconformity 1 Top to Unit C topset, which is 110 ms (~138 m). The truncated feature representing the erosion can be observed on the right side of seismic (i). The erosional activity is proved by the significant thickness difference between hangingwall and footwall blocks. The seismic line (ii) is crossing the 31/8-1 well (with gamma ray log) showing the similar progradational character between well and seismic interpretation.
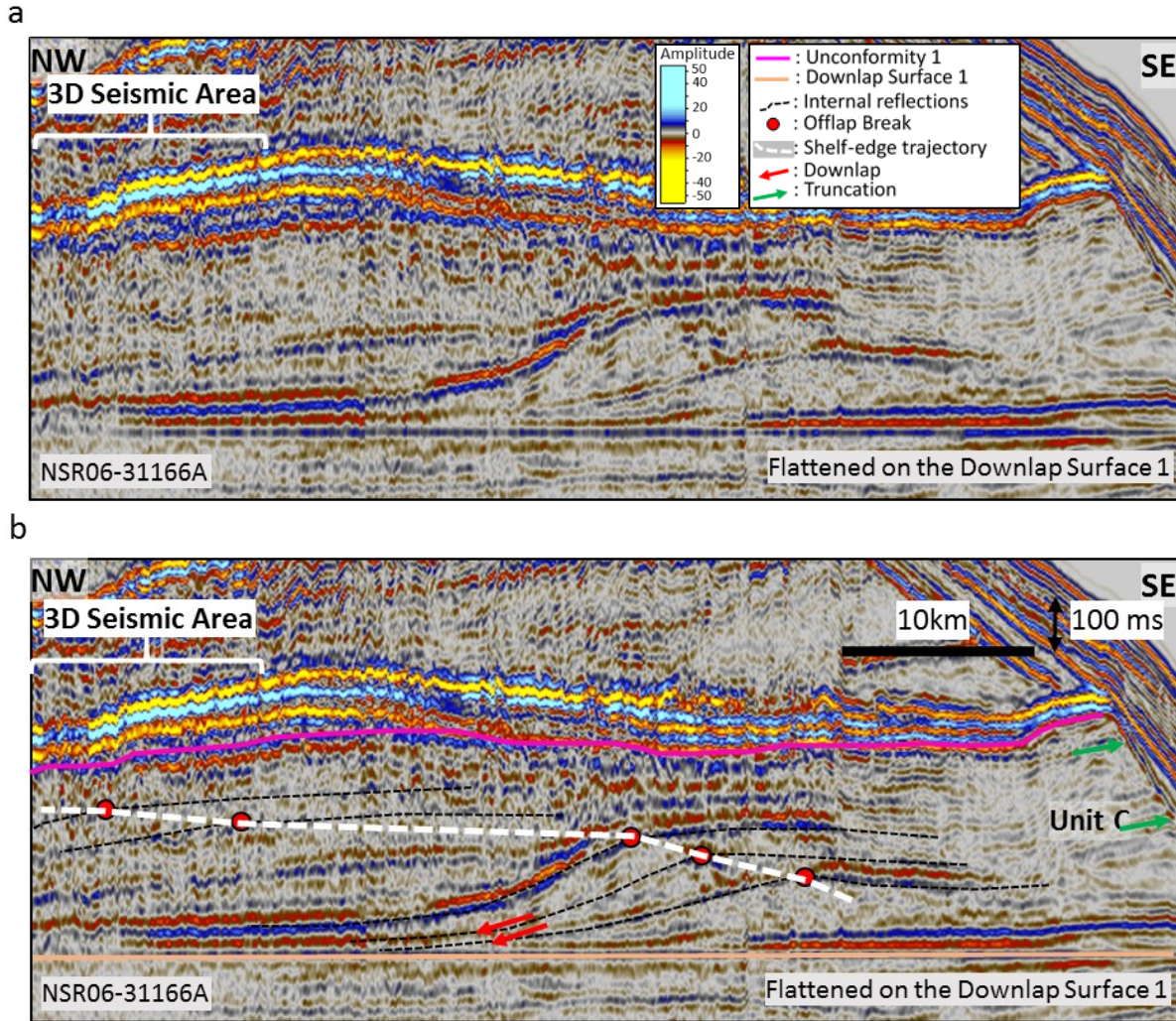
Figure 30: (a) Uninterpreted and (b) interpreted northwest-southeast 2D seismic lines representing the internal seismic character of Unit C. The seismic line is flattened on the Downlap Surface 1. The interpreted offlap breaks is observed as ascending and convex-upward, which represent highstand normal regression (Catuneanu et al., 2011; Figure 9b). The downlap features of the internal reflections can be observed on the western side of the seismic line, while the truncated shape can be identified on the eastern side of the seismic line. The location of the section is shown in Figure 23.

Figure 30 displays a northwest-southeast 2D seismic line flattened on the Downlap Surface 1. It shows the progradational stacking pattern of the internal reflections of Unit C, which downlaps onto the Downlap Surface 1. The offlap breaks determine the shelf-edge trajectory of this group, exhibiting the ascending and convex-upward (Figure 30). The thickness of this unit decreases towards the paleo-highs in the Troll and Oseberg Field areas.

68

5.1.3.3 MAPS AND OBSERVATIONS

The Unconformity 1 time-structure map (Figure 25e) illustrates the dipping direction of this surface that is towards the southwest of the study area. The paleo-highs during the deposition of this unit were the Oseberg and the Troll Fault Blocks, and Øygarden Fault Complex, which is proven by onlap and erosional features onto these highs (Figure 25e). The deepest part of the Unconformity 1 is around 2400 ms (~3032 m). The activity of the faults decreased during this time, except in around the Troll Fault Block and Øygarden Fault Complex.

The isochron map of Unit C (Figure 26e) shows the southeastern area of the study area as the location of this unit depocenters and trending northwest-southeast to west-east. This unit thins towards the north and west. Unit C is the thickest package of the Cretaceous interval, which can reach approximately 350 ms (~442 m).

5.1.3.4 INTERPRETATIONS

The erosional features observed in the Oseberg and Øygarden Fault Complex area suggest that these areas were still active during the Early Hauterivian to Early Cenomanian (133.9-99.6 Ma). The dominant contributor to sediment supply was the Øygarden Fault Complex inferred by the north-northwest offlap lineaments (Figures 29b and 29c). As mentioned before, Unit C is the thickest unit of the Cretaceous strata, which means that large amount of sediments was delivered to the basin most likely from the Øygarden Fault Complex and the eastern Norway during this time.

The seismic lines show the thickness difference between hangingwall and footwall block in the Troll Area of around 110 ms (~139 m; Figure 29c). The sediments are thinner in the footwall block rather than in the hanging wall block of the Troll Fault Block. The thickness difference is probably due to the footwall uplift after deposition of Unit C. The uplifting lead to erosion of Unit C sediments deposited on the footwall block. This is supported by the truncation features at top of this unit on the footwall block (Figure 29c (i)). In addition, the progradational features observed on the hangingwall and footwall block of the Troll Fault infer that this fault was active after deposition of Unit C (Figures 29c (i) and (ii)).

A 3D seismic line crossing the 31/8-1 well illustrates the similar progradational pattern of Unit C. The lithology of this unit from the 31/8-1 well description is claystone, which is grading to silty claystone, inferring that this well is representing the distal deposits of the potential sand-rich clinoform.

The progradational stacking pattern of Unit C is also shown in the NSR06-31166A 2D seismic line after flattening on the Downlap Surface 1. It displays the ascending shelf-edge trajectory with convex-upward shape, which is interpreted as a highstand normal regression (Catuneanu *et al.,* 2011; Figure 9b). This forms due to higher sediment supply than accommodation space during the last stage of relative sea-level rise. The Unconformity 1 can be identified as the subaerial unconformity based on Posamentier *et al.* (1998) as it represents the none deposition or erosion on the highs, and/or the correlative conformity where there is no time gap between underlying and overlying sediment.

Unit C is the Highstand Systems Tract 1 (HST 1), bounded by the Maximum Flooding Surface 1 (MFS 1) at the base and the Subaerial Unconformity 1 (SU 1) or the Correlative Conformity 1 (CC 1) at the top (Figure 36). This unit represents the upper part of the Åsgard, Sola, and Rødby formations (Figure 22). This unit records the shelf edge with possible sand sheet on the shelf and mud-prone on the slope, which is supported by siltstones in the well 31/8-1. The interpreted sandstone lithology on the shelf is predicted as time equivalent to the Agat sandstone, but no wells have penetrated any sandstones in this unit.

5.1.4 UNIT D

The Unconformity 1 forms the base of Unit D and the Top Unit D forms the upper boundary of the Unit D. This unit was deposited during the Early to Late Cenomanian period (99.6-94 Ma).

5.1.4.1 WELL LOGS

The typical gamma ray response of Unit D is a fining upward combined with slightly increasing sonic log (Figure 19). At the top of this package, the gamma ray response moves rapidly from

low to high gamma ray values followed by increasing sonic log. The maximum thickness based on key wells is 60 m in the 31/8-1 well.

The lithology description from five wells shows that this unit consists of claystones, marls, and limestones at the bottom. The 31/8-1, 31/6-8, and 31/6-2 wells are dominated by claystones and marls, while the 30/9-1 and 30/9-9 wells are dominated by limestones. The typical claystones are medium light grey, light grey, firm to moderately hard, blocky, very calcareous and grading to limestone, silty, disseminated glauconite, and in part abundant glauconite. The characteristics of limestones are very light grey to light grey, soft to firm, non-argillaceous to very argillaceous and in part grading to marls, no glauconite to abundant glauconite, and microcrystalline. The typical marls are light to medium grey and soft to firm.

5.1.4.2 SEISMIC OBSERVATIONS

The character of Top Unit D is a semi-continuous, low to medium peak amplitude (occasional high amplitude) (Figure 24c). The paleo-highs during deposition of Unit D were the Oseberg Fault Block and Øygarden Fault Complex. Top Unit D onlaps towards the Oseberg Fault Block (Figure 24b) and is truncated in the Øygarden Fault Complex area (Figure 24c). Both 2D and 3D seismic data shows downlap features within this unit (Figures 24c and 31). The internal reflections display continuous to semi-continuous, medium to low amplitude, occasional high amplitude, and low frequency. The progradation of internal reflections can be clearly seen in 2D seismic lines, in particularly when flattening on the flooding surface beneath of this unit (Figure 31). The reflection configuration of this unit consists of gentle sigmoidal clinoforms. The shelf-edge trajectory of Unit D is ascending and concave-upward based on the offlap breaks position within this unit (Figure 31).

In the western part of the study area, the internal reflections of Unit D represent high peak amplitudes (Figure 24b). It is very different with its character in the eastern part, which is low to medium amplitude (Figure 24b).

5.1.4.3 MAPS AND OBSERVATIONS

Top Unit D time-structure map (Figure 25f) shows the distribution and the configuration of this surface, where it is dipping towards southwest. The mapped paleo-highs during this time were the Oseberg Fault Block and the Øygarden Fault Complex areas, where this unit is absent. The deepest part of Unit D is approximately 2400 ms (~3032 m; Figure 25f). The subcrop area on top of the time-structure map shows no deposition of this unit in some parts of the Oseberg Fault Block. The north-south trending faults can still be observed to be active during deposition of this unit (Figure 25f).

The isochron map of Unit D (Figure 26f) displays the location of depocenters of this unit that is in the eastern part of the study area. Unit D thins towards the south and the west. The thickest part of this unit reaches around 130 ms (~164 m).

5.1.4.4 INTERPRETATIONS

The onlap features onto the Oseberg Fault Block and truncated reflections in the Øygarden Fault Complex infer that these highs were still active during the Cenomanian period. The large area of the non-deposition or erosion of Top Unit D in the Oseberg Fault Block illustrates this (Figure 25f). This means that the Oseberg Fault Block was uplifted during this time. The Øygarden Fault Complex was most likely the sediment source for this unit, where the thickest part is located in the eastern part of the study area (Figure 26f). The progradational stacking pattern of the internal reflections is clearly seen in the southwest-northeast 2D seismic line, which is potentially proves it (Figure 31).

The dominant medium to low amplitude, continuous to semi continuous of the reflections, low frequency seismic characteristic, and claystone description from well data indicate that this unit consists of mud-rich lithology of the pelagic and hemipelagic deposits. The high amplitude internal reflections are related to the limestones. This typical high amplitude reflections are dominant in the western part of the study area compared to the eastern part, particularly in the Oseberg Fault Block. This means that there is different lithologies between these two areas. Well data also support assumption, which are showing limestone deposits in the Oseberg Fault Block, while claystone to marls sediment are observed in the Troll Fault Block (Figure 19).

Figure 31: (a) Uninterpreted and (b) interpreted northeast-southwest 2D seismic lines, flattened on flooding surface beneath of this unit, showing the internal seismic character of Unit D. The progradation of offlap breaks are ascending and concave upward representing lowstand normal regression (Catuneanu et al., 2011; Figure 9a). The downlap features can be observed towards the basin in the seismic line. The location of the section is shown in Figure 23.

The ascending and concave-upward of Unit D's shelf-edge trajectory is interpreted as a lowstand systems tract (Catuneanu *et al.,* 2011; Figure 9a). This represents decreasing rate of progradation and increasing rate of aggradation. Top Unit D is categorized as the transgressive surface or the maximum regressive surface (Catuneanu *et al.,* 2011) as it bounds the lowstand normal regression and the transgression.

Overall, Unit D represents the Lowstand Systems Tract 2 (LST 2), which is bounded at its base by the Subaerial Unconformity 1 (SU 1) or Correlative Conformity 1 (CC 1) and at its top by the Transgressive Surface 2 (TS 2) (Figure 36). This unit is related to the Svarte Formation (Figure 22), and it was deposited in the distal shelf setting. Well data in the Oseberg Fault Block show that this unit is dominated by limestone in the Oseberg area, while well data from the Troll Fault Block show claystones. It is inferred that the limestone could be deposited due to lack of siliciclastic sediment in the Oseberg Fault Block, while small amount of sediments in the eastern area was still delivered from the Øygarden Fault Complex.

5.1.5 UNIT E

Unit E seismic package comprises the Late Cenomanian to Early Turonian sediments (94-93.6 Ma) and is bounded by the Top Unit D at the base and the Downlap Surface 2 at the top.

5.1.5.1 WELL LOGS

Unit E shows fining upwards combined with slightly increasing sonic log (Figure 19). Towards the upper part of this unit, the Downlap Surface 2 is determined as the highest gamma-ray value correspond with high sonic log data. The thickness of this unit is very thin, where the thickest deposit based on key well data is only 15 m from the 31/6-8 well.

The lithologic description from all five wells shows that this unit consists of claystones. The characteristics of the claystones are olive black, very light grey, firm to moderately hard, blocky calcareous, silty, and in part slightly glauconitic.

5.1.5.2 SEISMIC OBSERVATIONS

The characteristic of the Downlap Surface 2 is a semi-continuous and low to medium peak amplitude (Figures 24a-c and 32). This surface drapes over almost all the structures (The Oseberg and The Troll Fault Blocks, and The Bjørgvin Arch), except in the Øygarden Fault Complex. The Downlap Surface 2 is truncated in the Øygarden Fault Complex area (Figure

24c). The character of internal reflections of Unit E is sub-parallel, semi-continuous to convergent, low-amplitude, and low frequency (Figure 32). The onlap features can only be observed on 2D seismic lines, as this unit is very thin in the 3D seismic area (Figures 24a-b and 32). These features step gradually toward the eastern part of the study area.

Figure 32 illustrates a northeast-southwest 2D seismic line flattened on a flooding surface beneath this unit. The internal reflections of this unit can be traced, though they are subtle due to low amplitude. The offlap breaks show the backstepping patterns, which are moved toward the northeast.

5.1.5.3 MAPS AND OBSERVATIONS

The Downlap Surface 2 time-structure map (Figure 25g) shows the dipping direction of this surface, which is toward southwest. The Downlap Surface 2 covered almost all the structural highs in the study area, except the Øygarden Fault Complex (Figure 25g). The deepest part of the Downlap Surface 2 is around 2400 ms (~3032.4 m), with some of the major N-S and NE-SW faults still active during the formation of this surface (Figure 25g).

The isochron map of Unit E (Figure 26g) illustrates the position of the main depocenter during the Late Cenomanian-Early Turonian (94-93.6 Ma). The main depocenter of Unit E was located in the northeastern part of the study area (Figure 26g). An area of non-deposition occurs in Unit E isochron map because Top Unit D was not present in that location. In general, the sediments were delivered towards the southwest, where the thickest part is only 70 ms (~88 m). The sediment source area for this unit was most likely from the Øygarden Fault Complex.

5.1.5.4 INTERPRETATIONS

The onlap features of the Downlap Surface 2 in the Troll and the Oseberg Fault Blocks are interpreted to be caused by thickness. The thickest sediment of this unit, which can be observed in the well data is only 15 m. The 30/9-9 well is located on the high of the Oseberg Fault Block with the thickness of this package is only 6 m (Figure 21). This thickness is below vertical

seismic resolution used in the study, which is 26 m (Table 2). Since the seismic resolution is higher than the thickness of this unit, the reflection does not represent this group individually.
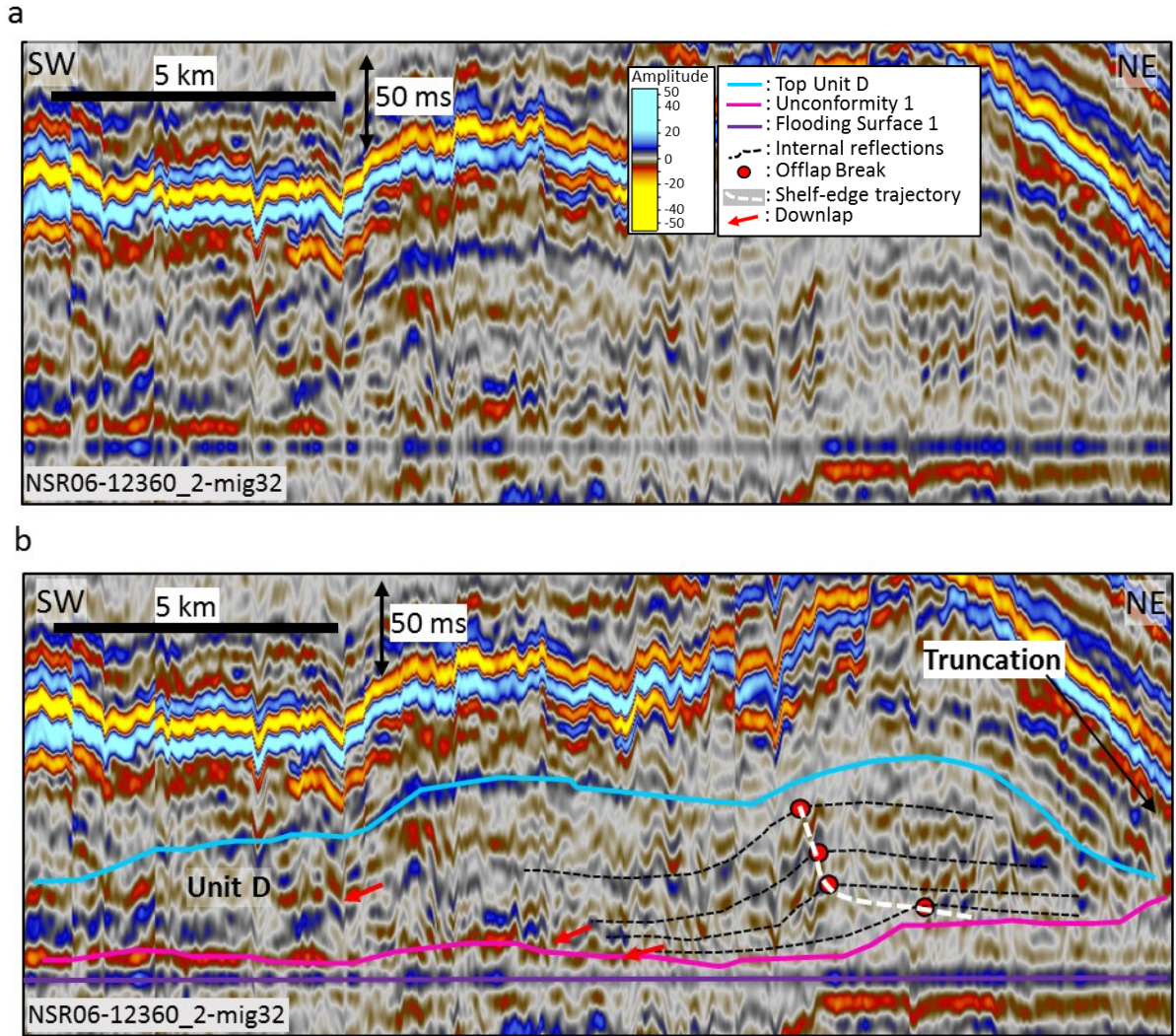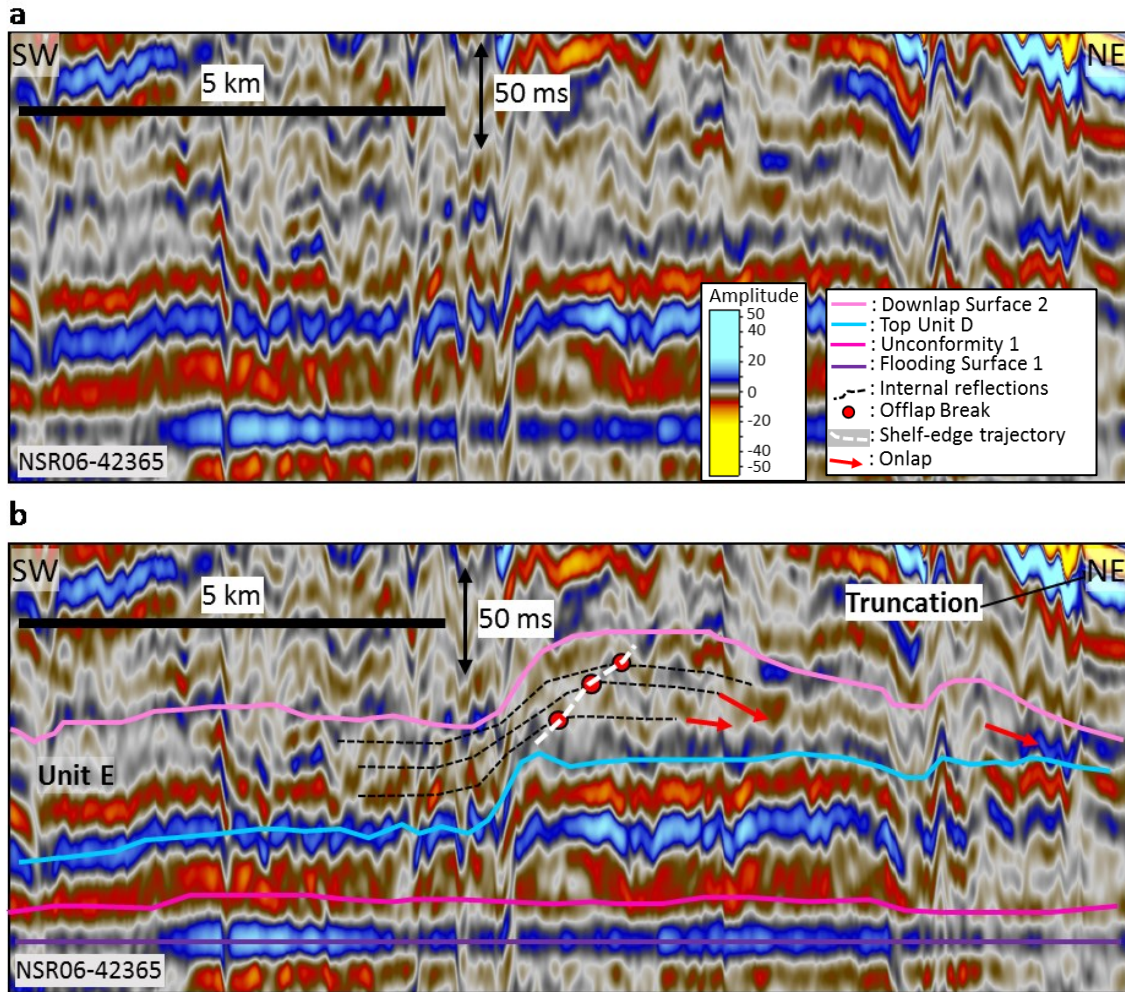

Figure 32: (a) Uninterpreted and (b) interpreted northeast-southwest 2D seismic lines, flattened on flooding surface beneath of this unit illustrating the internal character of Unit E. The offlap breaks show retrogradational stacking pattern representing accretionary transgression according to Hansen and Hampson (2009) (Figure 8c). This stacking pattern of this unit is only clearly seen in northeast 2D seismic lines. The location of the section is shown in Figure 23.

Still, the sediment source for this unit is thought to be from the Øygarden Fault Complex and the Norwegian mainland. The erosional area was approximately the same as before (Figure 25g), which resulted in minor amounts of sediment deposited. However, this unit is the first in Cretaceous to drape all the structural highs in the northern Stord Basin area, except the

Øygarden Fault Complex, and this infer a drowning of the entire area related to a relative sea-level rise.

A 2D seismic line in the northeastern part of the study area illustrates the backstepping of Unit E. This shape is similar with accretionary transgression from Hansen and Hampson (2009) (Figure 8c). The accretionary shape was most likely formed due to the high gradient of the inherited structures during sedimentation. The previous deposits of Unit D created progradational features, which affected the deposition of Unit E. In addition, the backstepping shape was probably influenced by relative base-level rise causing the rate of accommodation space being greater than rate of sediment supply. The decreasing rate of sediment supply could have been triggered due to limited subaerial paleo-highs as the existing highs were flooded. Also, the gamma ray fits this interpretation as it consists of a retrogradational stacking pattern (Figure 19).

Accordingly, Unit E can be classified as the transgressive systems tract (TST) from Hansen and Hampson (2009) based on the backstepping trajectory. This unit was most likely deposited at the beginning of the transgressive event until the maximum flooding period. The Downlap Surface 2 is consistent with the maximum flooding surface from Catuneanu *et al.* (2011) as it bounds the top of the transgressive unit and the base of the succeeding highstand clinoform unit.

In summary, Unit E forms the Transgressive Systems Tract 2 (TST 2), bounded by the Transgressive Surface 2 (TS 2) at the bottom and by the Maximum Flooding Surface 2 (MFS 2) at the top during the Late Cenomanian to Early Turonian time (94-93.6 Ma) (Figure 36). This unit corresponds to the Blodøks Formation penetrated in the 31/8-1 well (Figure 22).

5.1.6 UNIT F

Unit F seismic package comprises the Early to Late Turonian sediments (93.6-88.6 Ma). It is bounded by the Downlap Surface 2 at its base and by the Unconformity 2 at its top.

5.1.6.1 WELL LOGS

The typical gamma ray log of Unit F is coarsening upward with slightly decreasing sonic log values (Figure 19). The boundary at the top of this unit is represented by an abrupt decrease of the gamma ray values. The maximum thickness of Unit F is around 118 m in the 31/8-1 well.

According to lithology description from all five wells, this unit consists of marls or claystones (silty) with occasional limestones. The characteristics of the marls are light to medium grey and soft to firm. The typical claystones characteristics are olive black, firm to moderately hard, blocky calcareous, silty, and in part slightly glauconitic. The limestones are characterized by dark red brown, hard, blocky, microcrystalline, and they are grading to dolomite.

5.1.6.2 SEISMIC OBSERVATIONS

The seismic character of the Unconformity 2 reflection in Unit F is a relatively continuous, consistent character, and strong trough amplitude (Figures 24a-c). This surface is truncated against the Øygarden Fault Complex (Figure 24c). The Unconformity 2 seems to onlap in the Oseberg and the Troll Fault Blocks (Figures 24a-b). The typical seismic characteristics of Unit F is continuous to semi-continuous, medium to low amplitude, gentle sigmoidal clinoform features, and low frequency reflections (Figures 24b and 33). The downlap features within this unit can be observed on 2D and 3D seismic data (Figure 24b), while the offlap break of the sigmoidal features can only be identified in the area covered by 2D seismic data (Figure 33).

Figure 33 shows a northeast-southwest 2D seismic line flattened on the Downlap Surface 2, with representative the seismic facies of Unit F. The offlap breaks can also clearly be observed within seismic profile, which infer progradation towards the southwest. The pattern of the offlap breaks within this unit is ascending and convex -upward.

Figures 34a and 34b exhibit the variance and RMS amplitude map Unit F. Figure 34c (i) illustrates that the 3D seismic line crossing the 31/6-2 well shows the progradational features. This fits with the well data showing the coarsening upward gamma ray log pattern within thin unit. Figure 34c (ii) also shows this progradation of internal reflections within Unit F. In the variance map, there are several discontinuity lineaments that is trending in a north-south

direction (Figures 34a and 34b). The RMS amplitude map shows slight amplitude variation along the lineaments (Figure 34b). The anomalously high amplitude in the RMS amplitude map are interpreted to be due to the thickness of this unit, which is below vertical seismic resolution (Figure 34b).
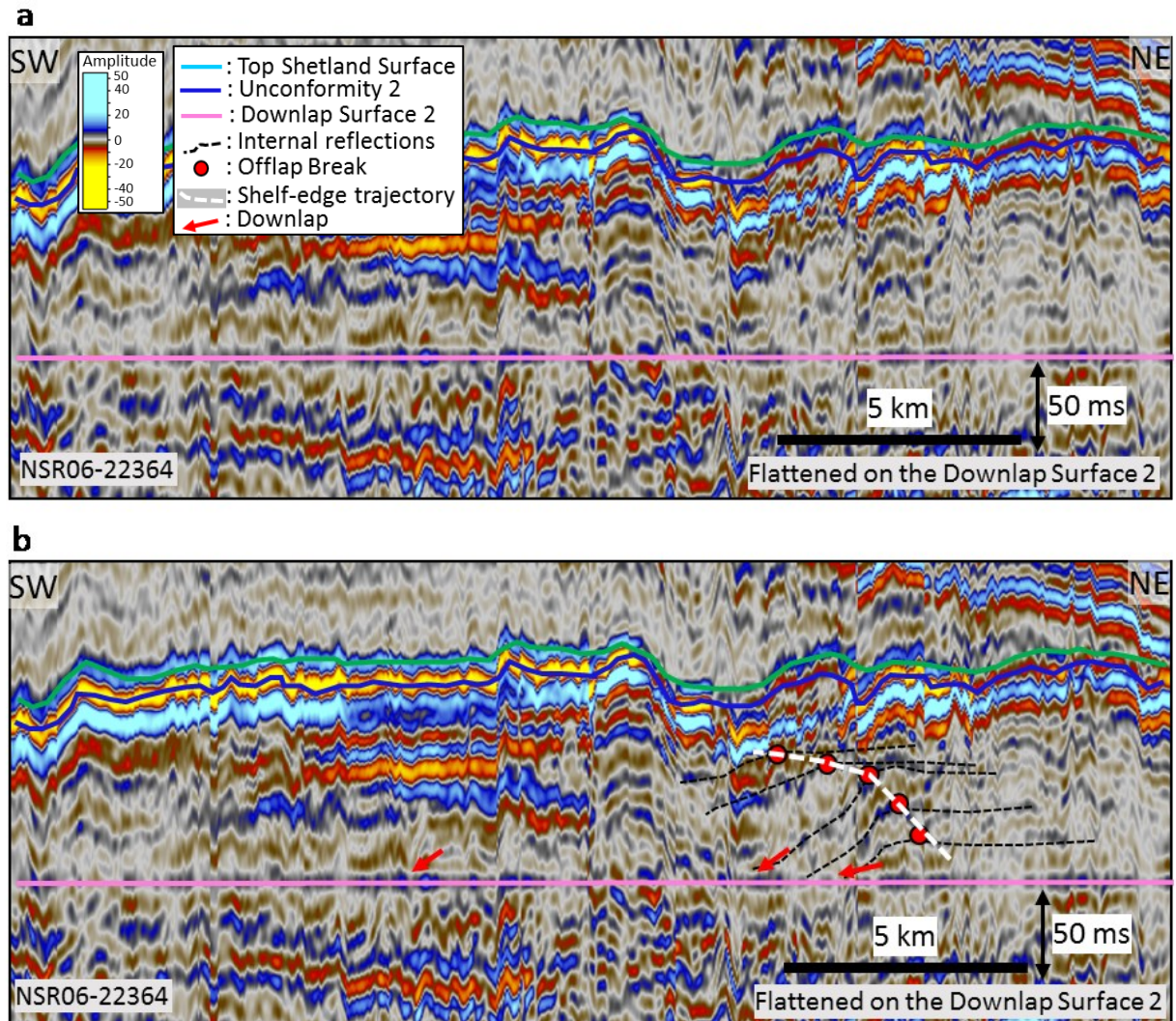
Figure 33: (a) Uninterpreted and (b) interpreted northeast-southwest 2D seismic lines illustrating the internal seismic reflections of Unit F. The downlap features within this unit can be observed on the seismic lines, which are flattened on the Downlap Surface 2. The type of the shelf-edge trajectory of this group is ascending and convex-upward, which is defined by the offlap break positions. This suggests highstand normal regression based on Catuneanu et al. (2011) (Figure 9b). The location of the section is shown in Figure 23.
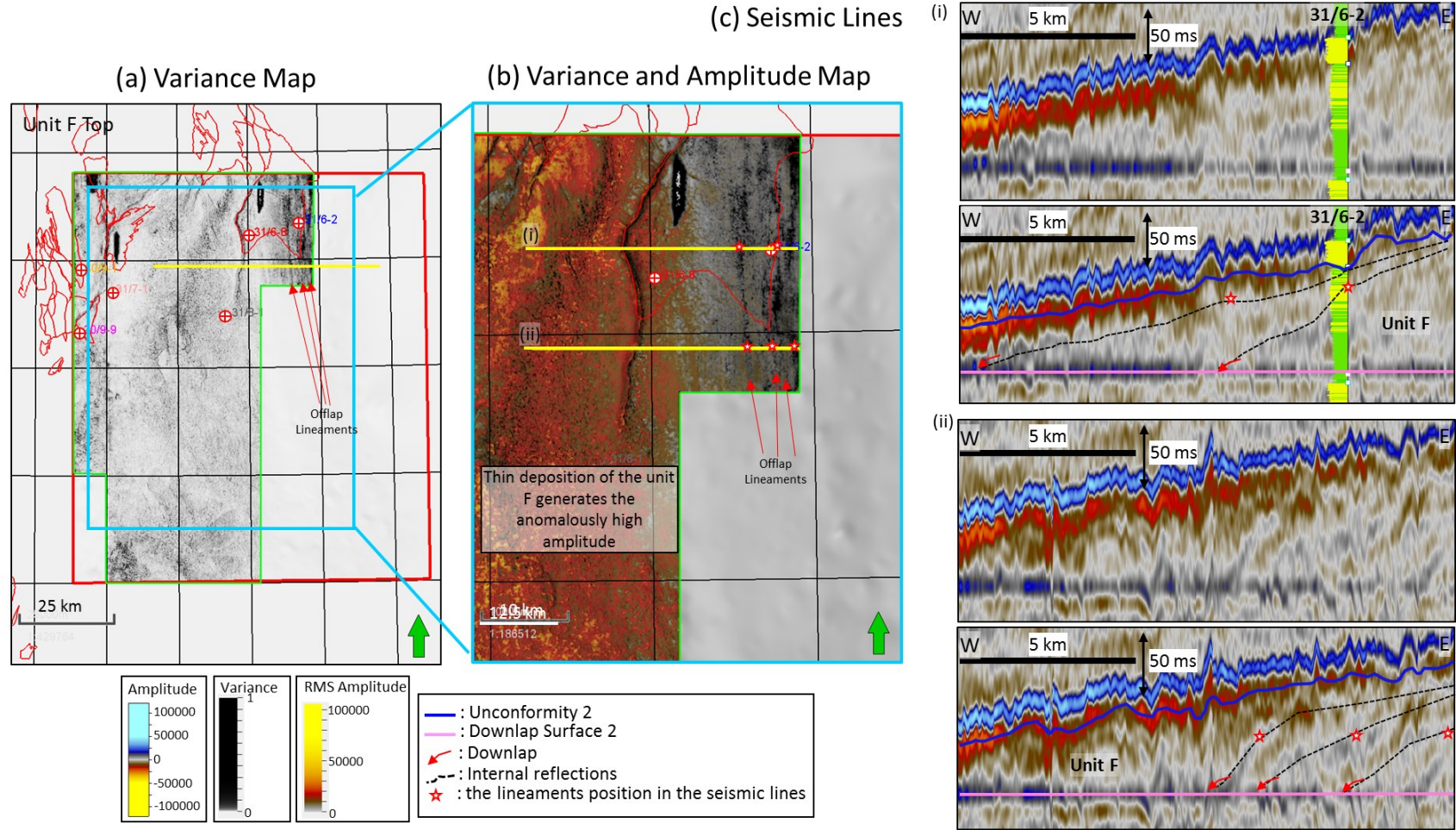
Figure 34: (a) Variance map and (b) variance and RMS amplitude maps, (c) two uninterpreted and two interpreted west-east 3D seismic lines representing the internal seismic reflections of Unit F in the northern Stord Basin. The north-south offlaping lineaments can be identified on the variance map. The anomalously high amplitude in the western part of the study area is caused by the thin sediment layer and interference of the overlying reflections. The RMS amplitude map displays weak north-south amplitude trends. The seismic lines show the progradational stacking pattern of internal reflections, which coincide with the position of offlap lineaments on the variance map.

5.1.6.3 MAPS AND OBSERVATIONS

The Unconformity 2 time-structure map (Figure 25h) shows a dip towards the southwestern part of the study area and therefore most likely the basin position. The present-day deepest part of this surface is around 2400 ms (~3032 m). The paleo-high during deposition of this unit was only the Øygarden Fault Complex area, where this group is truncated. The deposition of Unit F did not seem to have been affected by tectonic activities, except in the Øygarden Fault Complex.

The isochron map of Unit F (Figure 26h) illustrates the depocenter location of this unit, which was in the northeastern part of the study area. The north-south normal fault, which is dipping toward the west, influenced the depocenters of this unit. The sediments thin toward south and west. The thickest deposit of this unit is around 160 ms (~202 m).

5.1.6.4 INTERPRETATIONS

Minor fault activities during the Early to Late Turonian sediments (93.6-88.6 Ma) relatively tectonic quiescence during this time. The dominant sediment source was still from Øygarden Fault Complex, with the sediment depocenter in the northeastern part of the study area (Figure 26h). The distribution of this depocenter seems also to have been controlled by the north-south fault system. This unit drapes all the highs, except the Øygarden Fault Complex, which means the relative sea-level rose and flooded the intervening highs.

The progradational stacking pattern of Unit F displays the ascending shelf-edge trajectory with convex-upwards shape from Catuneanu *et al.* (2011). This feature represents highstand normal regression since the rates of progradation increases with time and the rates of aggradation decreases with time. Therefore, Unit F is consistent with the highstand systems tract (HST) from Catuneanu *et al.* (2011; Figure 9b) most likely due to sediment supply is relatively higher compared to rate of accommodation space during the later stage of the relative base-level rise. The Unconformity 2 can be defined either as the subaerial unconformity according to Posamentier *at al.* (1998) because it represents the erosion or none-deposition during subaerial condition, or the correlative conformity, represented by no missing time gap between upper and lower units.

Overall, Unit F is interpreted as the Highstand Systems Tract 2 (HST 2), bounded by the Maximum Flooding Surface 2 (MFS 2) at the base and the Subaerial Unconformity 2 (SU 2) or the Correlative Conformity (CC 2) at its Top (Figure 36). This unit represents the Tryggvason Formation (Figure 22), which was deposited either in an outer shelf or an upper bathyal setting consisting of the mud-prone deposits in the relatively basin area, with corresponding sand sheets on the shelf. However, these clinoforms are proximal to the Øygarden Fault Complex, therefore the majority of sandstone is predicted to have been eroded by the following tectonic activities.

5.1.7 UNIT G

Unit G seismic package consists of the Late Turonian to Danian sediments (88.6-65.5Ma) and is bounded by the Unconformity 2 at its base and the Top Shetland Surface at the top.

5.1.7.1 WELL LOGS

The gamma ray values of Unit G shows coarsening upward pattern. The sonic values also show a slight fall within this unit (Figure 19). At the top of Unit G, the gamma ray response increases abruptly from low to high gamma ray values corresponding to increasing sonic values. The maximum thickness of this unit based on the key well data is 33 m from the 31/6-2 well.

The lithology description from the key wells documents that this group mainly consists of limestones, with occasional claystones or marls. The characteristics of limestones are white, chalky, soft to moderately hard, micritic, and cryptocrystalline with glauconite disseminations, trace pyrite, and it is occasional argillaceous. The claystones or marls are characterized by olive black to olive grey, medium light grey to medium dark grey, blocky, loose to moderately hard, trace glauconite, trace pyrite, and occasional silty.

5.1.7.2 SEISMIC OBSERVATIONS

The seismic character of the Top Shetland Surface reflection is a consistent, relatively continuous, and strong peak amplitude within the study area (Figures 24a-c, and 35). The

existing paleo-high during deposition of Unit G was the Øygarden Fault Complex, while the sediments of this unit draped the other paleo-highs. Unit G is truncated in the Øygarden Fault Complex area and this is shown in Figure 24c. The internal seismic reflections of this unit consists of two types: parallel and imbricated. The parallel features are characterized by continuous, high amplitude, high frequency, and parallel reflection configuration (Figure 35a (ii)). While the imbricated geometries are defined by discontinuous, high amplitude, high frequency, and imbricated reflection configuration (Figure 35a (ii)).

Figure 35a exhibits the variance attribute map combined with two northwest-southeast 3D seismic lines in the southern part of the study area compared with the Tor Formation in the Central Graben (Figure 35b). The seismic lines in the figure area are flattened on the Downlap Surface 2 and show the parallel and imbricated features of the internal reflection (Figures 35a (ii)). The parallel reflections of this unit are located in the northern part of the study area while the imbricated features are situated in the southern part of the study area (Figure 35a (i)). These imbricated features created discontinuity in the variance map within this unit. The variance map also shows the half-circular trend in the southeastern part of the study area, which spreads out towards the northwest (Figure 35a (i)). These features have a northeast-southwest trend extending towards the northwestern part of the study area. Figure 35b, illustrates geomorphological interpretation in the Central Graben in a variance map of the Tor Formation; and then these features are compared with northeast-southwest 3D seismic lines from this study area. The discontinuities on the seismic lines are interpreted as small thrust faults within the Tor Formation (Das, 2015), which is also a very plausible explanation for the observation in the northern Stord Basin as well.

5.1.7.3 MAPS AND OBSERVATIONS

The time-structure map of the Top Shetland Surface (Figure 25i) shows the dipping direction of this surface, which is towards southwest of the study area. The present-day deepest part of the Top Shetland Surface is approximately 2200 ms (~2779 m). The paleo-high was still in the Øygarden Fault Complex area, where this unit is truncated (Figure 24c). The very few faults cross the Top Shetland Surface and the ones penetrating it are concentrated in the northern part of the study area (Figure 25i).
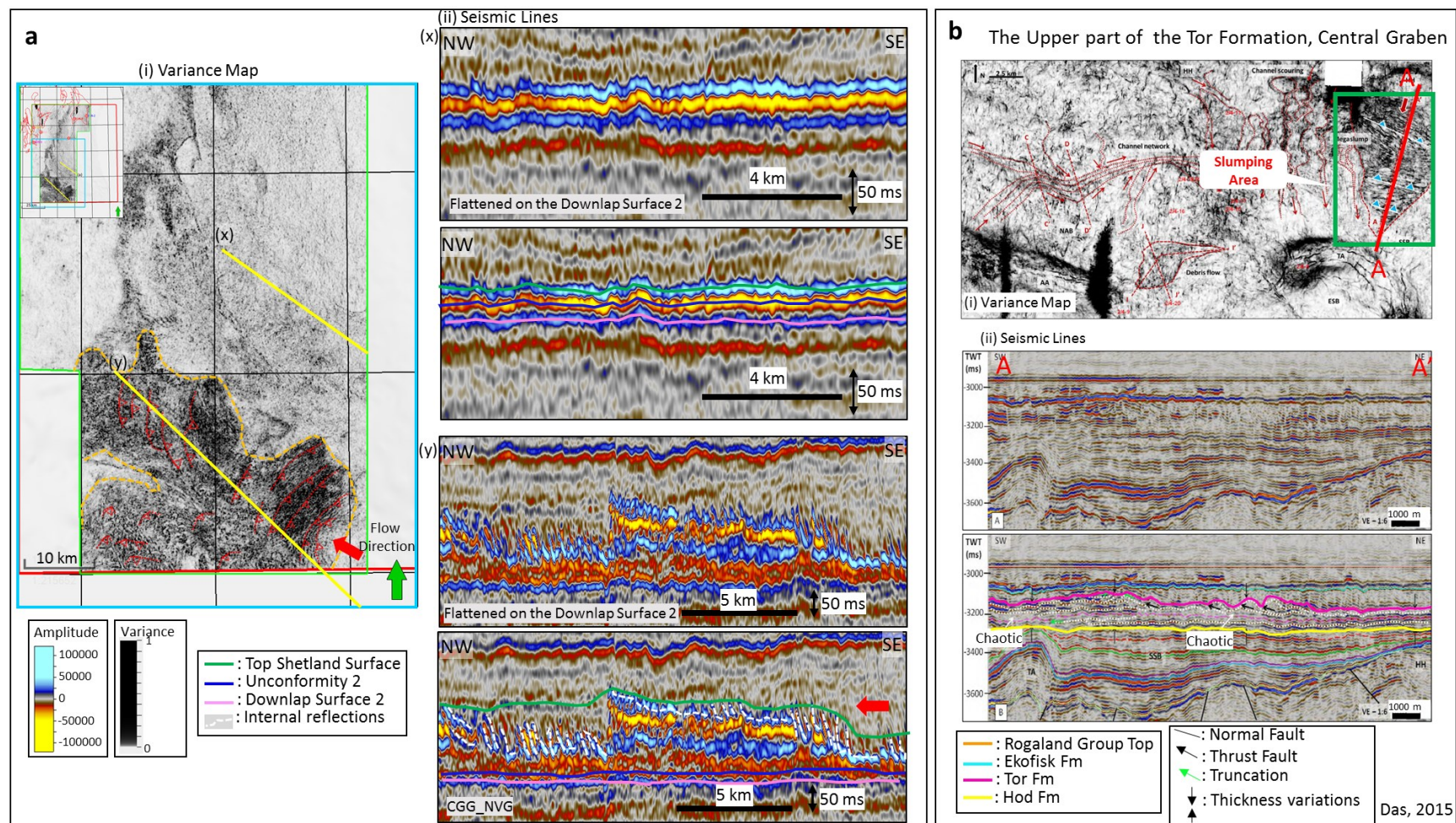
Figure 35: (a) (i) Variance map and (ii) two uninterpreted and interpreted northwest-southeast 3D seismic lines exhibiting the different internal characteristics of Unit G in the northern Stord Basin. Figure (b) (i) Variance map and (ii) uninterpreted and interpreted seismic lines representing the morphological features of the Tor Formation in the Central Graben (Das, 2015). The seismic lines in Figure (a (ii)) flattened on the Downlap Surface 2 shows a continuous, parallel and high amplitude reflection (x) and also the imbricated features (y) within Unit G. The variance map illustrates the half-circular pattern spread out towards the basin, which may represent slumping characteristic with a northwest-southeast trend. This geomorphological feature is almost similar with the Tor Formation in the Central Graben, where they are interpreted as the small thrust faults. These faults corresponded to the slumping feature in the Central Graben area (Das, 2015).

Unit G isochron map (Figure 26i) illustrates the depocenters in the southwestern part of the study area. Towards the western part, a north-south paleo-high separated the depocenters into two sub depocenters. This unit thins towards the north and the east, with the thickest part reaching 180 ms (~228 m).

5.1.7.4 INTERPRETATIONS

Group G drapes all the paleo-highs in the study area during the Late Turonian to Danian time (88.6-65.5 Ma). It means that during this time, the study area was flooded, except in the Øygarden Fault Complex area, lead to the limitation of sediment source. This is also supported by the lithology description from well data, which describe chalky limestone as the main lithology found for this unit (Figures 19 and 22) as the chalky limestone was deposited in open marine environment where the clastic supply is restricted.

The parallel reflections of Unit G represent the chalky limestone corresponding to pelagic deposition. The continuity of the reflections suggest that this unit was widely distributed as thin layers due to very slow settling of the chalk constituent particles (Brasher and Vagle, 1996). The thickness of this features is less than 40 ms (~50 m) (Figure 26i), which is thinner than the imbricated geometries in the southern part of the study area.

The imbricated features show the discontinuous internal reflections generating some segmentation of the reflections. This could be related to small contractional faults associated with slumping. These little thrust faults within this unit are seen in Figure 35a (ii)). The analog for this unit is the Tor Formation in the Central Graben (Figure 35b; Das, 2015). Several northeast-southwest thrust faults observed in the 3D seismic coincide with northeast-southwest discontinuity lineaments in the variance map. In the Central Graben study, these lineaments were interpreted as thrust faults generated by slumping activities (Das, 2015).

Gravity mass flow activities most likely caused the thrust faulting during the deposition of Unit G in the southern part of the study area. These events may have been triggered by the impact of the regionally uplifting tectonic or uneven basin-floor subsidence. It can be inferred that the southeastern part of the study area was uplifted during this time, which resulted in these slumping features with a northwest-southeast direction.

The coarsening upwards in the well data of this unit represents the progradational stacking pattern, which may correlate to a lowstand systems tract. The base of this unit is the Subaerial Unconformity 2 or Correlative Conformity 2, while the top of this unit is the Top Shetland Surface. The Top Shetland Surface is corresponding to the transgressive surface, which is separating underlying lowstand normal regression from the overlying transgression (Catuneanu *et al.,* 2011). The postulated uplift in the southeastern part of the study area during deposition of this unit may have led to a falling base-level.

Overall, Unit G is interpreted to be the Lowstand Systems Tract 3 (LST 3), which is bounded by the Subaerial Unconformity 2 (SU 2) or the Correlative Conformity 2 (CC 2) at the base and Transgressive Surface 3 (TS 3) at the top (Figure 36). This unit represent upper part of the Tryggvason and the Ekofisk formations according to 31/8-1 well, which refer to the Hardråde Formation at the Horda Platform (Figure 22), generally consisting of chalky limestone. The slumping features in the southern part of the study area, indicating widespread mass movements of the chalky limestone that re-deposited the sediments in a slope to a basinal settings. These features were probably generated by compression and inversion related to early phases of the Alpine Orogeny (Surlyk *et al.* 2003) and the early opening of the North Atlantic Ocean (Biddle and Rudolph, 1988; Coward et al., 2003).
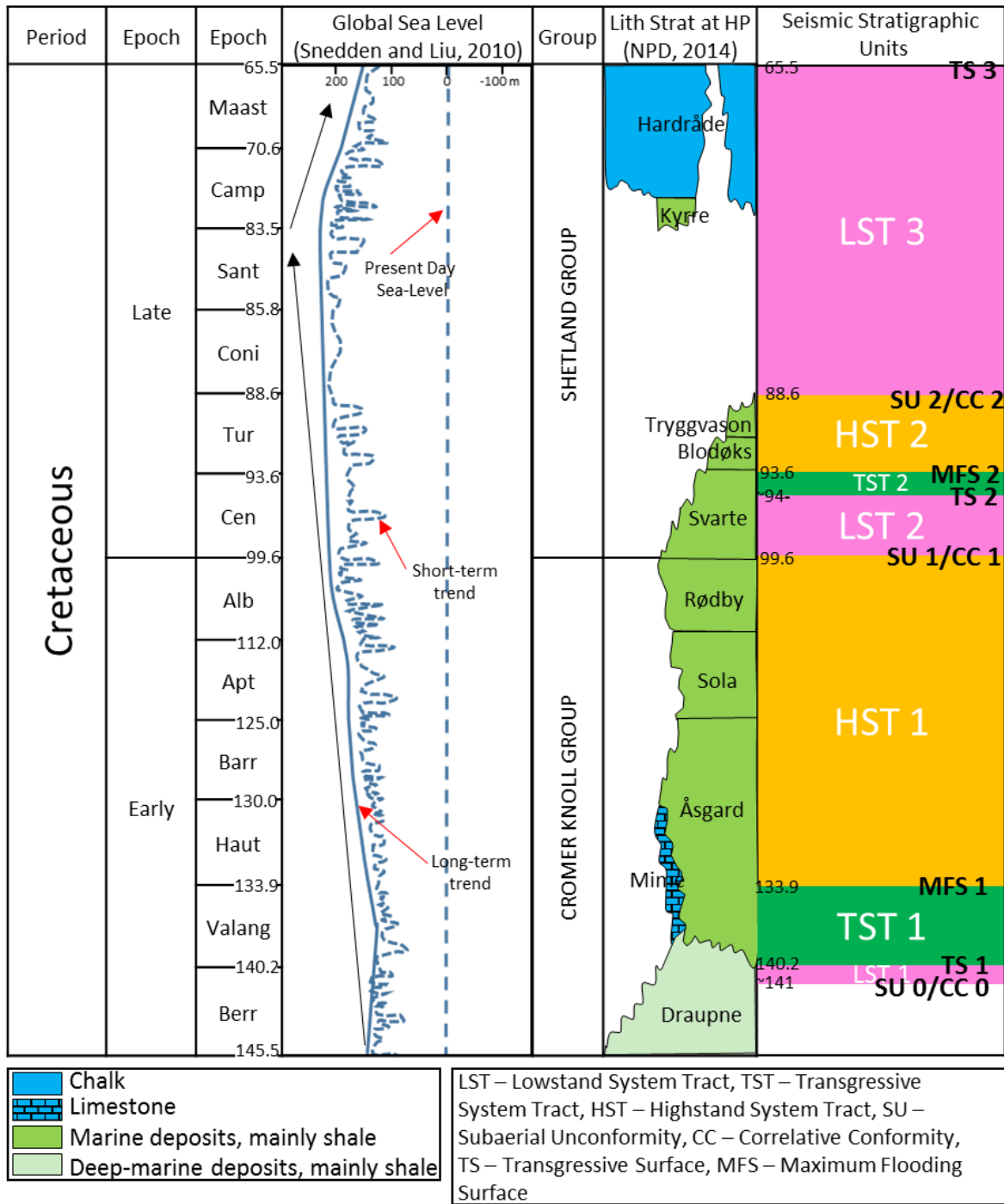
Figure 36: Interpretation of the chronogram (shown in Figure 22), according to this study. Each systems tract represents the interpreted seismic units of the Cretaceous interval bounded by the key stratigraphic surfaces. The global sea-level is based on Snedden and Liu (2010). The lithostratigraphic chart follows NPD (2017).

5.2 CHRONOSTRATIGRAPHIC CHARTS

In this study, two chronostratigraphic charts were constructed and these are presented in Figures 38 and 40. These charts are based on 2D seismic interpretation of a northwest-southeast and a northeast-southwest sections (Figure 23). The aim of generating these charts is to get a better understanding of the temporal relationships of the depositional systems, and their relation to surfaces of erosion, non-deposition, and condensation (units with no or minor thickness). Therefore, they reflect both significant factors in chronostratigraphy: space and time, and they follow the fundamental principle of the seismic stratigraphy; seismic reflections representing timelines. Hence, these reflections can be transferred to a time-scale after identifying and numbering the seismic packages and their component reflections.

5.2.1 OBSERVATIONS

Figures 37a and b display the northwest-southeast NSR08-41165 2D seismic lines across the northern Stord Basin, which was used in generating a chronostratigraphic chart. Figure 37a is the uninterpreted seismic line while Figure 37b is the same interpreted line with interpreted seismic units and stratigraphic surfaces superimposed. As previously mentioned, the paleo-high was located in the southeastern area (Øygarden Fault Complex; Figure 23), while the assumed basin center is in the western part of the study area. The depositional environments, based on the well data and seismic interpretation from the previous sub-chapter, were summeriesed in Figure 37. The character of the internal seismic reflections was identified and numbered in order of age. The numbers define the relative age of the deposition of the Cretaceous strata, where the lower value is older than the higher values. The internal reflections can generally be interpreted within each unit in this seismic line, except for Unit E due to very thin sediments (Figure 37b). The progradational pattern can be seen for Units A1, A2, C, D, and F, while retrogradational characteristics can be observed within Unit B.

Figure 38a shows the same seismic line as Figure 37 with the distribution of each Cretaceous units some clearer as no seismic is in the background. Figure 38b illustrates the chronostratigraphic chart that was generated based on interpretation of the seismic reflection from Figures 37 and 38a. In this figure, seismic unit was constructed in time in the

chronostratigraphic chart, except Unit E due to lack of its seismic reflection in this particular seismic section. The left side of each marked reflection represents downlap features, while the right side illustrates onlap and truncated features (Figure 38b). This figure also shows similarity of different unit location and stratal termination reflecting potential same system tract type within a different sequence (*e.g.* Units A2 and D or Units C and F). The lithology data, based on existing wells, were also included in this chart to determine the temporal and spatial of depositional environments.

Figure 39 shows (a) the uninterpreted and (b) the interpreted northeast-southwest NSR06-22364 2D seismic line, which was also used to generate a chronostratigraphic chart. The seismic facies and stratal terminations were observed for each seismic unit. The lithology defined from the well data was extrapolated to the different seismic units. Again, the relative age was given for each internal reflection. The internal reflections of Units A1, A2, C, D, and F show progradational stacking patterns, while horizons show retrogradational stacking patterns in Units B and E.

Figure 40a illustrates the interpreted seismic units and the key stratigraphic surfaces from the previous line without the seismic data in the back. Figure 40b displays a chronostratigraphic chart comprising the stratigraphic surfaces and seismic units generated from the 2D seismic line. The left boundary of seismic reflections illustrates downlapping reflections, while the right edge represents onlapping and truncating reflections. Interpreted lithology from well and seismic data is also integrated into this chart. Again, similar systems tracts show the same behavior, even though they are in different sequences (*e.g.* Units A2 and D, Units B and E, Units C and F).
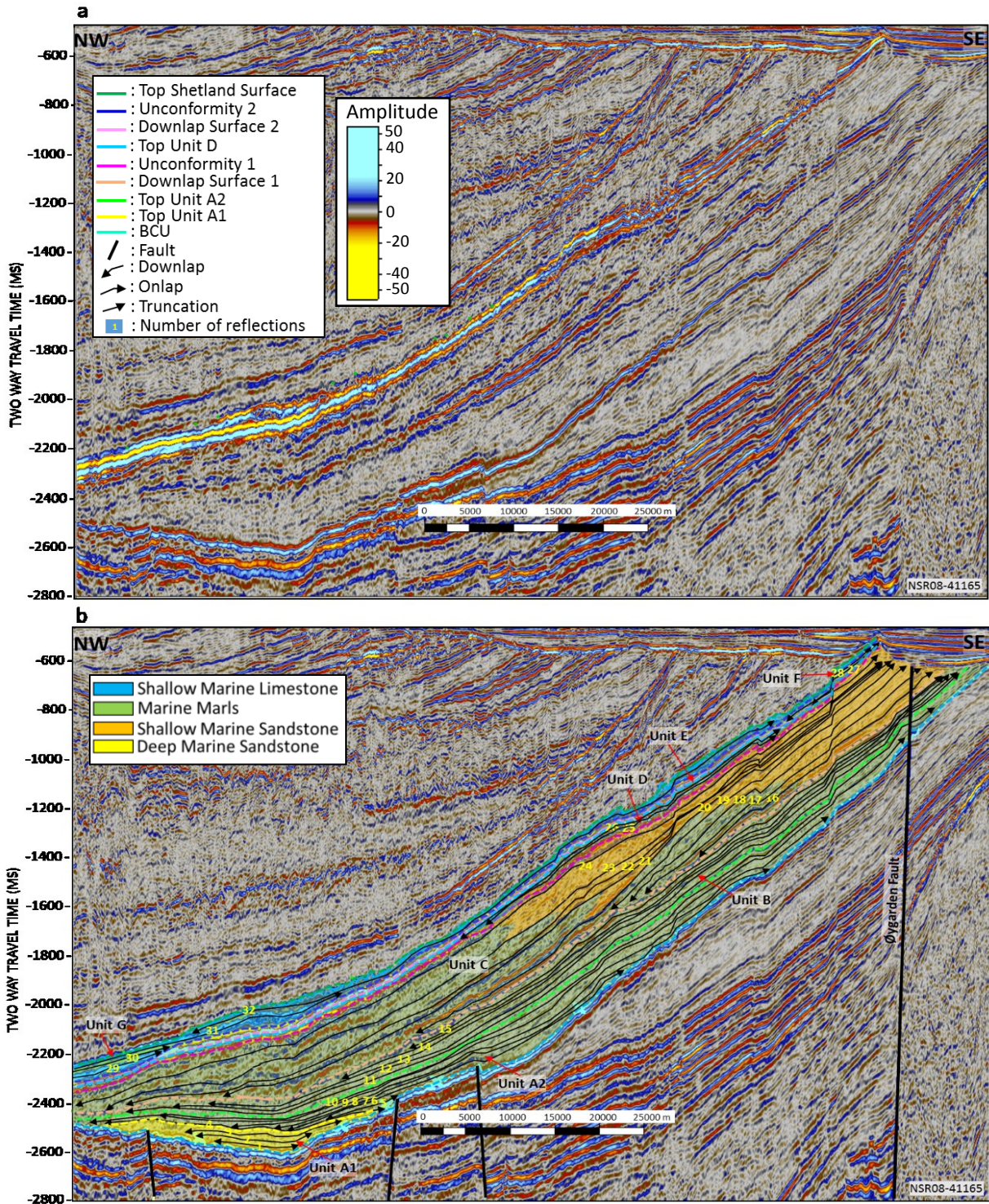
Figure 37: (a) Uninterpreted and (b) interpreted NSR08-41165 2D seismic lines illustrating typical seismic units within the Cretaceous strata. The stratal terminations and the stratigraphic surfaces were identified in order to classify the seismic unit. The interpreted lithology distribution was extrapolted to the different seismic units. These interpretations were then applied for generating the chronostratigraphic chart. All the seismic units show their internal reflections, except of Unit E due to its thickness in this particular seismic line. The location of the sections is shown in Figure 23.

90
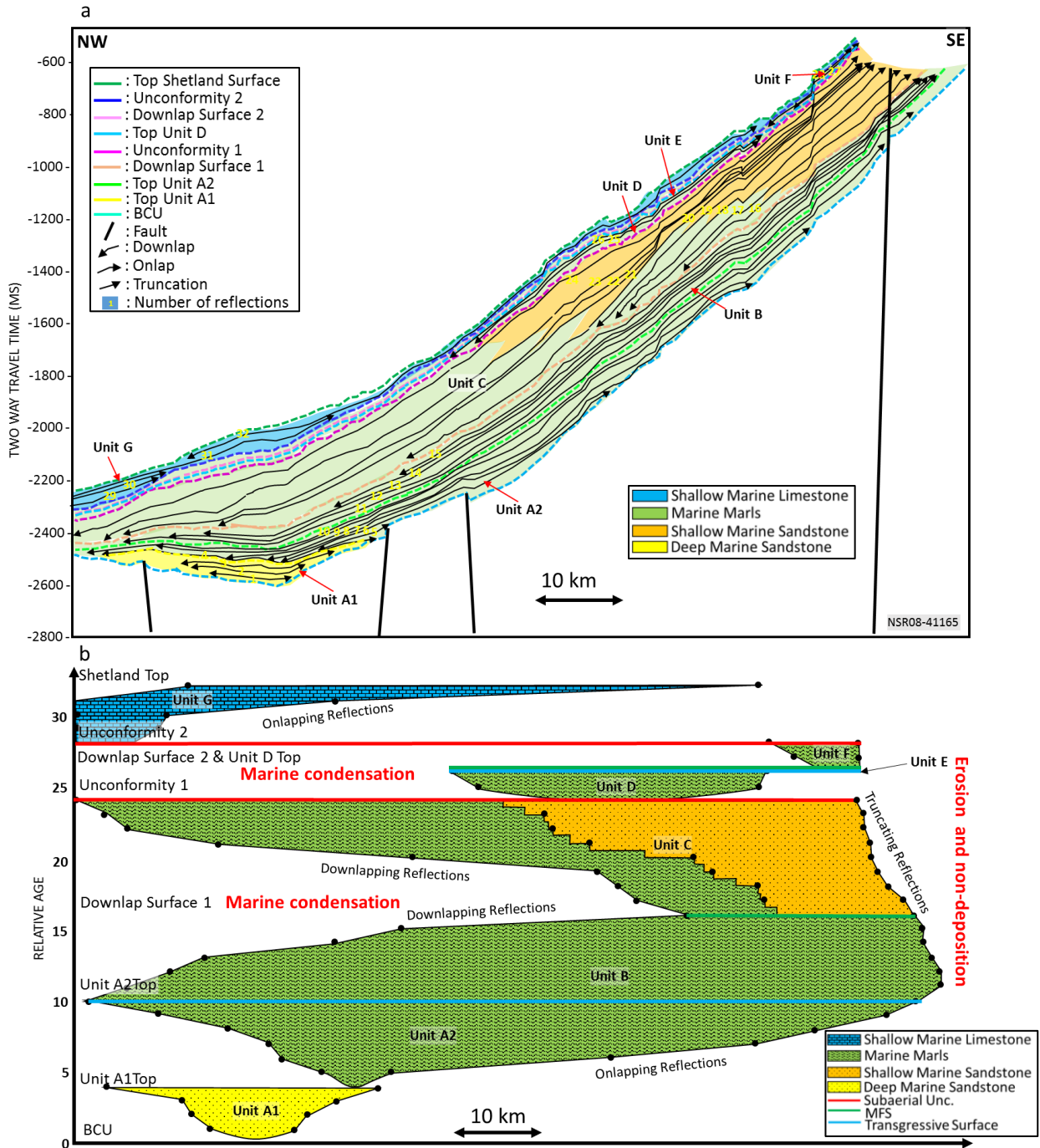
Figure 38: (a) The previous figure interpreted cross section illustrating seismic units and their internal reflection characters within the Cretaceous interval without the masking of the seismic, supplemented with lithological well data. (b) The chronostratigraphic chart build from the cross section in (a) illustrating the position of zones of erosion and non-deposition (blank area on the right side), condensed sections (blank area on the left side), and prograding clinoforms (Units A2, C, D, and F). The main base-level fall occurred during the time markers 0 and 25, corresponding to the BCU (Late Berriasian, ~141 Ma) and the Unconformity 1 (Early Cenomanian, ~99.6 Ma). The highest base-level rise in the study area occurred during the time marker 26 (Turonian, ~93.6 Ma). However, there was another maximum flooding surface at the time marker 13 (Early Hauterivian, ~133.9 Ma). The location of the section is shown in Figure 23.
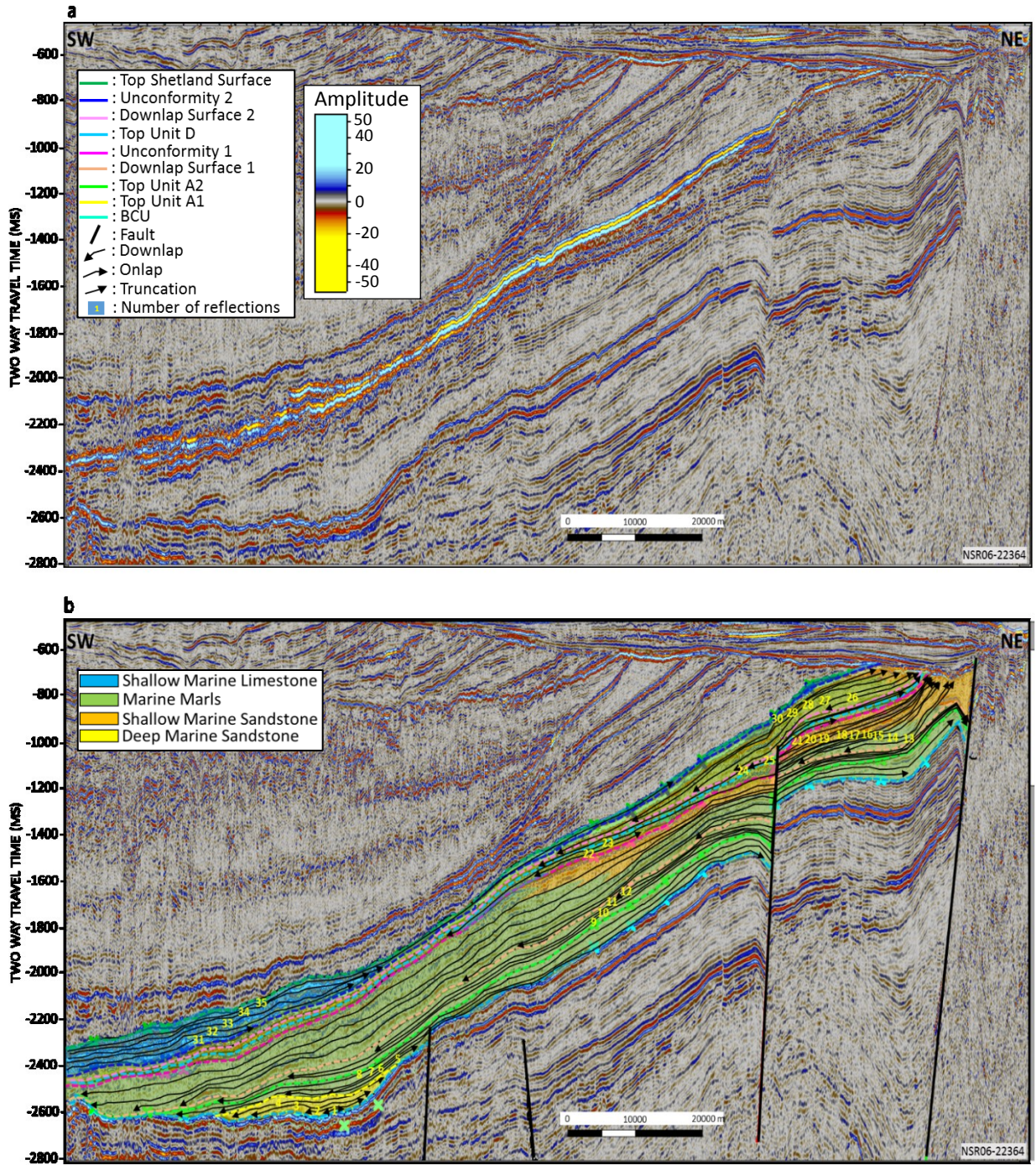
Figure 39: (a) Uninterpreted and (b) interpreted NSR06-22364 2D seismic lines clearly illustrating the internal characteristics of the seismic units within the Cretaceous interval that was used to build another chronostratigraphic chart. The reflection terminations were picked and the seismic surfaces were determined. Each internal reflection was numbered as a time marker and a relative age. The lithologic distribution was also included in the interpretations based on existing well data and seismic interpretation. The location of the section is shown in Figure 23.
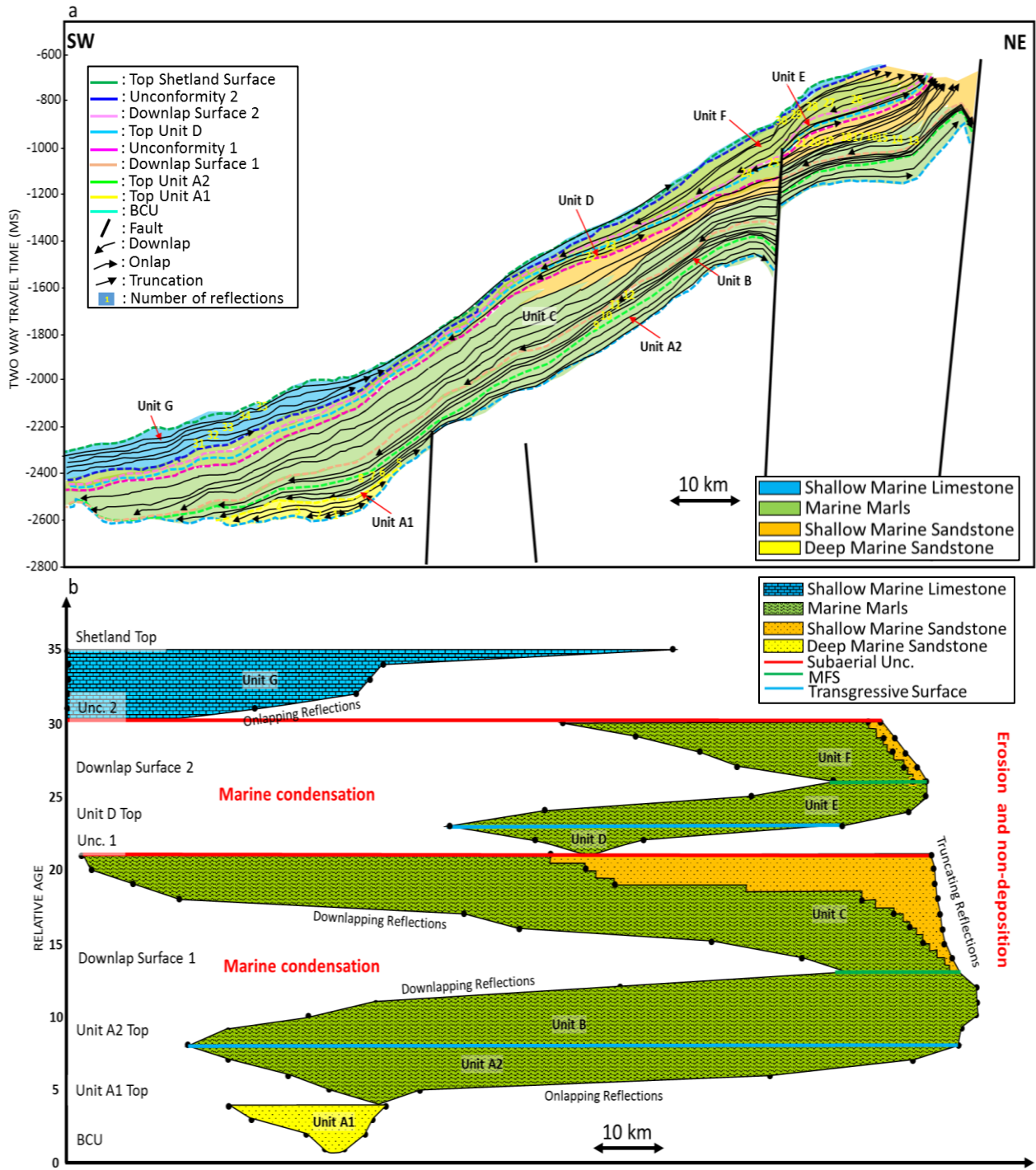
Figure 40: (a) The previous figure interpreted cross section without the background seismic and (b) The chronostratigraphic chart generated from the interpretation cross section in (a) illustrating the zone of erosion and non-deposition (blank area on the right side), condensed sections (blank area on the left side), and prograding clinoforms (Units A2, C, D, and F). Two major significant base-level falls can be observed at the time marker 0 and 21, which corresponds to the BCU (Late Berriasian, ~141 Ma) and the Unconformity 1 (Early Cenomanian, ~99.6 Ma). The maximum flooding surface occurred during the time marker 13 and 26, with the largest base-level rise during the time marker 26 corresponding to the Early Turonian (~93.6 Ma). The location of the section is shown in Figure 23.

5.2.2 INTERPRETATIONS

Figures 38b and 40b illustrate the temporal and spatial distribution of all seismic units of the Cretaceous interval in time and space. The charts suggest two major sequences occurred during the Cretaceous, where each sequence is bounded by unconformity surfaces (refers to Depositional Sequence, according to Posamentier *et al.,* 1988; or Depositional Sequence IV, according to Catuneanu *et al.,* 2011; Figure 7). The first sequence consists of Units A1, A2, B and C; while the second sequence comprises Units D, E, and F. Unit G represents part of a third incomplete sequence.

The area internal seismic reflections of Units A1, A2, D, and G become pointed towards the basin center (southwest), where the reflections onlap towards the underlying unconformity surface. This geometry form due to the duration of the unconformity surface formation will be the least towards the basin center and greatest towards the basin margin. The erosion and non-deposition zones occurred in the blank area on the right side of these charts (Figures 38b and 40b).

The character of the marine condensation or condensed-section interval on the basin margin is bounded by the downlapping reflections, represented by the blank area in the left side of these chronostratigraphic charts (Figures 38b and 40b). The duration of this interval is the least towards the margin and the greatest towards the basin. The apex of this wedge shape is associated with maximum flooding (*e.g.,* downlap surfaces in Figures 38b and 40b).

The prograding clinoforms in the chronostratigraphic chart is shown as the area of deposition, bounded above by a truncated or onlap line and below by a diagonal downlap line, *e.g.,* Units A2, C, D, and F (Figures 38b and 40b). The area of clinoform deposition within Unit A2 moves rapidly out into the basin, prograding over the sub marine fan below (Unit A1).

The zones of erosion or non-deposition prograded 73-94 km basinward during the BCU (time marker 0 in Figures 38b and 40b), and ~25-57 km basinward during the Unconformity 1 (time marker 25 in Figure 38b and time marker 21 in Figure 40b). These events corresponded to two significant relative base level falls, which were characterized by significant basinward shift of the deposition. Unconformity 2 was also probably related to low influx of sediments, as the

sediment units are thin and internal seismic reflection trends cannot obviously be determined at the basin margin.

The two main base-level falls in the study area corresponds to the BCU or the Subaerial Unconformity 0 or the Correlative Conformity 0 (Late Berriasian, ~141 Ma) and the Unconformity 1 or the Subaerial Unconformity 1 or the Correlative Conformity 1 (Early Cenomanian, ~99.6 Ma) surfaces. This is slightly different to the published base-level fall events in in the Central and Northern North Sea according to Oakman (2005). He highlighted that the regional flooding initially occurred in the Late Jurassic and continued until the Early Cretaceous, but this event was interrupted by two main base-level falls, one during the Late Valanginian to Early Hauterivian, and another one in the Aptian. It is predicted that tectonic event occurred during Cenomanian in the northern part of North Sea, hence it affected the relative base-level in the study area. While the study from Oakman (2005) is more referring to the Central North Sea, where the impact of this tectonic was probably not significant.

The time of maximum flooding (shown as the downlap surface) happened during the time mark 16 and 26 (Figure 38b), and time mark 13 and 26 (Figure 40b). The largest base-level rise within the Cretaceous interval in the northern Stord Basin occurred during time mark 26 (Figures 38b and 40b), which is corresponding to Downlap Surface 2 or Maximum Flooding Surface 2. This occurred during the Early Turonian time (~93.6 Ma). In addition, the maximum flooding surface occurred at time marker 13 corresponds to Early Hauterivian age, (~133.9 Ma). The internal reflection within Unit E was difficult to identify due to the limited thickness of this unit (below vertical seismic resolution) (Figure 38b). The thin sediments of this unit was probably due to a result of a combined decrease in sediment supply and a transgression, which flooded the paleo-highs during that time (Figure 38b). Therefore, the amount of sediment supplied to the basin decreased significantly as subaerial erosion stopped.

5.3 SEISMIC FACIES ANALYSIS

Seven types of seismic facies within the study area were deduced on the basis of the reflection configuration (geometry of seismic facies units), reflection continuity, reflection amplitude, and frequency. These variables are important in providing valuable information related to the

depositional environments and processes, sediment transport direction, and estimates of lithology (Mitchum *et al.,* 1977).

5.3.1 SEISMIC FACIES 1 (SF 1)

Seismic Facies 1 consists of medium to high amplitude, medium frequency, and continuous to semi-continuous reflections. The reflection configuration of this facies is mounded shape, bi-directional downlaps, convex-upward, and progradational (Table 4; Figure 27). This seismic facies is observed for Unit A1.

This seismic facies is interpreted to represent deep-marine basin-floor fan deposition, which is typical for convex-upward, mounded geometry, and progradational configuration (Figure 27). The high amplitude and continuous reflection of the upper surface record a contact between two different acoustic impedance zones, which is interpreted to be overlying slope shale above lower fan sandstone (Mitchum, 1985).

5.3.2 SEISMIC FACIES 2 (SF 2)

Seismic Facies 2 comprises medium to low amplitude, low frequency, and continuous to semi-continuous reflections. The typical reflection configuration of this unit is gentle sigmoidal clinoforms, with ascending shelf-edge trajectory and concave-upward (Table 4; Figures 28 and 31). This seismic facies corresponds to Units A2 and D (in the eastern part of the study area).

Seismic Facies 2 is defined as a mud-rich lithology of the pelagic and hemipelagic sediments in a shelfal to slope area, according to the 31/8-1 well data. The sigmoidal geometry of this facies represent rapid base-level rise or rapid basin subsidence that helped preserve the topsets. This seismic facies is consistent with the interpreted relatively low-energy sedimentary regime by Mitchum *et al.* (1977).

5.3.3 SEISMIC FACIES 3 (SF 3)

Seismic Facies 3 consists of low amplitude, low frequency, and semi continuous reflections. The reflection configuration of this unit is sub-parallel to convergent reflections with backstepping pattern (Table 4; Figures 28 and 32). This seismic facies is observed within Units B and E.

The seismic characteristics is identified as pelagic or hemipelagic claystone or marl in the shelfal and slope area, referring to the 31/8-1 well data. The convergent configurations may represent continuous tilting of the depositional surface, or the lateral differences in the sedimentation rate (Mitchum *et al.,* 1977).

5.3.4 SEISMIC FACIES 4 (SF 4)

Seismic Facies 4 comprises medium to low amplitude, low frequency, and continuous to semi-continuous reflections. It is characterized by gentle sigmoidal clinoforms with ascending shelf-edge trajectory that is convex-upward (Table 4; Figures 30 and 33). This seismic facies corresponds to Units C and F.

Seismic Facies 4 is interpreted to represent shelf edge depositional environment with the possibility of sand sheet deposition on the shelf, and mud-prone sedimentation on the slope. The sigmoidal feature in this unit probably represents up-building in the topsets due to rapid base-level rise or rapid basin subsidence (Mitchum *et al.,* 1977).

5.3.5 SEISMIC FACIES 5 (SF 5)

Seismic Facies 5 consists of medium to low amplitude, low frequency, and continuous to semi-continuous reflections. The typical reflection configuration is parallel to subparallel (Table 4). This seismic facies is also observed within Units C and F, but basinward of the Seismic Facies 4.

The seismic facies is interpreted as pelagic or hemipelagic claystones or marls in a shelfal area, according to the 31/8-1 well data. The parallel to subparallel reflection configurations represent constant sedimentation rates on a steadily subsiding shelf (Mitchum *et al.,* 1977).

5.3.6 SEISMIC FACIES 6 (SF 6)

Seismic Facies 6consists of high amplitude, high frequency, and discontinuous reflections. The reflection configuration is imbricated forms (Table 4; Figure 35). This seismic facies is related to Unit G in the southern part of the study area.
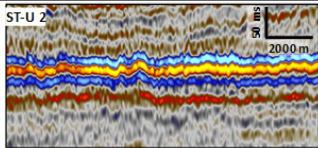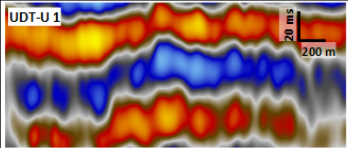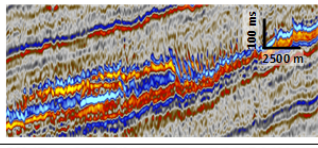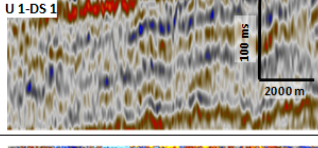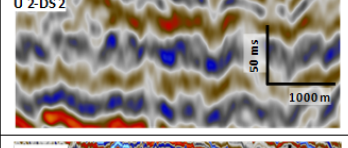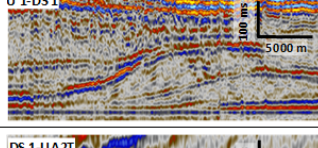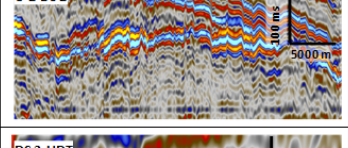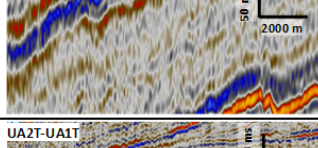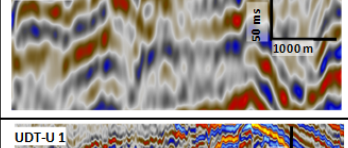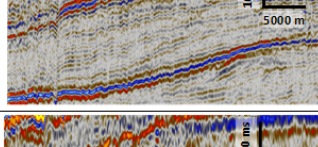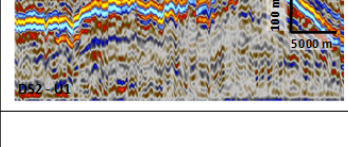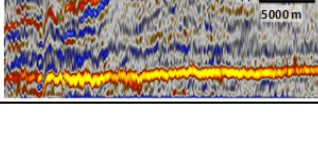
Seismic Facies 6 is interpreted to represent gravitational collapse (slumping) deposits of the chalky limestone. The direction of the thrust faults defined within this facies can infer the direction of slumping, which trends northwest in the study area.

5.3.6 SEISMIC FACIES 7 (SF 7)

Seismic Facies 7 consists of high amplitude, high frequency, and continuous reflections. The reflection configuration is parallel forms (Table 4; Figure 35). This seismic facies is related to Unit D in the western part and Unit G in the northern part of the study area.

This facies is identified as chalky limestone derived from pelagic deposition. The parallel reflections represent bedding resulting from slow settling of the chalk particles from suspension (Brasher and Vagle, 1996). Therefore, it only created thin beds compared to Seismic Facies 6.

Table 4: The seven seismic facies recognized in the study area, which were identified from reflection configuration, continuity, amplitude, and frequency. The interpretation of these parameters is with reference to Mitchum et al. (1977). Observations are from both 2D and 3D seismic data.

Seismic Facies	Seismic Interval	Reflection Configuration	Reflection Continuity	Reflection Amplitude and Frequency	Sedimentary Facies Interpretation	Examples
SF 7	Top Shetland Surface-Unconformity 2 and Top Unit D-Unconformity 1	Parallel	Continuous	High amplitude and high frequency	Limestones in shelf area	
SF 6	Top Shetland Surface-Unconformity 2	Imbricated	Discontinuous	High amplitude and high frequency	Gravitational collapsed (Slumping)	
SF 5	Unconformity 1-Downlap Surface 1 and Unconformity 2-Downlap Surface 2	Parallel-subparallel	Continuous to semi continuous	Medium to low amplitude and low frequency	Pelagic or hemipelagic claystones or marls in shelf	
SF 4	Unconformity 1-Downlap Surface 1 and Unconformity 2 - Downlap Surface 2	Gentle sigmoidal clinoforms, ascending shelf-edge trajectory, and convex up	Continuous to semi-continuous,	Medium to low amplitude and low frequency	Possible sand sheets in shelf, and mud-prone in slope	
SF 3	Downlap Surface 1-Top Unit A2 and Downlap Surface 2-Top Unit D	Sub-parallel to convergent reflections, and backstepping pattern	Semi-continuous	Low amplitude and low frequency	Pelagic or hemipelagic claystones or marls in shelf and slope area	
SF 2	Top Unit A2-Top Unit A1 and Top Unit D-Unconformity 1	Gentle sigmoidal clinoforms, ascending shelf-edge trajectory, and concave up	Continuous to semi continuous	Medium to low amplitude and low frequency	Pelagic and hemipelagic deposits in shelf-slope area	
SF 1	Top Unit A1-BCU	Mound-shaped, bidirectional downlaps, and prograding	Continuous to semi continuous	Medium to high amplitude and medium frequency	Basin floor fan	

6. DISCUSSION

The Cretaceous interval of the northern Stord Basin is divided into seven major seismic units (Units A-G) bounded by seven key stratigraphic surfaces. This was done by using integration of seismic, well, and biostratigraphic data. Unit A was further divided into two subunits (Units A1 and A2) by the mapping the presence of different configuration, amplitude, and frequency of the internal reflections within this unit.

Seismic stratigraphic analysis of the internal characteristics of each unit reveal a low-frequency, regional flooding during the Cretaceous period interrupted by two base-level falls in the Latest Berriasian and Cenomanian. These events are highlighted on the chronostratigraphic chart (Figures 38b and 40b), illustrating seaward stepping hiatus. These basinward shifts occurred over approximately 73-94 km and 25-57 km distance during the Latest Berriasian and Early Cenomanian, respectively. Also, this is consistent with the global sea-level curve from Snedden and Liu (2010) that shows a sea-level fall during the Berriasian-Valanginian and Cenomanian (Figures 22 and 36). Oakman (2005) highlighted two main base-level falls in the North Sea, which occurred during the Late Valanginian to Early Hauterivian and in the Aptian time. These base-level fall events during the Cretaceous are interpreted to have generated a significant coarse clastic sediment supply. The paleo-highs probably provided numerous sediment sources terrains during base-level falls. The clastic sediments were eroded of the subaerial exposed paleo-highs, which bypassed the slope and were deposited on the structural lows onto the basin-floor.

Biostratigraphic results from wells imply that the depositional environment throughout the Cretaceous time in the study area was an open marine, distal, outer shelf to the upper bathyal environment, with water conditions changing from oxygen-deficient to well-oxygenated. The post-rift Early Cretaceous sediments are dominated by hemipelagic and pelagic claystones that onlap towards the structural highs. The dominance of claystone sedimentation during the Cretaceous indicates that there were limited sediment supply during this time, particularly during times when the limestone was widely distributed (*e.g.* Unit G). The paleo-highs defined in the study area are the Troll and Oseberg Fault Blocks, Bjørgvin Arch, and Øygarden Fault Complex. During the Late Cenomanian to Early Turonian, the post-rift stratigraphy covered the

100

entire study area, except the paleo-highs in the Øygarden Fault Complex area. This also occurs in the northern Viking Graben, where the Turonian sediments are the oldest Cretaceous deposits onlapping the Oseberg footwall crest (Zachariah *et al.,* 2009).

The Øygarden Fault Complex is interpreted as the primary sediment source for the Cretaceous strata in the study area, especially for the clastic-rich depositional geometries. This is predicted by clinoforms and offlap lineaments trends (away from the Øygarden Fault Complex) in some of the units, as well as the position of depocenters throughout the Cretaceous time.

However, for the Cretaceous interval in the Oseberg Fault Block, erosional activity was insignificant compared to the western part of the Oseberg Fault Block (close to the northern Viking Graben; Zachariah *et al.,* 2009). This is recorded for instance in the 30/9-9 well in the Oseberg Fault Block. This well shows that the Cretaceous interval overlies the Upper Jurrasic Draupne and Heather Shales. While in the western part of the Oseberg Fault Block, the Cretaceous stratum overlies directly the Early Jurassic sediments, where the Late Jurassic sediments are eroded (Zachariah *et al*., 2009).

6.1 SEQUENCE HIERARCHY

The seven main seismic units and two seismic sub-units in the Cretaceous strata, discussed in the previous chapter, represent the systems tracts bounded by key stratigraphic surfaces. These units can be classified into two complete and an incomplete sequences, where each sequence is bounded by unconformity surfaces (refers to Depositional Sequence, according to Posamentier *et al.,* 1988; or Depositional Sequence IV, according to Catuneanu *et al.,* 2011; Figure 7). Sequence 1 comprises Units A1, A2, B, and C; and it is bounded at its base by the BCU and its top by the Unconformity 1 (Figure 36). Sequence 2 consists of Units D, E, and F; bounded by the Unconformity 1 at its base and the Unconformity 2 at its top (Figure 36). Unit G was deposited on top of Sequence 2 and is part of the Sequence 3.

The stratigraphic cycles (Table 5) were determined by quantitatively analyzing two kinds of sequences: the depositional sequences (Posamentier *et al.,* 1988) and the genetic stratigraphic sequences (Galloway, 1989). Both depositional and genetic stratigraphic sequences have a time span of more than ten million years. The cycle order of each sequence interpreted in the seismic

data corresponds to a second-order cycle, which is based on biostratigraphic data, sequence stratigraphy correlation, and the duration of the sequence from Miall (2010) (Table 1). This implies that each sequence was formed by continental-scale mantle thermal processes and by plate kinematics, which formed eustatic cycles due to volume changes in mid-oceanic spreading centers and global cycles of basement movement (Miall, 2010).

Table 5: The Cretaceous stratigraphic cycles within the study area. The depositional sequence is the sequence type used in this study.

Type of Sequence	Number of Sequence	Boundary	Duration (Million years)
Depositional	Sequence 1	BCU to Unconformity 1	~40.6
Sequences	Sequence 2	Unconformity 1 to Unconformity 2	~11
Genetic Sequences	Sequence 1	Downlap Surface 1 to Downlap Surface 2	~40.3

6.2 TEMPORAL VARIABILITY OF THE POST-RIFT DEPOSITION

The Lower Cretaceous interval is characterized as post-rift sequences that is filling inherited basin-floor topography (Copestake *et al.,* 2003). In the study area, Unit A1 represents basin-floor fans deposited in the paleo-lows in the southwestern part of the study area (Figure 26b), which is part of the Seismic Facies 1 (SF 1; Table 4). The sediment supply at this time is interpreted to be from the Øygarden Fault Complex, based on the progradational trends and the offlap discontinuity lineaments (Figure 27). The distribution of this unit was limited by the paleo-highs surrounding the depocenter, which were: the Bjørgvin Arch and the Oseberg Fault Block (Figure 41a). This coincides with the "Jurassic upwards" pattern (Figure 2b), which is a depositional model concept for North Sea Cretaceous units proposed by Oakman (2005). This concept states that sediments cannot travel long distances due to existing paleo-topography.

Deposition of the sequence began by relative sea-level fall and ended by rapid, relative sea-level rise. Deep-water basin-floor fan sediment is deposited during this time of sea-level lowstand (Posamentier and Kolla, 2003). This implies that basin-floor fan in Unit A1 was deposited during a period of maximum base-level fall in the Latest Berriasian, and is therefore representing the falling-stage systems tract (FSST 1; Figure 36). The coarse sediments predicted to have been deposited during this event are related to the Åsgard Formation sandstones (Figure 36). This event corresponds to a global sea-level event from Snedden and Lie (2010), showing

eustatic sea-level fall during deposition of Unit A1 (Figures 22 and 36). Bugge *et al.* (2001) described uplift and erosion during the Hauterivian-Barremian in the northern Atlantic region, and Gabrielsen *et al.* (2001) highlighted that the early post-rift evolution (incipient stage) in the northern North Sea was followed by relative uplift or deceleration of the subsidence. The base-level fall in the study area is associated with the tectonic events in the northern Atlantic region (Bugge *et al.,* 2001) and the uplifting effect during the early post-rift evolution (Gabrielsen *et al.,* 2001).

Unit A2 consists of hemipelagic and pelagic claystones deposited in the shelf-slope setting during the Latest Berriasian. This sediment is related to the Åsgard Formation claystones, which forms part of the Seismic Facies 2 (SF 2; Table 4), and represents a lowstand systems tract deposit (LST 1; Figure 36). It is interpreted that the sediment source for this unit was multiple highs, such as the Bjørgvin Arch, the Oseberg and the Troll Fault Blocks, and the Øygarden Fault Complex (Figure 41b). However, the primary sediment source is believed to be from the Øygarden Fault Complex, as sediments of this unit prograde in a westward direction (Figure 28b). In addition, the depocenter locations were in the southwestern and southern part of the study area (Figure 26c). No coarse clastic sediments are recorded in any wells or seismic data which means that the base-level probably increased during this time.

A rising base-level continued during the Latest Berriasian to Early Hauterivian, which is proven by the retrogradational stacking pattern seen in Unit B. This unit is related to the Åsgard Formation claystones (Figure 36) and is part of the Seismic Facies 3 (SF 3; Table 4), which represent the transgressive systems tract (TST 1; Figures 19, 22, and 36). The depocenters of this unit prograded gradually towards the east (basin margin). This unit flooded most paleo-highs (*e.g.* Bjørgvin Arch) and reduced the sediment supply (Figure 41c).

In contrast to pelagic or hemipelagic deposition in Unit B, the clinoform features deposited in Unit C are interpreted to form due to the sediment supply is greater than the accommodation space during the later stage of relative sea-level rise (Catuneanu *et al.*, 2011). The sigmoidal shape implies that coarse sediments were deposited on the shelf, while mud-prone sediments were fed preferentially onto the basin-floor (Figure 41d). Unit C is related to the upper part of the Åsgard, Sola, and Rødby formations (Figures 19 and 36), which is related to the Seismic Facies 4 (SF 4) and Seismic Facies 5 (SF 5; Table 4). This unit represents the deposition of the

highstand systems tract (HST1; Figures 22 and 36). The depocenter of this unit (Figure 26e) moved towards the west, representing progradation of the sediments basinward. The seismic attributes and shelf-edge trajectory also display the aggradational and progradational patterns of Unit C westward. Hence, the sediment source was predominantly from the Øygarden Fault Complex.

The chronogram in Figure 22 shows the lack of Aptian sediments in most of the wells, which is probably due to the location of these wells on structurally highs, where unit C is not present. However, the 31/8-1 well is located in a relatively basinal area and this well shows the existence of the Late Aptian deposits (Figure 22). This indicates that the Aptian sediments were only deposited in the structural lower areas.

The coarse clastic sediments in Unit C correspond to the Agat sandstones, which are the reservoir in the Agat discovery of the northeastern North Sea (Bugge *et al.,* 2001). These reservoirs are a target play in the northern Viking Graben, Magnus Trough, and Atlantic Margin basins (Oakman, 2005). In addition, Copestake *et al.* (2003) reported that the development of Agat sandstones in the northern Viking Graben during the Late Aptian has been associated with the opening of the proto-North Atlantic and the Bay of Biscay.

However, later erosional activity occurred in the footwall block of the Troll Fault Block after deposition of Unit C (Figure 41d). This was defined by truncated features which are observed in the footwall block (Figure 29). The extent of erosion is nearly 110 ms (~139 m) (Figures 24b and 29). The eroded sediments from the footwall block in the Troll Field area were shed to the minor depocenter west of this area (Figure 26e). This erosional event is thought to be related to the tectonic uplift and tilting after deposition of Unit C.

Unit D, deposited during the Early to Late Cenomanian, contains a significant amount of limestone compared to previous units in the study area (Figure 41e). Two wells located in the Oseberg Fault Block (30/9-1 and 30/9-9) show the dominance of carbonate content within Unit D (Figure 19). The Oseberg Fault Blocks, which was one of the paleo-highs during deposition of this unit, shows that limestones were deposited in this area based on well data (Figures 19 and 41e) and these are part of the Seismic Facies 7 (SF 7; Table 4). This means that there were only limited parts of the Oseberg area that were subaerial exposed, leading to less erosion in this paleo-high and deposition of limestone surrounding this area. Another option is the

limestones were deposited on the highs while claystones were surrounding it. In addition, other key wells (31/8-1, 31/6-2, and 31/6-8) display claystone to marl deposits in the Troll Area, which correspond to the Seismic Facies 2 (SF 2; Figures 19 and 41e; Table 4). These wells are relatively more proximal to the Øygarden Fault Complex, hence the clastic material still could be deposited in this area. Also, Zachariah *et al.* (2009) highlighted that the limestone occurred in relatively shallower area in the northern Viking Graben.

The increasing limestone content may be related to warm-temperate and a pronounced "greenhouse" climate during the Late Cretaceous (Surlyk *et al.,* 2003). Zachariah *et al.* (2009) explained that the dominant carbonate content in the northern Viking Graben corresponded with a changing climate into a more arid and decreasing sediment supply. Unit D is related to the Svarte Formation (Figure 36), which represents the lowstand systems tract (LST 2; Figures 19, 22, and 36).

The deposition of this system corresponds to the second main base-level fall event in the northern Stord Basin. Lundin and Doré (1997) explained a significant regional unconformity within a Cenomanian age in the Træna Basin (Lofoten), which they explained by being connected to a poorly understood mid-Cretaceous tectonic event in the NE Atlantic margin. Hence, the main base-level fall event in the study area is probably also related to this event. However, since the sediment supply decreased dramatically, the amount of clastic sediment input was insignificant at this time.

Unit E corresponds to the Blodøks Formation (Figure 36), which is related to the Seismic Facies 3 (SF 3) (Table 4). It represents the transgressive systems tract deposits (TST 2) from the Late Cenomanian to Early Turonian (Figures 19, 22, and 36), which is identified by retrogradational stacking patterns. The Blodøks Formation represents a condensed section of organic-rich claystones representing a well-known transgressive event in the Cretaceous. This formation is equivalent to a pronounced condensed section found in Svalbard to Italy and Plenus Marls Formation in the North Sea (Bugge *et al.,* 2001; Copestake *et al.,* 2003). This formation draped all the paleo-highs in the study area, except the Øygarden Fault Complex (Figure 41f). In the northern North Sea, the relative sea-level covered all paleo-highs and the majority of the eastern basin margin in the Santonian time (Bugge *et al.,* 2001).
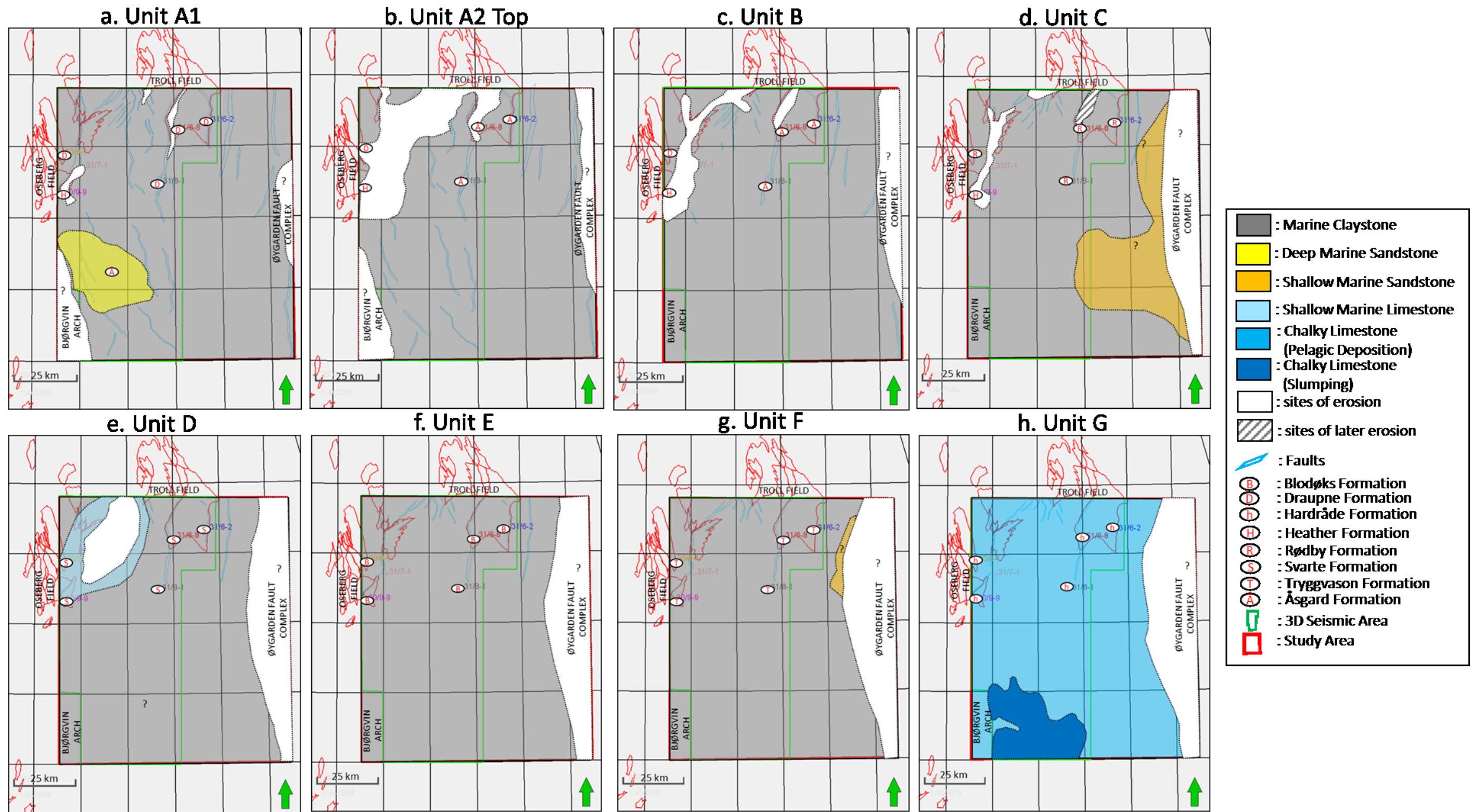
Figure 41: The Paleogeographic maps of all the units identified in the Cretaceous interval (Figure 22). Each map shows fault locations, lithologic distribution, and position of paleo-highs throughout the Cretaceous. The structural highs were believed to act as the sediment sources for the post-rift Cretaceous interval. The main highs in this area defined by seismic stratigraphic interpretation were the Troll and the Oseberg Fault Blocks, the Bjørgvin Arch, and the Øygarden Fault Complex. The lithologic distribution was inferred by integrating the seismic stratigraphic interpretation and well data. Two clastic-rich depositional geometries can be observed in Units A1 and C, representing the deep basin-floor fan and the shallow marine prograding sandstones, respectively. The chalky limestone in Unit G is predicted to have good reservoir parameters, according to Brasher and Vagle (1996).

Changing base-level can also be observed for Unit F during the Early to Late Turonian time, shown by the progradational pattern in the seismic section (Figures 33 and 34), associated with the Seismic Facies 4 (SF 4) and Seismic Facies 5 (SF 5). The attribute map displays the north-south offlap discontinuity lineaments with a westward progradation for this unit. The thickness map illustrates the northwestern part of the study area as the location of these depocenters (Figure 26h), which suggest a sediment source from the northern part of the Øygarden Fault Complex.

The Øygarden paleo-highs is predicted as the main sediment source for almost all of the previous units. Hence, this paleo-high would have been peneplained into a more gentle topography during deposition of Unit F with little sediments delivered to the structural lows. It is proven by the thickness of Unit F (HST 2), which is thinner than Unit C (HST 1) that was deposited during the similar highstand system tract. Therefore, the distribution of shallow marine sandstones is predicted to be limited to the northeastern part of the study area. This unit is related to the clastic sediments of the Tryggvason Formation (Figure 36).

Unit G—the youngest seismic unit in this study—is dominated by limestone deposition and it represents lowstand systems tract deposit (LST 3) during the Late Turonian to Danian time (Figures 19, 22, 36, and 41h). This unit is either time equivalent to the upper part of the Tryggvason and Ekofisk formations, according to the 31/9-1 well; or younger than Hardråde Formation, with reference to the lithostratigraphic chart from the Horda Platform given by NPD (Figure 36). Emery and Myers (2009) explained that carbonate could still be deposited during lowstand, but then carbonate systems are generally less productive due to the reduction in shallow-water carbonate production area. The seismic data shows strong amplitude within this unit throughout the study area, suggesting that limestone defined in this group was widely distributed and covered the entire study area, except for in the Øygarden Fault Complex area.

There are two seismic facies corresponding to this unit: Seismic Facies 6 and 7 (Table 4). The Seismic Facies 7 displays parallel reflection configuration representing pelagic deposition of chalky limestone (Table 4; Figure 35a (ii)). This seismic facies is related to the Category I chalks based on Brasher and Vagle (1996), which is characterized by pelagic deposition or the settlement of the finest particles from gravity flows. This will produce varying thickness with laminated to bedded, argillaceous to calcareous mudstone lithofacies. The Seismic Facies 6

shows imbricated features corresponding to slumping of the chalky limestone (Table 4; Figure 35a (ii)). This seismic facies is related to the Category III Chalk from Brasher and Vagle (1996). It is identified by re-deposition caused by gravity flows or slumping and is described as massive to chaotic, homogeneous, deformed, and comprising floatstone lithofacies (Brasher and Vagle, 1996).

The slumping activity in the southern part of the study are identified by the little thrust faults in the 3D seismic section. These features also show northeast-southwest discontinuity lineaments in the variance map. The tectonic activity likely defined the slumping and the gravity flow features. This is interpreted to be caused by the impact of tectonic compression of the Alpine Orogeny and rifting of the North Atlantic Ocean (Biddle and Rudolph., 1988; Surlyk *et al.,* 2003). These features are in contradiction to what was documented by Zanella and Coward (2003), where significant Late Cretaceous inversion structures were only inferred present in the southern part of the Central Graben in the Danish sector. The slumping features in Unit G show that the tectonic inversion in the Late Cretaceous still has a significant influence in the northern Stord Basin.

6.3 COMPARISONS WITH ANALOGOUS SYSTEMS

The clastic-rich depositional geometries in the Cretaceous interval consist of the basin-floor fans in Unit A1, and shallow marine sandstones in Units C and F. These units are predicted to contain good reservoir quality sandstones. In addition, the slumping-related chalky limestone deposits has probably good reservoir parameters in Unit G. Some analogues for the basin-floor fans geometries are the Kutei Basin, Indonesia (Fowler *et al.,* 2001) and in the northern Viking Graben, North Sea (Zachariah *et al.,* 2009). The shelf-margin clinoforms in the South China Sea (Gong *et al.,* 2015) is an analogue for the shallow marine sandstone within Units C and F; while an analogue of chalky limestone is the Tor Field, Central Graben, North Sea (Brasher and Vagle, 1996; Gennaro *et al.,* 2013; Das, 2015).

Fowler *et al.* (2002) described the character of recent basin-floor fans in the Kutei Basin as medium to high amplitude and continuous reflections, commonly concave-upward patterns, which represented dominantly sand-prone deposits. These sandy basin-floor fans formed due

to a change from a confined system to an unconfined system. The dimension of these large basin-floor fans are up to 23 km wide and 110 m thick. The basin-floor fan in the study area (Figure 27) is around 12 km wide and 90 ms (~113 m) thick. The difference in size between the basin-floor fan in Unit A1 and in the Kutei Basin is likely an affected by the paleo structures controlled the distribution of the basin-floor fan geometry. Inherited structures from previous rift episodes in the northern Stord Basin generated paleo-highs, which served as both sediment sources and paleo highs. The existence of the Oseberg Fault Block and Bjørgvin Arch as highs during deposition of Unit A1, limited the distribution of the basin-floor fan within this unit in between these highs (Figure 41a). The base-level fall during this time were probably connected to the uplift process during the early post-rift evolution (Gabrielsen *et al.,* 2001) as well as the tectonic activity in the north Atlantic region during the Hauterivian-Barremian time (Bugge *et al.,* 2001). The postulated effect of these tectonic activities was to increase the amount of preserved sediment in the basin center. The Øygarden Fault Complex is interpreted as the uplifted area during this time, which was consequently the primary sediment source of Unit A1.

Zachariah *et al.* (2009) observed that the basin-floor fans deposited in the K1 Unit in the northern Viking Graben have an unconfined and widespread distribution. This particular geometry is different to Unit A1, which was suggested to have been deposited in a similar depositional settings. The discrepancy could be caused by the unconfined paleogeomorphology of the basin-floor in the northern Viking Graben during deposition of Unit K1, which allowed for sedimentation without constrain from structural barriers. The dimension of the basin-floor fan observed in the northern Viking Graben is up to 20 km wide and 100 ms thick. The larger size of the basin-floor fan in this location is interpreted as the likely effect of the steeper slope gradient, which significantly increased the volume of sediments deposited towards the basin-floor area (Fowler *et al.,* 2001; Zachariah *et al.,* 2009).

Gong *et al.* (2015) divided the shelf margin clinoforms in the South China Sea into strongly progradational, strongly aggradational, and mixed progradational-aggradational clinoforms. The sigmoidal features identified in Units C and F in the study area (Figures 30b and 33b) have a similar pattern with the mixed progradational and aggradational clinoforms in the South China Sea (Figure 42a and 42b). This implies that the clinoforms in Units C and F also could represent mixed sand-mud submarine channel and/or canyon systems with moderate sand-shale ratios. It

is also predicted that the majority of the clastic-rich sediments were stored on the shelf, while the finer-grained sediments were deposited in the slope to basinal setting (Figures 37b and 39b).
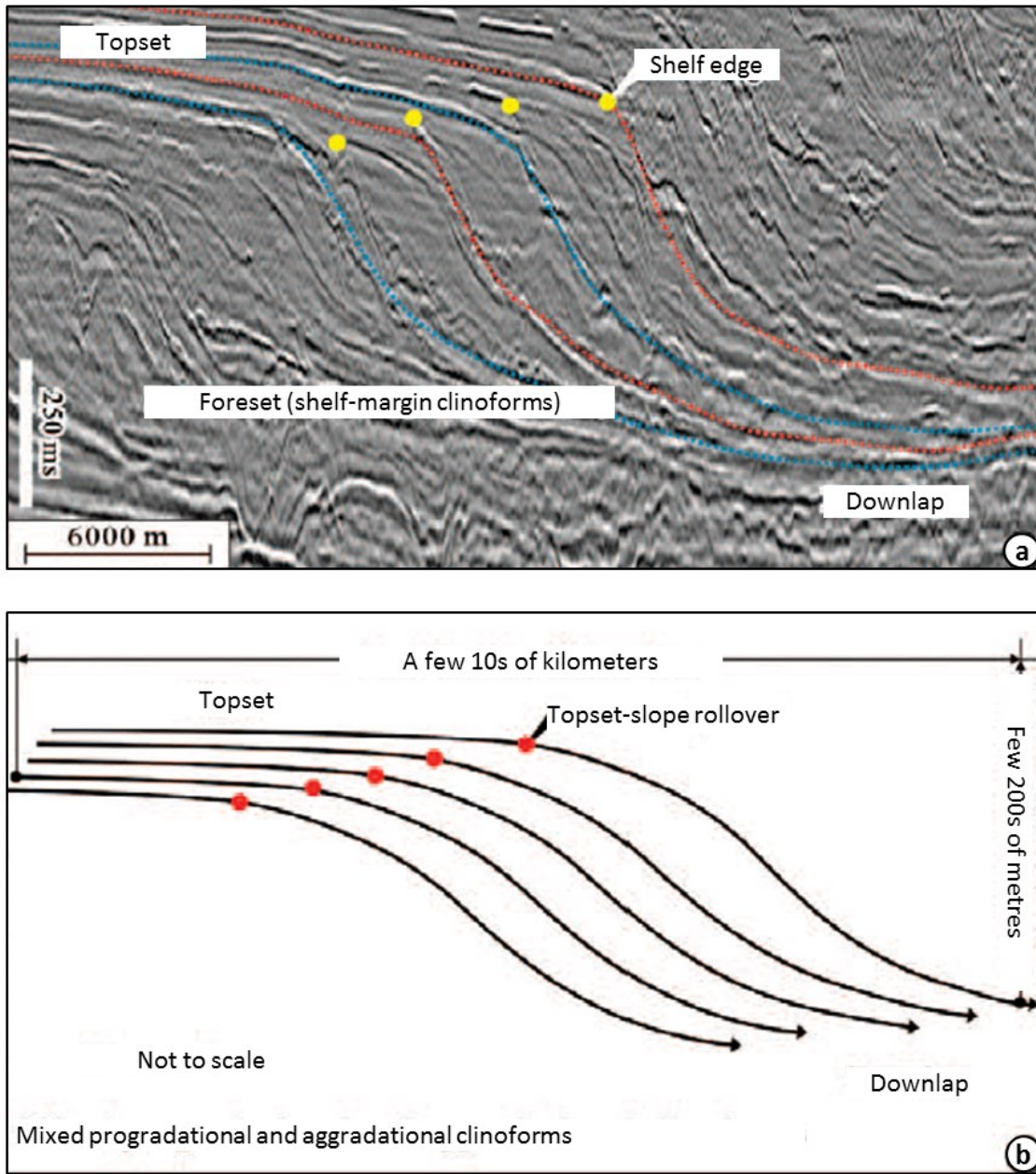
Figure 42: (a) The cross-sectional seismic expression and (b) architectural styles illustrating "the Mixed Progradational and Aggradational Clinoforms" interpreted in the South China Sea (Gong et al., 2015). The clinoform shapes in Units C (Figure 30b) and F (Figure 33b) shows the sigmoidal features which are similar with the Mixed Progradational and Aggradational Clinoforms in the South China Sea. These features indicate that sandstones were deposited in the shelfal area, while the claystones and marls were more abundant towards the basin.

Brasher and Vagle (1996) reported on the typical chalks in the Norwegian North Sea Chalk reservoirs based on core data, dipmeter, and borehole imagery logs. They identified three kinds of chalks: Category I, II, and III chalks. The Category I chalks correspond to the pelagic deposition, Category III chalks are affiliated with slumping, while Category II chalks are intermediate between III and I. They also established that Category I chalks have the poorest reservoir properties, while Category III chalks have the best reservoir properties. Das (2015) and Gennaro *et al.* (2013) showed the compressional ridges on seismic lines and coherency maps corresponding to slumping geometries in the Norwegian Central Graben (Figure 35b). This geometry has a similar pattern to Unit G in the southern part of the study area (Figure 35a (i)). Therefore, the slumping-related chalky limestone of Unit G is predicted to have good reservoir properties (Figure 41h).

6.4 PETROLEUM SIGNIFICANCE

The interpreted seismic sequence stratigraphic framework has assisted in the understanding of facies distribution and depositional environments. This can be used to predict the petroleum system elements of the Cretaceous interval in the northern Stord Basin. The transformation of seismic reflections into time domain in the Wheeler Diagram has improved the depositional history concept of each unit and enhanced the prediction of seismic facies and litho-facies. It contributed to determining potential source rocks, reservoir rocks, and cap rocks in an area with limited well control.

6.4.1 SOURCE ROCKS

The potential source rocks in the Cretaceous strata are the Sola and the Blodøks formations in Units C and E, respectively (Figures 19, 22, 41d, and 41f). Bugge *et al.* (2001) explained that dark shales of the Sola Formation, identified by high gamma log response, were deposited in a deep marine environment. They also mentioned that this formation is time-equivalent to the organic-rich claystones of the Fischschiefer source rock in Germany. In addition, as noted earlier, the Blodøks Formation corresponds to a condensed section of organic-rich claystones (Bugge *et al.,* 2001; Copestake *et al.,* 2003). Moreover, the gamma ray log in the 31/8-1 well

shows very high and high gamma ray response for the Sola and the Blodøks formations, respectively (Figure 19). These potential source rocks were deposited during early highstand systems tract (Sola Formation) and transgressive systems tract (Blodøks Formation) (Figures 38b and 40b).

However, there are some issues related to the lateral and vertical distribution of these source rock units. The thickness of the Sola Formation is relatively thick, which is around 137 m in the 31/8-1 well (Figure 19), but this formation was not deposited over all the study area (Figure 41b). The Blodøks Formation draped the entire study area, but the thickness of it is only 16 m in the 31/6-8 well (Figure 19), where the thickest part is around 70 ms (~88 m) (Figure 26g). The depocenter depth for the Sola (Unit C) and the Blodøks (Unit E) formations are approximately 1900 ms (~2400m) and 1200 ms (~1516 m), respectively (Figures 25d, 25f, 26e, and 26g). According to maturity data from the 31/8-1 well, an early mature oil window (0.6% Ro) occurs at ~2400 m and source rock in peak oil generation window (0.8% Ro) occurs around 3000 m. This information suggests that the Sola Formation is in the early mature oil window phase, while the Blodøks Formation is still considered as an immature source rock in the northern Stord Basin.

6.4.2 RESERVOIR ROCKS

Potential reservoir rocks in the Cretaceous interval are the Åsgard deep-marine basin-floor fans sandstones, and the potential shallow marine sandstones of the Agat Formation in Unit C, and the Tryggvason Formation in Unit F (Figures 41a, 41d, and 41g). These primary reservoirs were mainly formed during lowstand systems tract and highstand systems tract (Figure 36). However, the reflection configuration in Units C and F implying that coarse sediments were deposited only in the shelfal area to the east (Figures 41d and 41g). In addition, the slumping-related chalky limestone of Unit G (Tryggvason and Ekofisk formations) in the southern part of the study area may potentially represent a good reservoir (Figure 41h).

6.4.3 CAP ROCKS

The Åsgard claystones are potential cap rocks for the underlying Åsgard sandstones; while, the potential seal rocks for the Agat, Tryggvason, and Ekofisk formations are expected to be intra-formational shales and ultimately by the overlying claystones of the Cenozoic sediments (Figure 24c).

6.4.4 TRAPS

Insignificant tectonic activity occurred during the Cretaceous in the northern Stord Basin, except in the Late Aptian and Late Cretaceous inversions. There were some fault activities, in particularly in the Troll area after deposition of unit C, though the active normal faults generally decreased trough time from the Early to Late Cretaceous (Figure 41a-h).

The stratigraphic traps observed in the study area are (1) the stratigraphic pinch-out of the Åsgard basin-floor fans sandstones (Unit A1; Figure 24c) and the Tryggvason-Ekofisk limestones (Unit G; Figure 24a); (2) the truncational traps within the shallow marine sandstones of the Agat (Unit C) and Tryggvason (Unit F) formations (Figure 24c). However, a normal fault in the up-dip part of the Åsgard sandstones (Unit A1) has potential to make these sandstones to be trapped as a downfaulted structural closure (Figure 24c). Generally, the stratigraphic traps are the main traps type in the study area.

6.4.5 HYDROCARBON CHARGING

There is no well data proving a mature source rock interval in the northern Stord Basin. This leads to the uncertainty of source rock maturity within this area. Therefore, the hydrocarbon charging is expected to be from the Viking Graben in the eastern part of the study area. Sørensen and Tangen (1995) also explained that the possibility of hydrocarbon migration from the Viking Graben exists. However, this scenario is seen to have a high risk due to long-distance migration.

6.4.6 RISKS

The main risks for possible hydrocarbon-filled sandstones in Units C and F are top seal, biodegradation, and charge. The cap rock lithology is uncertain, especially in the overlying claystones of the Cenozoic sediments due to no well penetrates in the Øygarden Fault Complex area. If it is assumed that the seal has sufficient capacity to contain the hydrocarbons, another issue is the depth of the traps, which is only observed in the shallow area (700 ms (~884 m); Figure 24c). At this relatively shallow depth, microorganisms can destroy oil components resulting in biodegraded oil. For the hydrocarbon-filled chalky limestone in Unit G, cap rock is uncertain since no well penetrates close to this area. The limited data of the Cretaceous interval in the study area lead to the uncertainty about mature source rocks, as well as the lateral and vertical distribution of the source rocks. Therefore, the hydrocarbons are expected to be from the Viking Graben though this charging is risky due to long-distance migration.

7. CONCLUSIONS

The Cretaceous interval in the northern Stord Basin, northern North Sea, was divided into seven main seismic units: Unit A (Latest Berriasian), Unit B (Latest Berriasian-Early Hauterivian), Unit C (Early Hauterivian-Early Cenomanian), Unit D (Early-Early Cenomanian), Unit E (Late Cenomanian-Early Turonian), Unit F (Early Turonian-Late Turonian), and Unit G (Late Turonian-Danian). Unit A was further divided into two subunits (Unit A1 and A2) due to the differences in internal characters within this unit.

Two base-level fall events occurred in the Latest Berriasian and in the Cenomanian times. The base-level fall events in the Latest Berriasian is interpreted as a result of a combination of tectonic uplift during the early post-rift evolution of the northern North Sea, and tectonic processes in the north Atlantic region during the Hauterivian-Barremian. Relative sea-level fall in the Cenomanian was as a result of the mid-Cretaceous tectonic event at the NE Atlantic margin.

A prevailing open marine, outer shelf to bathyal depositional environment has been interpreted for the Cretaceous interval in the study area inferring mainly basinal hemipelagic and pelagic deposition, intervened by clastic-prone and limestone sedimentation. The Troll and the Oseberg Fault Blocks, the Bjørgvin Arch, and the Øygarden Fault Complex were the paleo-highs controlling the deposition of the Cretaceous interval, with the Øygarden Fault Complex interpreted as the primary sediment source for the early post-rift deposits.

For the Cretaceous strata in the northern Stord Basin two complete and an incomplete sequences were identified, bounded by the observed unconformities (depositional sequences). These sequences consist of a falling-stage systems tract (FSST 1), three lowstand systems tracts (LST 1, 2, and 3), two transgressive systems tracts (TST1 and 2), and two highstand systems tracts (HST 1 and 2). In addition, these sequences are related to second-order cycles, which postulate that the sequences were affected by continental-scale mantle thermal processes and by plate kinematics.

The integrated analysis of seismic stratigraphy interpretations, geomorphology tied to key well data, biostratigraphic data, and the chronostratigraphic chart helped determine the stratigraphic

evolution and thus the clastic-rich geometries in the study area. These geometries consist of deep-marine basin-floor fans within Unit A1, and shallow marine sandstones in Units C and F. The Oseberg Field and Bjørgvin Arch constrained the distribution of the basin-floor fans for Unit A1. The sandstone distribution in Units C and F suggests deposition only occurred on the paleo-shelf in the eastern parts of the study area during this stage.

The later erosional activity of Unit C in the footwall block of Troll Field suggests that tectonic uplift and tilting occurred after deposition of this unit. The absence of Aptian sediments (part of Unit C) in most of the wells in the study area, is interpreted due to the position of the wells being located on highs where non-deposition took place. This argument is confirmed by the evidence of sediments deposited in the basin recorded in the 31/8-1 well in the Stord Basin. The deposition of carbonate-rich lithologies in Unit D during the Early to Late Cenomanian was likely due to warmer temperatures and decrease in sediment influx. The slumping features in Unit G represent tectonic inversion caused by the Alpine Orogeny and North Atlantic Ocean rifting.

Two potential source rocks identified in the study area are the Sola and the Blodøks formations. The Sola Formation is assumed to be in the early oil mature stage, while the Blodøks Formation is still an immature source rock. The reservoir rocks are: the Åsgard Formation deep-marine basin-floor fan deposits in Unit A1; the Agat and the Tryggvason formations shallow marine sandstones in Units C and F; and the Tryggvason and the Ekofisk formations slumping-related chalky limestones in Unit G. The cap rocks are the Åsgard claystones, intra-formational claystones, and ultimately the overlying claystones within the Cenozoic succession. The main traps are interpreted as stratigraphic traps as no significant tectonic activity occurred during the Cretaceous in the northern Stord Basin. However, there is a potential structural trap within Unit A1, defined as a downfaulted trap.

REFERENCES

Allen, G, P., and Posamentier, H, W. 1993. Sequence Stratigraphy and Facies Model of An Incised Valley Fill: the Gironde Estuary, France. *Journal of Sedimentary Petrology 63*, Vol. 3, pp. 378–391.

Badley, M, E., Egeberg, T., and Nipen, O, V. 1984. Development of Rift Basins Illustrated by the Structural Evolution of the Oseberg Feature, Block 30/6, Offshore Norway. *J. Geol. Soc.*, Vol. 141, pp. 639-649. DOI: 10.1144/gsjgs.141.4.0639

Beach, A., Bird, T., and Gibbs, A. 1987. Extensional Tectonics and Crustal Structure: Deep Seismic Reflection Data from the northern North Sea Viking Graben. Continental Extensional Tectonics. Dewey, J F, and Hancock, P L (editors). *Special Publication of the Geological Society of London*, No. 28, pp. 467-476. DOI: 10.1144/GSL.SP.1987.028.01.29

Biddle, K, T., and Rudolph, K, W. 1988. Early Tertiary Structural Inversion in the Stord Basin, Norwegian North Sea. *Journal of the Geological Society,* 145**,** pp**.** 603-611. DOI: 10.1144/gsjgs.145.4.0603

Brasher, J., and K. Vagle. 1996. Influence of Lithofacies and Diagenesis on Norwegian North Sea Chalk Reservoirs: AAPG Bulletin, 80, pp. 746-768.

Brown, L, F, Jr., and Fisher, W, L. 1977. Seismic Stratigraphic Interpretation of Depositional Systems: Examples from Brazilian Rift and Pull Apart Basins. In: Payton, C. E. (ed.), *Seismic Stratigraphy – Applications to Hydrocarbon Exploration*. AAPG Memoir 26, pp. 213–248.

Bugge, T., Tveiten, B., and Bäckström, S. 2001. The Depositional History of the Cretaceous in the Northeastern North Sea. Sedimentary Environments Offshore Norway. *NPF Special Publication*, No. 10, pp. 279-291. DOI: 10.1016/S0928-8937(01)80018-7

Catuneanu, O. 2002. Sequence Stratigraphy of Clastic Systems: Concepts, Merits, and Pitfalls. *Journal of African Earth Sciences 35*, pp. 1–43. DOI: 10.1016/S0899-5362(02)00004-0

Catuneanu, O., Abreu, V, Bhattacharya, J, P., Blum, M, D., Dalrymple, R, W., Eriksson, P, G., Fielding, C, R., Fisher, W, L., Galloway, W, E., Gibling, M, R., Giles, J, A., Holbrook, J, M., Jordan, R., Kendall, C, G, S, C., Macurda, B., Martinsen, O, J., Miall, A, D., Neal, J, E., Nummedal, D., Pomar, L., Posamentier, H, W., Pratt, B, R., Sarg, J, F., Shanley, K,

W., Stell, R, J., Strasser, A., Tucker, M, E., and Winker, C. 2009. Towards the Standardization of Sequence Stratigraphy. *Earth-Science Reviews*, 92, pp: 1-33. DOI: 10.1016/j.earscirev.2008.10.003

Catuneanu, O., Galloway, W, E., Kendall, C, G, S, C., Miall, D, A., Posamentier, H, W., Strasser, A., Strasser, A., and Tucker, M, E. 2011. Sequence Stratigraphy: Methodology and Nomenclature. *Newsletters on Stratigraphy,* Vol. 44, pp. 173-245.

CGG. 2017. URL:
http://www.cgg.com/en/Media-and-Events/Media-Releases/2016/11/Integrated-Geoscience-Unlocks-Potential-in-Northern-Viking-Graben (available from: 27.02.2017).

Copestake, P., Sims, A., Crittenden, S., Hamar, G., Ineson, J., Rose, P., and Tringham, M. 2003. Upper Cretaceous. In D. Evans, et al. (Eds.). *The Millennium Atlas: Petroleum Geology of the Central and Northern North Sea*. The Geological Society of London, pp. 441-489.

Coward, M, P., Dewey, J., Mange, M, A., Hempton, M., and Holroyd, J. 2003. Tectonic Evolution. In D. Evans, et al. (Eds.). *The Millennium Atlas: Petroleum Geology of the Central and Northern North Sea*. The Geological Society of London, pp. 67-88.

Das, Sarasi. 2015. Seismic Stratigraphy and Geomorphology of the Chalk Group of the Central Graben, North Sea. *Master Thesis*, University of Stavanger.

Emery, D., and Myers, K. 2009. *Sequence Stratigraphy*. John Wiley & Sons, pp. 304.

Faerseth, R, B. 1996. Interaction of Permo-Triassic and Jurassic Extensional Fault-Blocks during the Development of the Northern North Sea. *Journal of the Geological Society*, Vol. 153, pp. 931-944. DOI: 10.1144/gsjgs.153.6.0931

Fossen, H., Khani, H, F., Faleide, J, I., Kseinzyk, A, K., and Dunlap, W, J. 2016. Post-Caledonian Extension in the West Norway-Northern North Sea Region: The role of Structural Inheritance. *Geological Society, London, Special Publications*. DOI: 10.1144/SP439.6

Fowler, J. N., Guritno, E., Sherwood, P., and Smith, M. J. 2001. Depositional Architectures of Recent Deep Water Deposits in the Kutei Basin, East Kalimantan. *Proceedings, Indonesian Petroleum Association, Twenty-Eighth Annual Convention and Exhibition*, October 2001, pp. 409–422.

Gabrielsen, R, H., Kyrkjebø, R., Faleide, J, I., Fjeldskaar, W., and Kjennerud, T. 2001. The Cretaceous Post-Rift Basin Configuration of the Northern North Sea. *Petroleum Geoscience*, Vol. 7, pp. 137-154. DOI: 10.1144/petgeo.7.2.137

Gabrielsen, R, H., Steel, R, J., and Nøttvedt, A. 1995. Subtle Traps in Extensional Terranes: A Model with Reference to the North Sea. *Petroleum Geoscience*, Vol.1, pp. 223–235. DOI: 10.1144/petgeo.1.3.223

Galloway, W, E. 1989. Genetic Stratigraphic Sequences in Basin Analysis I: Architecture and Genesis of Flooding-Surface Bounded Depositional Units. *The American Association of Petroleum Geologists Bulletin*, Vol. 73, pp. 125–142.

Gennaro, M., Wonham, J, P., Gawthorpe, R., and Sælen, G. 2013. Seismic Stratigraphy of the Chalk Group in the Norwegian Central Graben, North Sea. *Marine and Petroleum Geology 45*, pp. 236-266. DOI: 10.1016/j.marpetgeo.2013.04.010

Gong, C., Wang, Y., Steel, R, J., Olariu, C., Xu, Q., Liu, X., Zhao, Q. 2015. Growth Styles of Shelf Margin Clinoforms; Prediction of Sand- and Sediment-Budget Partitioning into and across the Shelf. *Journal of Sedimentary Research*, Vol. 85, 209–229. DOI: 10.2110/jsr.2015.10

Helland-Hansen, W. and Hampson, G., J. 2009. Trajectory Analysis: Concepts and Applications. *Basin Research*, Vol. 21, pp. 454-483. DOI: 10.1111/j.1365-2117.2009.00425.x

Hunt, D., and Tucker, M, E. 1992. Stranded Parasequences and the Forced Regressive Wedge Systems Tract: Deposition During Base-Level Fall. *Sedimentary Geology 81*, pp. 1–9. DOI: 10.1016/0037-0738(94)00123-C

Isaksen, D. and Tonstad, K. 1989. A Revised Cretaceous and Tertiary Lithostratigraphic Nomenclature for the Norwegian North Sea. NPD-Bulletin No. 5, 59 pp.

Jordt, H., Faleide, J, I., Bjorlukke, K., and Ibrahim, M, T. 1995. Cenozoic Sequence Stratigraphy of the Central and Northern North Sea Basin: Tectonic Development, Sediment Distribution and Provenance Areas. *Marine and Petroleum Geology*, Vol. 12, pp. 845–879. DOI: 10.1016/0264-8172(95)98852-V

Lundin, E, R., and Doré, A, G. (1997). A Tectonic Model for the Norwegian Passive Margin with Implications for the NE Atlantic: Early Cretaceous to break-up. *Journal of the Geological Society,* 154, pp: 545-550. DOI: 10.1144/gsjgs.154.3.0545

McClay, K, R., Norton, M, G., Coney, P., and Davis, G, H. 1986. Collapse of the Caledonide Orogen and the Old Red Sandstone. *Nature,* London, Vol. 525, pp. 147-149. DOI: 10.1038/323147a0

Miall, A, D. 2010. *The Geology of Stratigraphic Sequences*. Second Edition. Springer-Verlag, Berlin, pp. 522.

Mitchum, R, M, Jr. 1985. Seismic Stratigraphic Expression of Submarine Fans: Chapter 7. In: Berg, O., R. and Woolvertoon, D., G. (eds). *Seismic Stratigraphy II: An Integrated Approach to Hydrocarbon Exploration.* AAPG, Memoir 39, pp. 117-135.

Mitchum, R, M, Jr. and Vail, P., R. 1977. Seismic Stratigraphy and Global Changes of Sea Level. Part 7: Stratigraphic Interpretation of Seismic Reflection Patterns in Depositional Sequences. In: Peyton, C.E. (Ed.), *Seismic Stratigraphy―Applications to Hydrocarbon Exploration*. AAPG Memoir 26, pp. 135-144.

Mitchum, R, M, Jr., Vail, P.R., and Sangree, J, B. 1977. Seismic Stratigraphy and Global Changes of Sea Level. Part 6: Stratigraphic Interpretation of Seismic Reflection Patterns in Depositional Sequences. In: Payton, C.E. (Ed.), *Seismic Stratigraphy―Applications to Hydrocarbon Exploration*. AAPG Memoir 26, pp. 205-212.

Norwegian Petroleum Directorate (NPD)-*FactPages*. 2017. URL: http://factpages.npd.no/factpages/Default.aspx?culture=en (available from: 05.02.2017).

Norwegian Petroleum Directorate (NPD). 2017. URL: http://www.npd.no/Global/Engelsk/2-Topics/Geology/Lithostratigraphy/NS-OD1409001.pdf (available from: 27.01.2017).

Nummedal, D., and Swift, D, J, P. 1987. Transgressive Stratigraphy at Sequence-Bounding Unconformities: Some Principles Derived from Holocene and Cretaceous Examples. In: Nummedal, D., Pilkey, O. H., Howard, J. D. (eds.) *Sea-level Fluctuation and Coastal Evolution*. SEPM Special Publication, No. 41, pp. 241–260. DOI: 10.2110/sepmsp.105.

Oakman, C. 2005. The lower Cretaceous Plays of the Central and Northern North Sea: Atlantean Drainage Models and Enhanced Hydrocarbon Potential. *Petroleum Geology: North-West Europe and Global Perspectives-Proceedings of the 6th Petroleum Geology Conference*. The Geological Society of London, pp. 187-198. DOI: 10.1144/0060187

Posamentier, H, W., and Allen, G, P. 1999. Siliciclastic Sequence Stratigraphy: Concepts and Applications. *SEPM Concepts in Sedimentology and Paleontology*, No. 7, 210 pp.

Posamentier, H, W., and Kolla, V. 2003. Seismic Geomorphology and Stratigraphy of Depositional Elements in Deep-Water Settings. *Journal of Sedimentary Research*, Vol. 73; No. 3, pp. 367–388. DOI: doi.org/10.1016/j.earscirev.2008.10.003

Posamentier, H, W., Jervey, M, T., and Vail, P, R. 1988. Eustatic Controls on Clastic Deposition. I. Conceptual Framework. In: Wilgus, C. K., Hastings, B. S., Kendall, C, G, St. C., Posamentier, H.W., Ross, C. A., Van Wagoner, J. C. (Eds.). *Sea Level Changes – An Integrated Approach*. SEPM Special Publication 42, pp. 110–124.

Ramsayer, G, R. 1979. Seismic Stratigraphy: A Fundamental Exploration Tool. In: *Proceedings of the Offshore Technology Conference*, Houston, Texas, April–May 1979, Vol. 3, pp. 1859–1867. DOI: 10.4043/3568-MS

Roksandic, M, M. 1978. Seismic Facies Analysis Concepts. *Geophysical prospecting 26*, pp. 383-398. DOI: 10.1111/j.1365-2478.1978.tb01600.x

Taner, M. T. 2001. Seismic attributes. *Canadian Society of Exploration Geophysicicts Recorder*, v. 26, no. 7, pp. 48-56.

Torsvik, T, H., Smethurst, M, A., Meert, J, G., Van der Voo, R., McKerrow, W, S., Brasier, M, D., Sturt, B, A., and Walderhaug, H, J. 1996. Continental Breakup and Collision in the Neoproterozoic and Paleozoic of Baltica and Laurentia. *Earth Science Reviews*, Vol. 40, pp. 229-258. DOI: 10.1016/0012-8252(96)00008-6

Schlumberger. 2006. URL: http://webcache.googleusercontent.com/search?q=cache:KqRjmH6KX_EJ:www.slb.com/~/media/Files/software/case_studies/varcube_cs.ashx+&cd=1&hl=no&ct=clnk&gl=no&client=firefox-b-ab (available from: 03.04.2017).

Sheriff, R, E. 2006. Encyclopedic Dictionary of Applied Geophysics. *Society of Exploration Geophysicists*, Tulsa. DOI: 10.1190/1.9781560802969

Sloss, L, L., Krumbein, W, C., and Dapples, E, C. 1949. Integrated Facies Analysis. In: Longwell, C. R. (ed.), *Sedimentary Facies in Geologic History*. Geological Society of America Memoir 39, pp. 91–124.

Snedden, J., and Liu, C. 2010. A Compilation of Phanerozoic Sea-Level Change, Coastal Onlaps and Recommended Sequence Designations. *Search and Discovery Article #40594*.

Surlyk, F., Dons, T., Clausen, K, C., and Higham, J. 2003. Upper Cretaceous. In D. Evans, et al. (Eds.). *The Millennium Atlas: Petroleum Geology of the Central and Northern North Sea*. The Geological Society of London, pp. 490-548.

Swift, D, J, P. 1975. Barrier-Island Genesis: Evidence from the Central Atlantic Shelf, Eastern U.S.A. *Sedimentary Geology 14*, pp. 1–43. DOI: 10.1016/0037-0738(75)90015-9

Sørensen, S., and Tangen, O, H. 1995. Exploration Trends in Marginal Basins from Skagerrak to Stord. Petroleum Exploration and Exploitation in Norway. *NPF Special Publication*, No. 4, pp. 97-114. DOI: 10.1016/S0928-8937(06)80039-1

Vail, P. R., Mitchum, R, M, Jr., and Thompson, S. 1977. Seismic Stratigraphy and Global Changes of Sea Level, Part Four: Global Cycles of Relative Changes of Sea Level. In Payton, C.E., ed., Seismic stratigraphy; applications to hydrocarbon exploration: *American Association of Petroleum Geologists Memoir 26*, pp. 83-98.

Van Wagoner, J, C. 1995. Sequence Stratigraphy and Marine to Non-Marine Facies Architecture of Foreland Basin Strata, Book Cliffs, Utah, U.S.A. In: Van Wagoner, J. C., Bertram, G.T. (Eds.), *Sequence Stratigraphy of Foreland Basin Deposits*. AAPG Memoir 64, pp. 137–223.

Van Wagoner, J, C., Mitchum R., M, Jr., Campion, K, M., and Rahmanian, V, D. 1990. Siliciclastic Sequence Stratigraphy in Well Logs, Core, and Outcrops: Concepts for High-Resolution Correlation of Time and Facies. *American Association of Petroleum Geologists Methods in Exploration*, Series 7, 55 pp.

Van Wagoner, J, C., Posamentier, H, W., Mitchum, R, M., Vail, P, R., Sarg, J, F., Loutit, T, S., and Hardenbol, J. 1988. An Overview of the Fundamentals of Sequence Stratigraphy and Key Definitions. In: Wilgus, C, K., Hastings, B. S., Kendall, C, G, St, C., Posamentier, H.W., Ross, C. A., Van Wagoner, J, C. (Eds.). *Sea Level Changes – An Integrated Approach*. SEPM Special Publication, No. 42, pp. 39-45.

Zachariah, A, J., Gawthorpe, R., Dreyer, T., and Corfield, S. 2009. Controls on Early Post-Rift Physiography and Stratigraphy, Lower to Mid-Cretaceous, North Viking Graben, Norwegian North Sea. *Basin Research 21*, pp. 189-208. DOI: 10.1111/j.1365-2117.2008.00371.x

Zanella, E., and Coward, P, M. 2003. Structural Framework. In D. Evans, et al. (Eds.). *The Millennium Atlas: Petroleum Geology of the Central and Northern North Sea*. The Geological Society of London, pp. 88-125.

Ågotnes, S, S. 2016. Permian-Triassic Tectono-Stratigraphic Evolution of the Stord Basin, Northern North Sea. *Master Thesis*, University of Bergen.